

This electronic thesis or dissertation has been downloaded from the King's Research Portal at <https://kclpure.kcl.ac.uk/portal/>



## **Fluctuations in non-equilibrium states from quantum to classical**

Myers, Jason

*Awarding institution:*  
King's College London

The copyright of this thesis rests with the author and no quotation from it or information derived from it may be published without proper acknowledgement.

### **END USER LICENCE AGREEMENT**



**Unless another licence is stated on the immediately following page** this work is licensed

under a Creative Commons Attribution-NonCommercial-NoDerivatives 4.0 International

licence. <https://creativecommons.org/licenses/by-nc-nd/4.0/>

You are free to copy, distribute and transmit the work

Under the following conditions:

- Attribution: You must attribute the work in the manner specified by the author (but not in any way that suggests that they endorse you or your use of the work).
- Non Commercial: You may not use this work for commercial purposes.
- No Derivative Works - You may not alter, transform, or build upon this work.

Any of these conditions can be waived if you receive permission from the author. Your fair dealings and other rights are in no way affected by the above.

### **Take down policy**

If you believe that this document breaches copyright please contact [librarypure@kcl.ac.uk](mailto:librarypure@kcl.ac.uk) providing details, and we will remove access to the work immediately and investigate your claim.

# Fluctuations in Non-Equilibrium States: From Quantum to Classical

*Jason Myers*

Supervised by:

*Benjamin Doyon*

*Joe Bhaseen*

*Rosemary Harris*

A dissertation submitted for the degree of

**Doctor of Philosophy**

of

**Kings College London.**

Department of Mathematics

Kings College London

December 27, 2019

I, Jason Myers, confirm that the work presented in this thesis is my own. Where information has been derived from other sources, I confirm that this has been indicated in the work.

# Abstract

The goal of this thesis is to obtain the statistics of transported quantities in non-equilibrium steady states of both classical and quantum systems. This transport is considered over a long time period where the large deviation principle is satisfied. Thus, the statistics of transported quantities will be described via the Scaled Cumulant Generating Functional (SCGF).

Initially I introduce a simple approach for obtaining the SCGF dubbed ‘bootstrapping’. This is limited to systems that display a chiral separation and satisfy the Gallavotti-Cohen fluctuation relation which is expressed as a symmetry on the SCGF.

I then present the primary result of this work, the Ballistic Fluctuation Formalism (BFF). This approach allows for the derivation of the SCGF for ballistically transported quantities in a maximal entropy state that has arisen in the long-time limit of a system governed by Euler hydrodynamics. The BFF represents an important new organisational principle for non-equilibrium states in both classical and quantum systems.

The remainder of this thesis is the application of the BFF to three different systems. The first is a generalised Totally Asymmetric Exclusion Process, a classical system, where the SCGF for current transport is obtained. The second is a  $d$ -dimensional Conformal Field Theory, a quantum system, where the first known expression for the SCGF of energy transport is obtained. Finally, the BFF is applied to integrable models that can be described by generalized hydrodynamics via the Thermodynamic Bethe Ansatz, where these can be either classical or quantum systems. The BFF is used to obtain a general expression for the SCGF applicable to any transported conserved quantity of any such system. These results are applied to the classical hard rod gas and the quantum Lieb-Liniger gas.

# Acknowledgements

To begin I would like to thank all my supervisors: Ben Doyon, Rosemary Harris and Joe Bhaseen. Having three great physicists who are also down-to-earth, friendly and kind has made me very self-conscious while others complain about their supervisors. This thesis wouldn't have been possible without you.

Next I would like to thank my partner in life and now my wife, Alison. You have put up with more complaining, moaning and tears than should be expected of any person. Thanks for being there with me through this entire process and always providing the encouragement I needed (even when hangry).

All my family have been incredibly supportive throughout, even if I was occasionally (often) asked why I was torturing myself. Thanks to all my parents for politely asking me questions about things that presumably bored you to tears. Further thanks to the rest of my large family but in particular Matty (the-moo) and Rox for putting me up in your home when I really needed a home-cooked meal and family close by.

Special thanks to my other partner in life, Tinashe, it was great having someone else going through the same ups and downs as me. I appreciate you always having my back.

Thanks to all my friends both inside KCL and outside. Particular shout out to my citrus family: Claudio, Gioia and Vito for being there through thick and thin. Particularly thanks to Claudio for having an equally childish sense of humour to me, it was always great to laugh with you (or at you).

I also would like to acknowledge the taxpayers of both the UK and SA for funding me throughout my academic career, it has been great receiving more tax than I pay in tax.

# Contents

<b>Introduction</b>	<b>1</b>
<b>1 Foundational concepts</b>	<b>10</b>
1.1 Non-equilibrium steady states . . . . .	10
1.2 Large deviation theory - a study of fluctuations . . . . .	11
1.3 Fluctuation relations . . . . .	16
1.4 Integrability and large numbers of conserved charges . . . . .	23
1.5 Basics of Euler hydrodynamics . . . . .	26
<b>2 The SCGF via bootstrapping</b>	<b>31</b>
2.1 Conformal field theory . . . . .	31
2.2 SCGF for transport of KdV charges . . . . .	34
2.3 Classical interpretation of KdV charge transport fluctuations . . . . .	38
2.4 Extended fluctuation relation introduced . . . . .	40
<b>3 Ballistic fluctuation formalism</b>	<b>44</b>
3.1 Maximal entropy states and fluctuating hydrodynamics . . . . .	45
3.2 Equations and assumptions of ballistic fluctuation formalism . . . . .	51
3.3 Application of ballistic fluctuation formalism to 1D CFT . . . . .	57
3.4 Extended fluctuation relation revisited . . . . .	59
3.5 Co-propagating modes and dynamical phase transitions . . . . .	62
3.6 Normal mode decomposition of SCGF . . . . .	64
<b>4 Fluctuations in the <math>\ell</math>-TASEP</b>	<b>68</b>
4.1 $\ell$ -TASEP . . . . .	68
4.2 SCGF for particle current in $\ell$ -TASEP . . . . .	72

4.3	Insights into the ballistic fluctuation formalism . . . . .	78
<b>5</b>	<b>Fluctuations in <math>d</math>-dimensional CFT</b>	<b>81</b>
5.1	Reduction to a one-dimensional hydrodynamic problem . . . . .	82
5.2	Exact SCGF and cumulants . . . . .	84
5.3	Fluctuation relations in $d$ -dimensional CFT . . . . .	88
5.4	Normal mode decomposition of $d$ -dimensional CFT . . . . .	91
<b>6</b>	<b>Ballistic fluctuation formalism applied to integrable models</b>	<b>93</b>
6.1	TBA and generalised hydrodynamics . . . . .	94
6.2	The SCGF of conserved quantity transport . . . . .	100
6.3	Cumulants for transport . . . . .	103
6.4	Classical hard rod gas . . . . .	104
6.5	Quantum Lieb-Liniger gas . . . . .	107
6.6	Fluctuation relation in integrable models . . . . .	113
	<b>Conclusions</b>	<b>117</b>
	<b>Appendices</b>	<b>121</b>
<b>A</b>	<b>Appendices to chapter 2</b>	<b>121</b>
A.1	Bootstrapping in $d$ -dimensional free massive theories . . . . .	121
A.2	1D CFT energy transport from classical particles on a ring . . . . .	123
<b>B</b>	<b>Macroscopic fluctuation theory</b>	<b>126</b>
<b>C</b>	<b>Appendices to chapter 4</b>	<b>129</b>
C.1	Zero range process flow equation . . . . .	129
C.2	$\ell$ -TASEP hydrodynamic quantities . . . . .	131
<b>D</b>	<b>Appendices to chapter 6</b>	<b>134</b>
D.1	Derivation of TBA for Lieb-Liniger . . . . .	134
D.2	Integrable SCGF specialisation to the Lesovik-Levitov formula . . . . .	138
D.3	Calculating $c_3$ and $c_4$ from integrable SCGF . . . . .	139
D.4	Occupation function in integrable models . . . . .	144

D.5	Thermal distribution of hard rod gas . . . . .	145
D.6	Details of Monte Carlo simulation of hard rod gas . . . . .	147
<b>Bibliography</b>		<b>148</b>



# List of Figures

1.1	3D representation of partitioning protocol for non-equilibrium steady states	11
4.1	Depiction of open $\ell$ -TASEP. . . . .	70
4.2	Phase diagram for the open boundary $\ell$ -TASEP for the bulk of the system.	71
4.3	SCGF for the particle transport in the $\ell$ -TASEP . . . . .	78
5.1	Numerical solutions for the SCGF of energy transport in a CFT with two and three dimensions. . . . .	88
5.2	SCGF for energy transport in CFT with two dimensions showing fluctuation relations. . . . .	90
5.3	SCGF for energy transport in CFT with five dimensions. . . . .	90
6.1	Comparison of theoretical predictions and Monte Carlo simulation of the first four energy flow cumulants in the classical integrable model the hard rod gas. . . . .	105
6.2	Heat maps for the first four cumulants of energy transport in the quantum integrable model, the Lieb-Liniger model. . . . .	110
6.3	Heat maps for the first four cumulants of particle transport in the quantum integrable model, the Lieb-Liniger model. . . . .	111
6.4	Figures showing the SCGF of energy transport for the Lieb-Liniger model in equilibrium and non-equilibrium states. . . . .	112
6.5	Figures showing the probability distributions for energy transport at different times for the Lieb-Liniger model in equilibrium and non-equilibrium states. . . . .	113

6.6	Probability distribution for energy currents in Lieb-Liniger showing a symmetrical curve in equilibrium state and an asymmetrical curve in non-equilibrium state. . . . .	113
6.7	Numerical evidence for the fluctuation-relation symmetry in the Lieb-Liniger gas. . . . .	115
6.8	Further numerical evidence for the fluctuation-relation symmetry in the hard rods gas. . . . .	115
6.9	Further numerical evidence for the fluctuation-relation symmetry in the Lieb-Liniger gas. . . . .	116
6.10	Numerical evidence for the fluctuation-relation symmetry in the Lieb-Liniger gas. . . . .	116
A.1	Figure showing two independent random walkers on a ring, where particle 1/2 hopping with rate $p_1/p_2$ to the right and $q/q'$ to the left. . . . .	125

# Introduction

As the title suggests, understanding fluctuating quantities in non-equilibrium states will be the primary goal of this thesis. To understand non-equilibrium states, it is perhaps optimal to begin with what is meant by equilibrium. An equilibrium state can be understood as fundamentally related to time reversibility, specifically an equilibrium state exists if the average rate of every process in the system is equal to the average rate of that process under time-reversal. Time-reversibility can only be achieved for a system in which the dissipation, or the total entropy change, is zero [1]. This immediately sets up the definition of a non-equilibrium state as that which is time-irreversible, a corollary of this is these states often display entropy production [1]. The best analogy is consider filming the system of interest. After filming play the resulting movie in reverse, if it is clear that the system in reverse is different to what was filmed then we can say the system is time-irreversible and is in a non-equilibrium state.

Non-equilibrium states are ubiquitous in nature and can be found in areas as diverse as: environmental science [2], geography [3], economics [4], biology [5] and many others to the realms of physics both large and small. Within condensed matter physics understanding such states may lead to a variety of technological applications, according to [6] expected applications are as diverse as: the development of new materials leading to revolution in use and production of energy, storage and transfer of quantum coherences leading to multiple quantum based technologies, conditions under which heat is rapidly transferred leading to smaller electronic devices and better control of spin transport leading to new secure ways to transfer information. Thus, it has become crucial to understand and describe non-equilibrium states in a variety of systems.

The goal for physicists working on non-equilibrium states is obtaining a framework as successful as equilibrium thermodynamics which provides a general approach to un-

derstanding the fluctuating quantities of an equilibrium state. Through the well-known statistical ensembles one can acquire information that encodes fluctuations based only on a few key properties such as entropy, temperature and free energies [7]. Although often taken for granted, the ability to describe behaviour of many-body systems based on only a few key observables is phenomenal. The successful approach of Boltzmann and his contemporaries has even been applied to quantum statistical systems, systems that were far beyond the imagination of the 19th century developers of the ideas. In contrast to the successes in the arena of equilibrium states, much less is known about non-equilibrium states in general. The primary difficulty with systems that are out-of-equilibrium is the important role played by dynamics that arises from the time-irreversible nature of such states [1, 8]. In non-equilibrium states one is interested in not only the stationary fluctuations of a system but those fluctuations that arise in time or, importantly for the present work, fluctuations of time integrated stochastic quantities. Thus, in addition to the usual scaling limits of large volume or large particle number one must also take into account time evolution. The additional scaling limits needed, which depend on the system and stochastic quantity studied, lead to tremendous challenges [8].

Work on an approach to non-equilibrium statistical mechanics has been progressing for over a century. In [9] three important figures in the field, R. Kubo, M. Toda, and N. Hashitsume, begin their history of non-equilibrium states with stochastic processes. However, in order to truly encapsulate all developments, I rewind slightly further back as the language of non-equilibrium can be understood in the older formalism of hydrodynamics, the foundations of which were introduced by Euler and Bernoulli in the 18th century. A good description relaying the importance of these ideas is found in [10]. Hydrodynamics is a study of dynamics of conserved quantities. In [10] it is explained that the reason these conserved quantities are of paramount importance is that when considering system dynamics, quantities that are not conserved during collisions of the constituents of the system will decay rapidly. Thus, the only surviving quantities after a short period of time are those that are conserved in collisions and it is these conserved quantities that will come to characterise the non-equilibrium behaviour of the system after some time has passed. With this simple explanation the importance of hydrodynamics is illuminated, and this work will come to rely heavily on hydrodynamics.

Using [9], I now continue with the historical overview of non-equilibrium approaches with the Einstein relation.

In [9] it is stated that “grasping physical phenomena as stochastic processes is one of the very fundamental methods of [non-equilibrium statistical mechanics]”. The first such description was undertaken by Einstein, highlighted by the Einstein relation [11]. The Einstein relation states that the diffusion of a Brownian particle is proportional to its mobility where diffusion describes the ‘natural’ movement of a particle under statistical fluctuations in the system and the mobility is related to an external force applied to the system. In the words of R. Kubo [12] “ [this describes a] relationship between the response of a given system to an external disturbance and the internal fluctuation of the system in the absence of the disturbance”, which is precisely the statement of the fluctuation-dissipation relation, the first step towards a cohesive framework non-equilibrium statistical physics. Importantly the internal fluctuations of the system must be understood as equilibrium or thermal fluctuations. One should also note the appearance of the hydrodynamics through the use diffusivity, initially a hydrodynamic concept developed by Fick in 1855, although used in a different way in this case. The fluctuation-dissipation can be understood as a perturbative result into non-equilibrium systems. In more specific language, the fluctuation-dissipation relation is the statement that the linear response of an equilibrium system driven into an out-of-equilibrium state is determined by fluctuations in the initial, equilibrium state [13]. The history of these discoveries is nicely laid out in [13], which I follow closely here. The Brownian motion fluctuation-dissipation relation was also found independently by Sutherland at the same time as Einstein’s work [14]. Later Johnson and Nyquist discovered a corresponding relation in electric circuits [12, 15, 16]. Some further steps were taken by Callen and Welton in applying these ideas to quantum systems [17]. These ideas were systematised by Green [18, 19] and then generalised to a large extent by Kubo [20], the same Kubo as referenced above. Kubo’s monumental work on fluctuation-dissipation relations extended to both classical and quantum systems. Further contributions to non-equilibrium systems were again made by Kubo through providing the framework for the Onsager-Casimir reciprocity relations [13]. Probably the most important outcome of Kubo’s work was to open an approach to the application of higher order fluctuation-dissipation rela-

tions, beyond linear regime [20]. More details on Kubo and the work that followed provide a fascinating history and much more could be said about this great man and others around him but unfortunately this would take me too far from the main purposes of the present work.

In the early 90's a new and modern wave of activity was set off by the work of [21] in which they conjecture the existence of so-called fluctuation relations based on numerical evidence. This conjecture was placed on firmer ground in the seminal work [22] in which these relations are shown rigorously, this original finding has come to be known as Gallavotti-Cohen fluctuation relations. The fluctuation relations express properties of the probability distribution for stochastic, fluctuating quantities that are general enough to apply to states both in equilibrium and far from equilibrium [23]. This provides an important step forward as the work of Kubo, even in a non-linear generalised form, fundamentally requires fluctuations to be Gaussian in nature whereas fluctuation relations move beyond this [24]. It can be shown that the fluctuation-dissipation relations of Kubo are a consequence of the fluctuation relations [24]. Various types of fluctuation relations have been found and these have largely been consolidated, [23] however it is still important to explicitly state the Jarzynski equality and Crooks' fluctuation relations as the first and archetypical examples of the fluctuation relations. Jarzynski's equality states that given the transition from an equilibrium state  $a$  to an equilibrium state  $b$ , the change in free energy,  $\Delta F$  is related to the work it took to perform this transition,  $W_{a \rightarrow b}$ , by  $\langle e^{-\beta W_{a \rightarrow b}} \rangle = e^{-\beta \Delta F}$  with  $\beta$  inverse temperature of the equilibrium system [25]. Although Jarzynski's equality came first, this was shown to be a simple consequence of the Crooks' fluctuation relation which states that the probability of a transition from equilibrium state  $a$  to equilibrium state  $b$  is related to the reverse transition in the following way:  $\mathbb{P}_{a \rightarrow b} / \mathbb{P}_{b \rightarrow a} = \exp(\beta(W_{a \rightarrow b} - F))$  [26]. These results are tremendously important as they are valid even if the system changes rapidly through a non-equilibrium process. In general the fluctuation relations can be understood as defining a relationship between a forward and reverse process, with details left for chapter 1. Only relatively recently have fluctuation relations been found in quantum systems where difficulties arise as transported or extensive quantities, the quantities of interest in non-equilibrium states, are very often not quantum observables under von Neuman measurement [27]. This prob-

lem is usually resolved through the two-measurement protocol whereby the fluctuating quantity of interest is obtained via a measurement at some initial time and some final time, this is discussed in greater detail in chapter 1. There has now been extensive experimental confirmation of the appearance of the fluctuation relations across a vast range of physical systems including: basic RC circuits [28], mesoscopic systems [29], chaotic systems such as granular systems [30] and even quantum systems through trapped ion experiments [31].

At the same time as the fluctuation relations were being uncovered, an older framework was rediscovered, a framework known as Large Deviation Theory (LDT) (presented in detail in chapter 1). In this framework one is interested in the statistics of extensive quantities correctly scaled. A trivial but widely cited example of this is the statistics of getting heads in a coin tossed a very large number of times. Clearly the number of heads obtained will grow with the number of coin tosses, however the number of heads divided by the number of tosses will provide meaningful statistics. The LDT states the probability distribution of such a situation is defined by a large deviation principle (LDP) where the probability distribution of heads is  $\lim_{N \rightarrow \infty} \mathbb{P}(XN = H) = \lim_{N \rightarrow \infty} \exp(-NI(H))$  with  $H$  the number of heads and  $N$  the number of tosses. This shows in the large limit the statistics of obtaining heads is dominated by an exponentially decaying function with the function  $I(H)$  known as the rate function. Not all systems satisfy an LDP, but a large number of physical systems seem to. In fact, applying these ideas to the energy statistics of a system in an equilibrium state results in the identification of  $I$  as the negative of entropy (see section 1.2.3). Crucially, the ideas of the LDT are applicable to systems far from equilibrium and provide an important toolkit for describing the statistics of non-equilibrium quantities. Of particular interest in the present work is the Legendre-Fenkel transform of  $I$ , the Scaled Cumulant Generating Functional (SCGF). The SCGF turns out to be a crucial object as it encodes information about all the fluctuations of stochastic quantities for non-equilibrium systems and can be shown to play the role of a non-equilibrium free energy (see section 1.2.3), thus knowing the SCGF is to understand fluctuations in non-equilibrium states. A further interesting aspect of the LDP is the fluctuation relations can be obtained within this formalism further bolstering its credentials as a fundamental language of non-equilibrium states. The

LDP was originally developed in mathematics, however work by Lanford [32], and generalised by Ellis [33] brought this framework to statistical physics and was reintroduced to a modern audience by the important review of Touchette [34]. Thus it seems, that the LDT may be at the core of statistical physics, and as Touchette himself states in [34], “[some already] see large deviation theory as the proper mathematical framework in which problems of statistical mechanics [both equilibrium and non-equilibrium] can be formulated and solved efficiently and, if need be, rigorously”. Due to the importance of the SCGF in non-equilibrium states, the primary focus of this thesis will be on calculation of this object for the transport of various fluctuating quantities in a range of systems in non-equilibrium states.

The SCGF has been calculated in numerous settings including both classical and quantum systems, where in mesoscopic physics this is equivalent to obtaining the full counting statistics. Explicit results have been found in: interacting particle models including the exclusion and the zero-range process [35] (discussed in chapter 4), systems modelled by stochastic differential equations [36], open quantum chains, [37, 38], free-fermions with the celebrated Lesovik-Levitov formula [39], harmonic chains [40] and free field theory [41, 42], certain integrable impurity models [43], and quantum systems at one-dimensional critical points [44, 45].

In spite of these developments no fully general organising principles for non-equilibrium states have been found. However, there has been recent success in developing a somewhat general approach describing non-equilibrium states through the LDP and hydrodynamics in combination, i.e. obtaining the rate function and/or SCGF within the hydrodynamic scaling limit. In some sense this brings this overview full circle as I stated at the start that the language of hydrodynamics has always played a prominent role in the study of non-equilibrium states. Arguably the most successful approach along these lines to date has been the macroscopic fluctuation theory (MFT) [46–48]. The MFT is based on a large deviation rate function of joint fluctuations of densities and currents in the Hydrodynamic-diffusive regime (see appendix B). It provides a general approach to calculate rate functions and the SCGF in classical stochastic systems that has reproduced known results as well as proving successful at obtaining new results [48].

In this thesis I move closer towards an organisational principle for non-equilibrium



systems through the development of the *Ballistic Fluctuation Formalism (BFF)* in chapter 3. Due to its reliance on diffusion, the MFT is not able to obtain information on the statistics of ballistically transported quantities i.e. quantities that do not diffuse while travelling through the system. This type of transport is of particular interest in a number of systems, especially quantum integrable systems which contain many (infinite) conserved charges and some classical lattice gasses. The BFF has been developed to provide a general approach for calculating the SCGF for ballistically transported quantities in the hydrodynamic limit of a system. Although similar in principle to the MFT, through the use of the LDP and hydrodynamics, in practice the BFF provides a very different approach based on hydrodynamics at the Euler scale - a scale which explicitly excludes diffusion. The BFF builds from ideas in fluctuating hydrodynamics [49, 50], a theory of hydrodynamic systems in the Euler limit (see section 3.1). Of particular importance, the BFF not only applies to quantum systems but, as I will show in chapters 4 and 6, it is applicable to classical stochastic systems that support ballistic transport. The application of the BFF to classical stochastic systems opens an interesting possible connection between the MFT and the BFF. The primary idea of the BFF is based on hydrodynamic equations of state and a basic knowledge of system correlations from which one can construct the SCGF of the transport of some statistical quantity. Armed with this new formalism I apply it to obtain new results in: classical lattice gasses; higher-dimensional conformal field theory which is a theory that describes quantum critical points; and most importantly, obtain a generally applicable and completely new formula for the SCGF of currents in classical and quantum integrable models. All three of these models are important within modern physics and the success of the BFF in unifying previously known results while obtaining new ones in this widely ranging set of systems provides evidence of the power of this formalism.

In chapter 2 I also provide a novel result which shows how, in a 1D conformal field theory, one can work backwards from knowledge of current and the existence of a fluctuation relation in order to obtain full knowledge of the SCGF of transported quantities. This provides completely new results in the context of these systems, unfortunately this approach is not easy to generalise. In particular this approach requires the assumption of chiral separation, which breaks down when considering non-critical systems that contain

interactions. In the attempt to obtain the SCGF for more general interacting models, the BFF was developed.

The thesis is structured as follows. In chapter 1, I introduce important basic ideas and tools used throughout the thesis such as the LDP, fluctuation relations and hydrodynamics. In chapter 2 I provide original but unpublished work in an attempt to define an organisational principle through the fluctuation relations and making use of chiral separation. Specifically, I obtain the statistics of the transport of conserved quantities in a one-dimensional conformal field theory. I introduce the existence of a classical structure underpinning this and expose the reader to a proposed relation, known as the extended fluctuation relation. In chapter 3 I present the BFF and explain certain ramifications of the theory, including a full treatment of the extended fluctuation relation. This chapter is based on work submitted for publication [51]. The remaining three chapters are applications of the BFF in three separate systems where the outcomes are analysed, given the BFF is a new formalism, most of the results of these chapters form original work both published and unpublished as of this point. In chapter 4 I show how the BFF is applied to a generalisation of the well-known lattice gas the *Totally Asymmetric Exclusion process* (TASEP) [52], where in the generalisation each particle takes up  $\ell$ -lattice sites. The  $\ell$ -TASEP [53], as it is known, provides a simple arena in which to elucidate many aspects of BFF, I also provide new results for fluctuations of the particle current when  $\ell > 1$  which is being written up for a journal submission. Chapter 5 is an application to a  $d$ -dimensional Conformal Field Theory (CFT). I not only obtain the SCGF for energy currents but also explore some of the results within the context of the fluctuation relations, which provides some interesting new insights. Most results in this chapter have been submitted for publication in [51], however some parts remain unpublished. The final chapter is, arguably, the most important outcome of the BFF in this thesis. In this chapter the BFF is used to obtain the SCGF of flows of conserved quantities in a general interacting 1D integrable model. The results obtained are applied to a classical system, the hard rods gas and the Lieb-Liniger model, a quantum model describing a 1D gas of Bosons with delta interactions. Analysis of these models is also provided. Most of the work in this chapter has been submitted for publication [54]. Finally, I present my conclusions and discuss potential outlooks for the BFF including potential future

applications, the addition of diffusive terms to the framework and ultimately links to the MFT which would go some way to developing a truly global organisational approach for non-equilibrium states.

## Chapter 1

# Foundational concepts

In this chapter I will expand on aspects of the introduction and discuss concepts that are necessary throughout this thesis. I will first address the specific type of non-equilibrium state considered in this thesis, the non-equilibrium steady state, and explain the partitioning protocol used to generate this (section 1.1). Then I undertake a more detailed exposé on Large Deviation Theory and associated concepts (section 1.2). I discuss the fluctuation relations in more detail, with specific focus on the Gallavotti-Cohen type used in this work and discuss the quantum fluctuation relations (section 1.3). I provide a brief introduction to the basic concepts of integrable systems and the associated Generalised Gibbs Ensemble as both of these appear across multiple chapters (section 1.4). Finally I introduce Euler-scale hydrodynamics, this theory plays a prominent role throughout this current work (section 1.5).

### 1.1 Non-equilibrium steady states

In the introduction I claimed, the key difference between equilibrium and non-equilibrium states is the effect of dynamics in the system. Specifically, as stated in [55], since equilibrium distributions are, by definition, stationary a theory for non-equilibrium requires an approach to deal with distributions varying in time. Reference [8] explains further that such a theory would require describing not only the stationary fluctuations of states but also the time-dependent fluctuating dynamics of the system as well as fluctuations of macrostates or observables integrated over time. It is this last type that is primarily considered in this thesis.

It is clear that the space of all possible non-equilibrium states is large and varied.

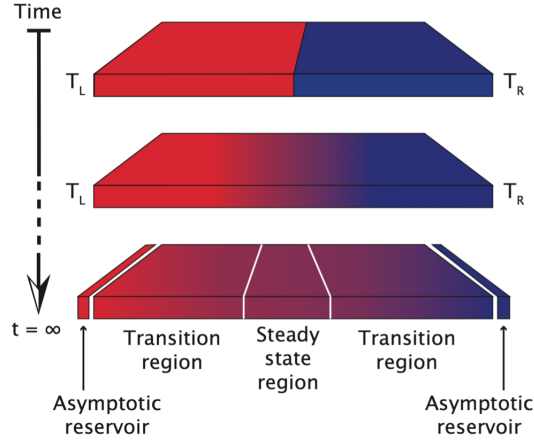


**Figure 1.1:** 3D representation of partitioning protocol for non-equilibrium steady states. At the initial time a system is comprised of two independently thermalised systems placed into contact with each other. After waiting a long time a growing steady state region is set up at the interface. This region is a non-equilibrium steady state.

To isolate non-equilibrium behaviour, the literature often turns to the ‘simplest’ type, non-equilibrium steady states (NESS), where these states are time-invariant but are not symmetric under time-reversal [56]. I will only consider states of the NESS type in this work.

A common way to generate an NESS is the partitioning protocol [57]. In this protocol one begins with a very large (infinite) system partitioned into two halves. Each half is independently thermalised to a different equilibrium state governed by independent Lagrange multipliers. At some time  $t = 0$  the two partitions are brought into contact with one another and the system is left to evolve for a very long time  $t \rightarrow \infty$ . At this very late time in system evolution an NESS exists at the junction of the two partitions (and within an increasing region around this junction). This state is fed by the reservoirs at the infinite edge of the two partitions that still remain in the original thermalised state, thus maintaining the non-equilibrium state. See figure 1.1 for clarity on this. I make use of the partitioning protocol often throughout this work. In hydrodynamics the problem of the partitioning protocol is known as the Riemann problem [58].

## 1.2 Large deviation theory - a study of fluctuations

As was explained in the introduction, large deviation theory (LDT) may provide the most natural language to describe statistical physics. However, large deviation theory

is more fundamental than this and is understood differently by different people. In the review, [34], it is stated that mathematicians understand LDT in a number of ways including: “A theory dealing with the exponential decay of the probabilities of large deviations in stochastic processes; A calculus of exponential-order measures based on the saddle-point approximation or Laplaces method; An extension of Cramér’s Theorem related to sample means of random variables; an extension or refinement of the Law of Large Numbers and Central Limit Theorem”. On the other hand, physicists understand the LDT as: An extension of Einstein’s fluctuation theory; A framework allowing for the calculation of entropies and free energies; A more formal formulation of statistical mechanics. Although [34] goes on to say that the LDT is all these things, for the purposes of this work the LDT can be understood as a fundamental re-writing of statistical physics which allows for generalisations that go beyond equilibrium.

### 1.2.1 Large deviation principle

The LDT is based on the large deviation principle (LDP) which states that the probability that some fluctuating quantity  $J^{(t)}$  takes the value  $tj$  is given by [34]:

$$\mathbb{P}(J^{(t)} = tj) \asymp e^{-tI(j)}, \quad (1.1)$$

where  $I(j)$  is known as the rate function and  $t$  can represent any quantity that the system scales with where in this work I only consider  $t$  to be time. The object  $\asymp$  signifies equality relationship on a logarithmic scale i.e. for two extensive quantities  $a_t, b_t$  then,  $a_t \asymp b_t \implies \lim_{t \rightarrow \infty} 1/t \log a_t = \lim_{t \rightarrow \infty} 1/t \log b_t$ . In the LDT the rate function becomes a central object in the theory. Knowing this object defines long-time fluctuations of the stochastic variable of interest. The rate function has two important properties, firstly  $\exists \bar{j}$  such that  $I(\bar{j}) = 0$  and if  $j \neq \bar{j}$ ,  $I(j) > 0$ . Thus, in the long-time limit there is an almost certain value of  $J^{(t)}/t$  and fluctuations around this value are suppressed as  $t \rightarrow \infty$ . This is why the rate function becomes such an important quantity, it describes the scaling of the fluctuations for some quantity. In fact, as will be shown in section 1.2.3 below, the rate function can be shown to be equivalent to the entropy in statistical mechanics.

There are a number of follow-on points. First, the exponent in (1.1) can scale with any power of  $t$ , which represents the system scaling. In all instances in this work the

exponent is 1. Secondly, the large  $t$  limit is important and can be understood as taking a thermodynamic limit in appropriate circumstances. Thirdly, and most importantly, not all systems are governed by a large deviation principle - although I will only consider those that are.

There are numerous types of quantities that can be described by LDT. Of particular interest in this work are time integrated currents,  $J^{(t)} = \int_0^t ds j(x, s)$ , in NESSs. Clearly this quantity is extensive in time and it represents transport in a system. The fact this quantity is extensive is precisely the need for taking a scaling limit.

### 1.2.2 Scaled cumulant generating function

Taking a Legendre transform of the rate function provides the central object for the purposes of this work, the scaled cumulant generating function (SCGF). To gain some sense of the importance of this object I refer to applications of the LDT to statistical physics. In statistical physics the Legendre transform of entropy is the specific free energy of the system. Similarly the Legendre-Fenchel transform of the rate function produces the SCGF ( $F$ ), an object that acts as a generalised free energy [34];

$$F(\lambda) = \sup_j \{\lambda j - I(j)\}, \quad (1.2)$$

where this may also be written more explicitly as a cumulant generating functional,

$$F(\lambda) = \lim_{t \rightarrow \infty} t^{-1} \log \left\langle e^{\lambda J^{(t)}} \right\rangle. \quad (1.3)$$

From (1.2), clearly  $\lambda$  is the conjugate parameter to  $j$  and as such will be referred to as the conjugate parameter of the SCGF. It is of particular importance to state that the SCGF can also be expressed as a infinite series of cumulants where each cumulant is scaled by  $t$  i.e.

$$F(\lambda) = \sum_{n=1}^{\infty} \frac{\lambda^n}{n!} c_n, \quad c_n = \lim_{t \rightarrow \infty} t^{-1} \left\langle (J^{(t)})^n \right\rangle^c. \quad (1.4)$$

The averages used are under the same probability measure used in the definition of the rate function through the large deviation principle and the superscript  $c$  denotes connected correlation functions.

Importantly, as a consequence of the LDP,  $F(\lambda)$  must be a convex function and from (1.4), the correct normalisation requires  $F(0) = 0$ . It can be used to determine cumulants of a fluctuating quantity, and it clearly encodes the large time limit probability distribution of the quantity through the rate function. It has the additional very important property of indicating the existence of dynamical phase transitions. Dynamical phase transitions are understood as analogous to usual, equilibrium, phase transitions. However, the non-equilibrium variety are expected to be even more diverse as they involve dynamics as an extra degree of freedom [59]. Simply stated these are phenomena in a non-equilibrium system where one obtains fundamentally different fluctuations in the system after altering of some quantity in some phase space of the system. Interestingly the phenomena of quantum dynamical phase transitions are also expected and have been theoretically predicted [60]. In analogy to equilibrium states, where discontinuities in the free energy indicate phase transitions, discontinuities in the SCGF are also proposed to mark dynamical phase transitions [61]. This particular property of the SCGF will provide many discussion points throughout chapters 3 and 4.

### 1.2.3 Application to equilibrium statistical mechanics

One can understand the rate function as the negative of entropy in a heuristic fashion as follows. Consider the macrostate of some statistical system. A higher number of microstates associated with the macrostate is equivalent to that macrostate having larger entropy. Given that a macrostate with more associated microstates is more likely to be observed in experiment, greater entropy of a macrostate can be associated with greater probability of observing that macrostate. Now consider the rate function, it governs the probability of macrostates in the system. Since a smaller value of a rate function corresponds to a higher probability of the macrostate, one can see that the rate function has the opposite behaviour to entropy which leads to the heuristic argument that the rate function is the negative of the entropy.

To place the above argument on a more solid foundation, I apply the LDT to equilibrium statistical physics. This section closely follows work appearing in [34].

Consider a closed system comprised of  $n$  particles. In such a system a microstate is defined by the state of the  $n$  particles where the microstate is written as  $\omega = (\omega_1, \omega_2, \dots, \omega_n)$  where the state of particle  $i$  is  $\omega_i$ . The set of all possible micro-states



is given by  $\Lambda^n$ . It is also possible to construct an energy function i.e. the Hamiltonian,  $H_n(\omega)$ , where the average energy per particle is defined by  $h_n(\omega) = H_n(\omega)/n$ . Consider the probability of the average energy per particle being in a given range  $du = [u, u + du]$  which is obtained from the probability distribution of the microstates,  $\mathbb{P}(d\omega)$  via

$$\mathbb{P}(h_n \in du) = \int_{\omega \in \Lambda^n: h_n(\omega) \in du} \mathbb{P}(d\omega), \quad (1.5)$$

where one integrates over the set of all micro-states  $\Lambda^n$  such that the  $h_n(\omega)$  is contained in the given range. In the microcanonical ensemble it can be assumed that all microstates are equally likely. This results in  $\mathbb{P}(d\omega) = d\omega/|\Lambda^n|$  where  $|\Lambda^n|$  is the size of the set of possible microstates. This is inserted into the above such that

$$\mathbb{P}(h_n \in du) = \frac{1}{|\Lambda^n|} \int_{\omega \in \Lambda^n: h_n(\omega) \in du} d\omega. \quad (1.6)$$

With this one uses (1.1) to find an expression for the rate function in terms of the probability distribution. This leads to

$$I(u) = \lim_{n \rightarrow \infty} -\frac{1}{n} \log \mathbb{P}(h_n \in du) \quad (1.7)$$

$$= \log |\Lambda| - s(u). \quad (1.8)$$

where  $s(u) = \lim_{n \rightarrow \infty} -\frac{1}{n} \log \int_{\omega \in \Lambda^n: h_n(\omega) \in du} d\omega$ . One can recognize  $\int_{\omega \in \Lambda^n: h_n(\omega) \in du} d\omega$  as the total number of microstates in the macrostate and thus  $s(u)$  is the entropy density. This results in the rate function as being identified with entropy up to some constant factor and up to a sign. The extra factor can be absorbed leaving the rate function as the negative of entropy.

To identify the relationship between the SCGF and free energy recall that free energy is the Legendre-Fenchel transform of entropy<sup>1</sup>. Then recall that by definition the SCGF is the Legendre-Fenchel transform of the rate function. Thus from the relationship between entropy and the rate function, this identifies the SCGF as negative free energy of the system up to some constant. Thus, I have shown that in equilibrium, the rate function corresponds to entropy and the SCGF to the free energy of the system.

---

<sup>1</sup>Although uncommon language in physics the usual Legendre transform is equivalent the Legendre-Fenchel used in the LDT community

### 1.2.4 Quantum large deviations

When one turns to quantum systems further care must be taken. This is primarily due to difficulties that can arise from considering quantum fluctuations related to quantum measurement [27]. In this work I consider time integrals of fluctuating quantities, usually energy or particle number. Physically measuring these in principle requires multiple measurements at different times of the system dynamics as the integral is a sum of values at different times. The problem is that the act of measuring a quantum system collapses the wave function, thus taking multiple samples of the quantum trajectory ultimately affects its nature through measurement. Fortunately, there are ways around this issue. Specifically, as introduced in [27], instead of considering time integrated quantities one can consider two-time measurements. In this case one determines the time integrated quantity by first measuring the quantity at some initial time then allowing the system to evolve and ultimately measuring the quantity at some final time where the difference of these is equivalent to the time integrated quantity. Each of these two measurements is valid and the system trajectory is evolved via quantum dynamics; i.e. the system remains undisturbed by any observer, avoiding collapse of the wave-function, during the period of interest [27]. This approach was proposed in [27] in order to determine the statistics of work performed on a quantum system. Through this process one can construct LDT results as obtained above. It is also possible to consider indirect measurements of the system whereby the system is weakly coupled to a probe on which the direct measurements are made [39]. Both procedures produce results that mirror the form found in usual classical LDT. Thus, I will assume that the LDT holds in a meaningful sense in quantum systems with the understanding that one of the two procedures described above is used to obtain physically relevant quantities.

## 1.3 Fluctuation relations

This section provides a more detailed exposé on the fluctuation relations (FRs) discussed in the introduction. I will begin with a discussion about the meaning and importance of these relations, followed by a derivation of an FR for a quantum system. Finally, I will expose the relationship between the large deviation principle and fluctuation relation of the Gallavotti-Cohen type which is used often throughout this work.

### 1.3.1 Meaning and importance

To facilitate discussion, I consider the archetypical example of a colloidal particle in a periodic potential driven by a non-conservative force interacting with a noisy environment [23]. I begin by defining  $\mathbb{P}_F(x)$  as probability of the particle following a particular forward trajectory  $x$  starting with the particle in equilibrium with its environment. I assume this trajectory is obtained via some driving force resulting in the process being time irreversible and thus a non-equilibrium process. Importantly it is assumed that this process is both Markovian and microscopically reversible which means each time step along the trajectory only depends on the previous step and each time step itself follows detailed balance [1]. Note that although each step satisfies detailed balance, the full trajectory remains time irreversible due to the driving force. At the end of the process the particle again equilibrates with its environment. Conversely, one defines  $\mathbb{P}_R(x)$  as the probability of a ‘backward trajectory’ where the particle starts at the end state of the previous trajectory and is governed by a reversed driving force. As the particle exists within a noisy environment both trajectories are stochastic. Then considering the probability of the work done moving from the initial state to the final state one obtains the Crooks’ relation as presented in the introduction [26],

$$\frac{\mathbb{P}_F(w)}{\mathbb{P}_R(-w)} = e^{\beta(w-\Delta F)}. \quad (1.9)$$

where  $w$  is the work done during the forward trajectory and  $\Delta F$  is the change in free energy between the start and end states. This expression provides a relationship between the probabilities of the forward trajectory and the reverse trajectory where the equilibrium scenario is obtained when  $\mathbb{P}_F(w) = \mathbb{P}_R(-w)$ , which is a statement about the system reversibility. Specifically, the Crooks’ relation encodes information about a non-equilibrium transformation on the system i.e. the system moves through a non-equilibrium state. This type of relation has vital ramifications for the study of non-equilibrium states as it provides a specific signature of such states. Specifically, the exponent in the Crooks’ relation is related to entropy production in the system, indicating a non-equilibrium state [23]. The Crooks relation has been used in experiments in order to obtain free energy landscapes of complex chemical molecules [62]. It has also been generalised to a form known as a detailed fluctuation relation which shows

the exponent is related to entropy production, again providing a consistent view with the understanding of a non-equilibrium system.

This relation has been generalised for stochastic processes and even found for quantum systems, as is detailed in the next section. In general, if one considers the ratio of a forward and backward trajectory of a system, the system is then said to satisfy a detailed fluctuation relation for some stochastic variable  $\mathcal{X}$  if,

$$\frac{\mathbb{P}_F(\mathcal{X} = x)}{\mathbb{P}_R(\mathcal{X} = -x)} = e^{vx}, \quad (1.10)$$

where  $x$  is some value the stochastic variable takes and  $v$  is some constant. From this expression one expects there to exist a relationship with the Large Deviation Theory, this is discussed further below. Before introducing the Gallavotti-Cohen type fluctuation relation used in this thesis, I first show how one goes about finding a detailed fluctuation relation for a quantum system.

### 1.3.2 Quantum fluctuation relations

Due to the difficulties with quantum systems, as mentioned in section 1.2.4 on quantum LDT, one must take care dealing with the measurement issues for quantum FRs. For what follows, I assume the two-measurement protocol, explained in section 1.2.4, where transport of some observable is found by measuring it at some initial time and at some final time and then using their difference to determine the transport. This protocol has been experimentally verified to produce results consistent with fluctuation relations [63]. In this section I produce a general expression for a quantum detailed fluctuation relation and use this general expression to obtain a quantum Crooks' relation. The results of this section are based on work in [64], which provides a fantastic review of quantum fluctuation relations.

Begin by considering a quantum observable,  $\hat{A}$ . This observable is measured at  $t_0$  and  $t$  where the outcomes of these measurements are  $a_0$  and  $a_t$  respectively. With this the joint probability of measuring  $(a_t, a_0)$  is,

$$\mathbb{P}(a_t, a_0) = \text{Tr} \left\{ \hat{P}_{a_t} \hat{U}(t, 0) \hat{P}_{a_0} \hat{\rho}_0 \hat{P}_{a_0} \hat{U}^\dagger(t, 0) \hat{P}_{a_t} \right\}, \quad (1.11)$$

where  $\hat{P}_a = |a\rangle\langle a|$  is a projection operator,  $\hat{U}(t, 0)$  is the usual quantum evolution oper-

ator and  $\hat{\rho}_0$  is the initial density matrix. The normalisation of  $\mathbb{P}(a_t, a_0)$  can be verified. From here one uses the definition of the projection operator,  $\langle a | \mathcal{O} | a \rangle$  is a number and by definition of complete states  $\text{Tr} \{ |a\rangle \langle a| \} = 1$ . This gives,

$$\mathbb{P}(a_t, a_0) = |\langle a_t | \hat{U}(t, x) | a_0 \rangle|^2 \langle a_0 | \hat{\rho}_0 | a_0 \rangle. \quad (1.12)$$

Now consider the same quantity except in the time reversed case. This means the system is evolved from the final density matrix  $\hat{\rho}_t$  back to a new initial density matrix under a reversed evolution operator. Due to the statistical nature of the dynamics the new initial density matrix is not expected to be the same as the old one. Thus, one considers:

$$\mathbb{P}^{\text{tr}}(a_t, a_0) = \text{Tr} \left\{ \hat{P}_{a_0} \hat{U}^\dagger(t, 0) \hat{P}_{a_t} \hat{\rho}_0^{\text{tr}} \hat{P}_{a_t} \hat{U}(t, 0) \hat{P}_{a_0} \right\}, \quad (1.13)$$

where  $\hat{\rho}_0^{\text{tr}} = \hat{U}(t, 0) \hat{\rho}_0 \hat{U}^\dagger(t, 0)$  and ‘tr’ stands for time-reversed. From here it is simple to show

$$\mathbb{P}^{\text{tr}}(a_t, a_0) = |\langle a_t | \hat{U}(t, x) | a_0 \rangle|^2 \langle a_t | \hat{\rho}_0^{\text{tr}} | a_t \rangle. \quad (1.14)$$

To show the FRs are satisfied I consider the log ratio between the forward and reverse expressions, where in a classical system this ratio is related to the irreversible contribution to a change in entropy. Calling this ratio  $R$  one finds:

$$R(a_t, a_0) = \log \frac{\mathbb{P}(a_t, a_0)}{\mathbb{P}^{\text{tr}}(a_t, a_0)} = \log \frac{\langle a_0 | \hat{\rho}_0 | a_0 \rangle}{\langle a_t | \hat{\rho}_0^{\text{tr}} | a_t \rangle}. \quad (1.15)$$

To get the fluctuation relation I define the probability distributions,

$$\mathbb{P}(R) = \sum_{a_t, a_0} \mathbb{P}(a_t, a_0) \delta(R - R(a_t, a_0)) \quad (1.16)$$

$$\mathbb{P}^{\text{tr}}(R) = \sum_{a_t, a_0} \mathbb{P}^{\text{tr}}(a_t, a_0) \delta(R - R^{\text{tr}}(a_t, a_0)), \quad (1.17)$$

where  $R^{\text{tr}}(a_t, a_0) \equiv \log \frac{\mathbb{P}^{\text{tr}}(a_t, a_0)}{\mathbb{P}(a_t, a_0)}$ . Note that the definition of  $R$  and  $R^{\text{tr}}$  means  $R^{\text{tr}}(a_t, a_0) =$

$-R(a_t, a_0)$ . Putting this together the detailed FR is obtained in a quantum system,

$$\begin{aligned}
\mathbb{P}(R) &= \sum_{a_t, a_0} \mathbb{P}(a_t, a_0) \delta(R - R(a_t, a_0)) \\
&= \sum_{a_t, a_0} e^{R(a_t, a_0)} \mathbb{P}^{\text{tr}}(a_t, a_0) \delta(R - R(a_t, a_0)) \\
&= e^R \sum_{a_t, a_0} \mathbb{P}^{\text{tr}}(a_t, a_0) \delta(R - R(a_t, a_0)) \\
&= e^R \sum_{a_t, a_0} \mathbb{P}^{\text{tr}}(a_t, a_0) \delta(R + R^{\text{tr}}(a_t, a_0)) \\
&= e^R \mathbb{P}^{\text{tr}}(-R),
\end{aligned} \tag{1.18}$$

where in the first line is obtained using (1.15), the second line is obtained by definition of the  $\delta$ -function, the third from  $R^{\text{tr}} = -R$  and the last is simply the definition from (1.17). This is consistent with the statement of FRs, (1.10).

To give this meaning I show how the above is used to determine a quantum Crooks' relation. In analogy with the classical case consider the Gibbs states,

$$\hat{\rho}_0 = \frac{e^{-\beta \hat{H}(0)}}{Z(0)}, \quad \hat{\rho}_0^{\text{tr}} = \frac{e^{-\beta \hat{H}(t)}}{Z(t)} \tag{1.19}$$

where  $Z(t) = \text{Tr} e^{-\beta \hat{H}(t)}$ ,  $\hat{H}$  is the Hamiltonian, and  $\beta$  the inverse temperature. In this case  $a_t$  and  $a_0$  in (1.12) and (1.14) are measured values of the Hamiltonian and can be interpreted as the energy of the system  $E_t$  measured at time  $t$  and  $E_0$  at time 0. Furthermore, as this is considered to be an isolated system there is no environment with which to exchange heat. Thus, the change in the system energy can be interpreted as work done by some driving force to get the system from the the initial to the final state i.e.

$$w = E_t - E_0. \tag{1.20}$$

There also exists some change in free energy defined by,

$$\Delta F(t) = -\beta^{-1} \log Z(t) + \beta^{-1} \log Z(0). \tag{1.21}$$

With the above it is clear that (1.15) becomes,

$$R(E_t, E_0) = \beta(w - \Delta F(t)). \quad (1.22)$$

Then using the fact that  $\Delta F(t)$  is not stochastic, one can insert the above into (1.18) to obtain.

$$\frac{\mathbb{P}(w)}{\mathbb{P}(-w)} = e^{\beta(w - \Delta F)}. \quad (1.23)$$

This is precisely the expression for the Crooks' relation however it was obtained via a two-measurement protocol for a quantum system.

### 1.3.3 Gallavotti-Cohen relations from LDT

In the introduction two types of FRs were discussed, the Crooks' relation which I have shown is a specific example of a detailed fluctuation relation and the Jarzynski equality which in general is known as an integrated fluctuation theorem [23]. Another form of the FRs is the Gallavotti-Cohen relation [22] where this form will be used at multiple places throughout this work. This were historically the first form of the FRs and can be presented as a symmetry on the SCGF. This form is obtained through the Large Deviation Principle thus showing the consistency of the LDP within the context of fluctuation relations.

Whereas the relation (1.10) holds in a very general setting, the Gallavotti-Cohen relations hold for systems in large scaling limits, in this thesis large time, for NESSs. Specifically [22] found that in the large time limit of some NESS there exists a relation for an extensive quantity  $\mathcal{X}_t$  which may be written as,

$$\lim_{t \rightarrow \infty} \frac{1}{t} \log \frac{\mathbb{P}_F(\mathcal{X}_t = xt)}{\mathbb{P}_R(\mathcal{X}_t = -xt)} = vx. \quad (1.24)$$

It is clear this expression is the long-time form of (1.10). Then if the LDP holds it is easy to show the above expression results in a symmetry on the SCGF. Assume that  $\mathbb{P}_F$  and  $\mathbb{P}_R$  satisfy LDPs, i.e.  $\mathbb{P}_F(\mathcal{X}_t = xt) \asymp e^{-tI(x)}$  and similarly  $\mathbb{P}_R(\mathcal{X}_t = -xt) \asymp e^{-tI(-x)}$ .

Inserting this into (1.24) gives [34]

$$I(-j) - I(j) = \nu j, \quad (1.25)$$

where  $\nu$  is the constant defined by the FR in (1.10). From (1.2), the Legendre-Fenchel transform of  $I(\lambda)$  is  $F(\lambda)$ . It can be shown that the Legendre-Fenchel transform of  $(I(-x) - \nu x)$  is  $F(-\lambda - \nu)$ . Thus, by transforming both sides of the above expression,

$$F(\lambda) = F(-\lambda - \nu). \quad (1.26)$$

This is the expression of the Gallavotti-Cohen fluctuation relations represented as a symmetry on  $F(\lambda)$ . This will prove to be useful as the existence of this symmetry can be used to ensure that many of the SCGFs obtained throughout this thesis are consistent with one of the very few general relations satisfied by non-equilibrium systems.

Recall that I largely focus on NESS generated by the partitioning protocol. Throughout this current work I will consider the scenario where in the NESS, both the dynamics and some conserved charge of interest,  $Q$ , are time-reversal invariant. Then if the partitioning protocol is constructed such that the initial state has an imbalance in  $Q$  only and satisfies (1.10), then in the long-time limit (1.26) is expected to hold with  $\nu = \beta_l - \beta_r$  [64–66] where  $\beta_l$  and  $\beta_r$  are the initial temperatures of the partitioning protocol. This can be seen using the results of the previous section on quantum FRs. The partitioning protocol assumes two partitions defined by Gibbs states,  $\rho_l = e^{-\beta_l \hat{Q}_l}$ ,  $\rho_r = e^{-\beta_r \hat{Q}_r}$  where  $\hat{Q}|Q\rangle = Q|Q\rangle$  and  $Q$  is a conserved quantity. One then considers an exchange occurs between the two partitions through the system of interest where this system is weakly coupled to the partitions. Thus, as was done in (1.19) I define the initial density matrices,

$$\hat{\rho}_0 = \hat{\rho}_0^{\text{tr}} = e^{-\beta_r \hat{Q}_r} e^{-\beta_l \hat{Q}_l} e^{-\beta_s \hat{Q}_s}, \quad (1.27)$$

where  $\beta_s$  is some parameter that describes the state of the system. Working through the



appropriate expressions it is clear from (1.15) that,

$$R(t, 0) = -\beta_r(Q_r^t - Q_r^0) - \beta_l(Q_l^t - Q_l^0) - \beta_s(Q_s^t - Q_s^0). \quad (1.28)$$

However, in this case, the system is considered to be weakly interacting with the partitions and conservation laws imply that changes in one system result in opposite changes in the other system such that,

$$Q_r^t - Q_r^0 \approx -(Q_l^t - Q_l^0) - (Q_s^t - Q_s^0). \quad (1.29)$$

Furthermore, recall that the partitions are assumed to be infinitely large. Since the system remains much smaller the possible change in energy  $Q_s^t - Q_s^0$  is much smaller than in the partitions. Thus, in the long time limit this change in energy is dominated by the two infinitely large partitions. Combining the above expression with this fact in the long-time limit, results in  $R(t, 0) \approx (\beta_l - \beta_r)(Q_r^t - Q_r^0)$ . Finally since  $(Q_r^t - Q_r^0)$  represents the current of interest in the partitioning protocol, one uses (1.18). The resulting expression shows this system satisfies a fluctuation relation, (1.10), where  $v = (\beta_l - \beta_r)$ . Thus using (1.26) I find the Gallavotti-Cohen fluctuation relation in the partitioning protocol satisfies,

$$F(\lambda) = F(-\lambda - (\beta_l - \beta_r)). \quad (1.30)$$

## 1.4 Integrability and large numbers of conserved charges

This section introduces quantum integrable systems in 1D. As was explained in the introduction, quantum integrable systems are of utmost importance for quantum systems in general. Due to special properties of integrable systems, one can obtain full solutions for these systems through general techniques where it is either very difficult or often impossible to find solutions for a general quantum system. This provides fundamental insights into the nature of quantum systems as a whole. In this section I also introduce an important generalisation of the usual Gibbs probability distribution, the *Generalised*

*Gibbs Ensemble (GGE)* where one takes into account the maximal entropy state of a system when it contains infinitely many conserved charges. In the next section distributions of the GGE type will become of particular importance.

### 1.4.1 Integrable systems

The length of this section cannot do justice to the richness and volume of research done on integrable systems, the only purpose is to provide a very brief introduction to quantum integrable systems and provide the background for the two important properties I make use of in this thesis.

Integrable models are of a large and rich variety that come in both classical and quantum flavours. The case of classical integrability is much older and very clearly defined thanks to Liouville so I start here and extend into quantum systems. Given a system Hamiltonian  $H$ , conserved quantities  $F_i$  are known to satisfy:

$$\frac{d}{dt}F_i = -\{H, F_i\} = 0, \quad (1.31)$$

where  $\{\cdot, \cdot\}$  are Poisson brackets and I have used the well-known equations of motion. These quantities are also known as integrals of motion. One can then define a classically integrable system as that which has as many integrals of motions  $F_i$  as there are degrees of freedom. Furthermore if the  $F_i$  are independent and everywhere differentiable with the further constraint that  $\{F_j, F_k\} = 0$  it is known as Liouville integrable [67].

In contrast to the clear definition of classical integrability, a precise statement of quantum integrability is not yet widely agreed upon [68]. Naively one would think that quantum integrability can be defined by the existence of a maximal set of independent commuting quantum operators with one conserved charge for each quantised degree of freedom, however this is trivially shown to be false. By the spectral theorem, all Hermitian Hamiltonians are diagonalizable. Thus, it is possible to construct a maximal set of commuting operators from the orthogonal state vectors of the Hamiltonian. This would mean all quantum systems can be considered integrable, clearly a false statement. Reference [68] goes on to present and reject further definitions used in the literature and finally arrives at a fairly technical definition for quantum integrability. What [68] refers to as ‘linear quantum integrable’ will be used as the definition of quantum integrability

in this current work since all integrable models considered are explicitly of this type.

To circumvent the issue of ‘too many’ conserved charges one turns to the concept of locality which requires using only those charges that are in some sense bounded. Given a conserved charge  $Q_i = \int dx q_i(x)$  where  $q_i(x)$  is a charge density and a Hamiltonian density  $h_i(y)$ , one states that  $Q_i$  is locally conserved if the charge density and Hamiltonian density commute i.e.  $[q_i(x), h(y)] = 0$  for  $x \neq y$ . Linear quantum integrable models are those models which have an infinite set of such locally conserved charges that commute with each other. Importantly the system is also required to be an extended 1D system.

An important consequence of an infinite set of locally conserved charges in 1D extended system is the curious behaviour of the scattering matrix (or  $S$ -matrix) that encodes interactions in the system. In such situations it is possible to show that the  $S$ -matrix can be written as the product of two particle scattering events [69]. This is an enormous simplification as an  $n$ -particle scattering event can be understood as comprised of only two-particle interactions [70].

In summary, the two important properties of quantum integrable systems used are the existence of the multiple local conserved charges and the factorization of the scattering matrix.

### 1.4.2 Generalised Gibbs Ensemble

In statistical mechanics one derives the Gibbs ensemble by maximising the entropy with respect to the energy which remains conserved and thus forms a system constraint. The Lagrange multiplier from this maximisation process is the inverse temperature of the system. However, as has been stated above, in an integrable model one has an infinite set of conserved quantities. In 1957 Jaynes [71, 72] showed how to define the maximal entropy for states comprised of multiple conserved charges. The full generalisation to a generalised Gibbs ensemble (GGE), which considers the case of infinite conserved charges and the physical ramifications in the context of integrability was presented in [73]. The end result is a density matrix of the following form:

$$\rho_{\text{GGE}} = e^{-\sum_i \beta^{(i)} Q_i} / \text{Tr}(e^{-\sum_i \beta^{(i)} Q_i}). \quad (1.32)$$

where  $\beta^i$  are Lagrange multipliers with index  $i$ , corresponding to the conserved charges  $Q_i$  where if  $Q_j$  is energy,  $\beta^j$  corresponds to inverse temperature. This is by no means a trivial statement with many issues arising related to the infinite series in the exponent. Further complications have also arisen as even with all locally conserved charges accounted for, such states may still be unsuccessful at describing thermalization after a quantum quench [74, 75], i.e. these states do not maximise the entropy. In such circumstances the infinite series in the exponent is expanded to include charges that are not fully locally but only quasi-local [76]. The ramifications of the existence of quasi-local charges is discussed in greater detail in section 3.1.1. The GGE has now been confirmed as the correct and natural distribution to use for a relaxed integrable system in many different contexts [77]. The GGE thus forms an important base when discussing integrable models in statistical contexts.

## 1.5 Basics of Euler hydrodynamics

In this section I introduce the basics of Euler hydrodynamics given the presence of many (including infinitely many) conserved charges. This generalisation is necessary for the introduction of hydrodynamics applied to integrable systems, although that is left for chapter 6. The primary result of this section, the derivation of the Euler hydrodynamic equations closely follows [78].

Hydrodynamics is concerned with the large space-time scaling limit where there is a significant reduction in the system's degrees of freedom. In the hydrodynamic limit one can consider the system to be comprised of local cells, called fluid cells. Since this limit is concerned with large space and large time scales each local cell is described by an equilibrium state or more generally, a state in which entropy is maximised called a maximal entropy state. In this sense a Hydrodynamic state can be understood as one in which all local fluid cells are in maximal entropy states. From statistical mechanics, maximal entropy states are known to be defined by the conserved quantities of the system,  $\{Q_i\}$ . Thus, the hydrodynamic limit is a way of describing the system through only its conserved quantities, this is the basis of the reduction in degrees of freedom and is a fundamental postulate of hydrodynamics. This property also leads to hydrodynamics being a powerful approach to describing systems out of equilibrium. As the only concern is local entropy maximisation, the system is not constrained globally, and one can

consider the transport of a quantity through such a system as long as the scale of this variation is very big compared to the scale of the individual fluid cell. The size of these fluid cells is determined by the expansion introduced in (1.37) below.

Seeing as conserved quantities are the building blocks of hydrodynamics, the fundamental hydrodynamic equations are based on the conservation laws. Given a conserved density  $q_i(x, t)$ , defined by  $Q_i = \int dx q_i(x, t)$ , conservation laws define the relationship between  $q_i(x, t)$  and a corresponding current density  $j_i(x, t)$  via:

$$\partial_t q_i(x, t) + \partial_x j_i(x, t) = 0, \quad (1.33)$$

As these are statistical in nature one is interested in expectation values of these quantities. These expectation values are defined by the local fluid cell's maximal entropy state. In general, the density matrix for these states are defined by a distribution  $\exp(-\sum_i \beta^i Q_i)$  where  $\beta^i$  are the Lagrange multipliers corresponding to the conserved charge  $Q_i$ . An example of such a state is the usual Gibbs state or a GGE as defined in the previous section. For ease of notation I define  $q_i(x, t) \equiv \langle q_i(x, t) \rangle_{\underline{\beta}}$ ,  $j_i(x, t) \equiv \langle j_i(x, t) \rangle_{\underline{\beta}}$  where  $\underline{\beta}$  is a vector of all the  $\beta^i$  that define the state. Given that behaviour is considered only at large scale i.e. much bigger than the fluid cells, system dynamics only concern expectation values of the conserved charges and currents where these are related by the conservation laws as,

$$\partial_t q_i(x, t) + \partial_x j_i(x, t) = 0, \quad (1.34)$$

This equation is of importance on recalling the fundamental postulate of hydrodynamics, introduced above, which states that a system can be described through the conserved quantities  $q$ . Formally the expectation values of some quantity  $\mathcal{O}$  can be written,

$$\langle \mathcal{O}(x, t) \rangle = F[q_{\bullet}(\bullet, t)](x, t), \quad (1.35)$$

where  $F$  is some functional and  $\bullet$  refers to the set of all possible values. In words at some time slice  $t$ , any expectation value can be written in terms of the set  $\{q_i(x, t)\}$  for all  $x$  and all conserved charges. Clearly this holds true for  $j$  too which means one can rewrite

(1.34) as,

$$\partial_t q_i(x, t) + \partial_x F_i^{(j)}[q_\bullet(\bullet, t)](x, t) = 0, \quad (1.36)$$

with  $F_i^{(j)}$  some functional such that  $j_i(x, t) = F_i^{(j)}[q_\bullet(\bullet, t)](x, t)$ . If one can solve the above equation for  $q$ , then through (1.35) any expectation value can be constructed exactly. Thus, solving this dynamical equation is the primary focus in hydrodynamics. In general, this is impossible to solve so one considers an appropriate expansion of  $F_i$ . Since entropy maximisation only occurs within local fluid cells when variation lengths are large, the local variations of  $F_i$  are expected to be very small, this allows one to express this in a derivative expansion [78],

$$\begin{aligned} j_i(x, t) &= F_i^{(j)}[q_\bullet(\bullet, t)](x, t) \\ &= \mathcal{F}_i(q_\bullet(x, t)) - \frac{1}{2} \sum_{j \in \mathcal{J}} \mathcal{D}_i^j(q_\bullet(x, t)) \partial_x q_j(x, t) + \mathcal{O}(\partial_x^2 q_j(x, t)). \end{aligned} \quad (1.37)$$

Inserting the above expression back into (1.34) provides the equations of hydrodynamics. To first order one obtains the Euler equation for Hydrodynamics, to second order the celebrated Navier-Stokes equations are obtained. This also provides the determining factor in the size of fluid cells, the variations between cells must be small enough such that the derivative expansion above holds. This work will focus on the Euler-scale hydrodynamic equations which in the rest of the thesis I will consider  $j_i(q)(x, t) = \mathcal{F}_i(q_\bullet(x, t))$ . With this definition of the current at Euler scale one obtains the Euler hydrodynamic equations as,

$$\partial_t q_i(x, t) + \partial_x \mathcal{F}_i(q_\bullet(x, t)) = 0, \quad (1.38)$$

where this can be written in a quasi-linear form by defining a matrix known as the flux Jacobian,

$$A_i^j(x, t) = \frac{\partial j_i(q)(x, t)}{\partial q_j(x, t)} = \frac{\partial \mathcal{F}_i(q_\bullet(x, t))}{\partial q_j(x, t)}. \quad (1.39)$$

Then using the chain rule in (1.38) leads to the quasi-linear Euler hydrodynamic equa-

tion,

$$\partial_t q_i(x, t) + \sum_j A_i^j \partial_x q_j(x, t) = 0. \quad (1.40)$$

This equation forms the basis of Euler scale hydrodynamics. It is a non-linear equation which supports ballistic transport but not diffusion. This also introduces  $A_i^j$  as an important component of hydrodynamic theory that will be discussed in far greater detail in chapter 3.

In the above I explained that hydrodynamics requires variations that are on a much larger scale than the fluid cells. In fact, for correlations on the Euler scale there is a more precise way to define this. What follows is based on [79]. Consider the expectation value of some operator under some  $\underline{\beta}$  at some initial time  $t = 0$  for convenience. Expectation values of each local observable are dependent only on the local cell which itself is defined by its set of  $\underline{\beta}$ . This leads to the observation that  $\langle \mathcal{O}(x, t) \rangle_{\underline{\beta}} = \langle \mathcal{O} \rangle_{\underline{\beta}(\underline{x}, 0)}$  i.e. in the Euler scale of the system the space-time dependence of expectation values can be defined by the local state. Then one can introduce a scaling parameter  $v$  for the  $\beta^i(x, 0)$  such that,

$$\langle \mathcal{O} \rangle_{\underline{\beta}, v} = \frac{\text{Tr} e^{-\int dx \sum_i \beta^i(v^{-1}x, 0) q_i(x)} \mathcal{O}}{\text{Tr} e^{-\int dx \sum_i \beta^i(v^{-1}x, 0) q_i(x)}}. \quad (1.41)$$

The  $v$  scaling will ensure that the relationship between the Lagrange multipliers,  $\beta^i$ , is only weakly dependent on position as I will use large  $v$  which means the spacial dependence goes to zero. Now define a fluid cell by  $\mathcal{N}_v(x, t)$  which is understood to be a space-time region defined by  $\mathcal{N}_v(x, t) = \left\{ (y, s) : \sqrt{(y - vx)^2 + (s - vt)^2} < v^\xi \right\}$  with  $\xi_0 < \xi < 1$ . The value of  $\xi_0$  depends on the sub-leading corrections to the dynamics i.e. if the system has diffusion then  $\xi_0 = 1/2$ . The volume of such a cell is defined by:  $|\mathcal{N}_v| = \int_{\mathcal{N}_v(x, t)} dy ds$ . With these definitions, correlations in the Euler scaling limit are defined by,

$$\begin{aligned} \langle \mathcal{O}_1(x_1, t_1) \dots \mathcal{O}_n(x_n, t_n) \rangle_{\underline{\beta}(\underline{x}, 0)}^{\text{Eul}} = \\ \lim_{v \rightarrow \infty} v^{n-1} \int_{\mathcal{N}_v(x_1, t_1)} \frac{dy_1 ds_1}{|\mathcal{N}_v|} \dots \int_{\mathcal{N}_v(x_n, t_n)} \frac{dy_n ds_n}{|\mathcal{N}_v|} \langle \mathcal{O}_1(y_1, s_1) \dots \mathcal{O}_n(y_n, s_n) \rangle_{\underline{\beta}(\underline{x}, 0), v}^c \end{aligned} \quad (1.42)$$

for fixed  $x_k$  and  $t_k$ . The  $c$  superscript represents the connected correlators and  $\underline{\beta}(\underline{x}, 0)$  means the initial state. The important aspect of this definition is the  $v \rightarrow \infty$  limit, which means one defines a very smooth function where the  $\beta^i$  are nearly completely independent of the position. In this limit the appearance of the integrations over the fluid cells, the  $\int_{\mathcal{N}_v(x_n, t_n)}$  factors, play the important role of avoiding non-Eulerian oscillations [79]. Notice that the averaging is a controlled way of considering  $\langle \mathcal{O}_1(vx_1, vt_1) \dots \mathcal{O}_n(vx_n, vt_n) \rangle_{\underline{\beta}, v}^c$ , which would be the naïve result of the  $v$ -scaling. Reference [79] goes on to note that in the one-point-function it can be shown, numerically, that the averaging over fluid cells isn't important which implies  $\langle \mathcal{O}(x, t) \rangle_{\underline{\beta}(\underline{x}, 0)}^{\text{Eul}} = \lim_{v \rightarrow \infty} \langle \mathcal{O}(vx, vt) \rangle_{\underline{\beta}, v}$ . This completes the formal definition of Euler-scaling. I will use the ideas again in section 3.1.

I now move onto original research included as part of this thesis.



## Chapter 2

# The SCGF via bootstrapping

In this chapter I present unpublished but original work on 1D Conformal Field Theories and non-interacting quantum models. As was stated in the introduction, Conformal Field Theories (CFTs) provide a description for quantum systems at critical points and are thus very important in describing universal behaviour of quantum theories. Free theories, in turn, are used as a check throughout this work when finding results for interacting quantum models and thus are important to understand as well as possible. This chapter primarily focuses on CFTs however results obtained here can be applied to free theories as is pointed out throughout the chapter.

I start this chapter with a short introduction to CFTs and focus on the integrable description of CFTs through so called Korteweg-de-Vries conserved charges and the hydrodynamic description of the CFT. I then introduce the primary focus of this chapter, the further development of a technique introduced in [44] that uses the Gallavotti-Cohen symmetry, (1.26), to obtain the SCGF of flows related to the Korteweg-de-Vries charges. This approach to obtaining the SCGF is dubbed ‘bootstrapping’. I show the unexpected result that fluctuations of these fundamentally quantum flows are strongly associated with those in a classical system. I also introduce the Extended Fluctuation Relation (EFR), a proposed relation between the SCGF of flows and the steady state expected current of the system.

## 2.1 Conformal field theory

CFT plays an important role in physics. These are quantum field theories which are invariant under transformations by the conformal group where the conformal group is the

set of transformations of space-time that preserve angles [80, 81]. In other words, CFTs can be understood as those field theories which are unchanged under a local rescaling of the metric. From statistical physics it is well known that systems approaching their critical points have a correlation length that goes to infinity, which directly implies that the system is invariant under scaling. With this, the physical interpretation of CFTs is as a description of a quantum critical points. Although the study of CFTs is a very important topic with a vast body of work I forgo an in-depth discussion and only highlight the important features and properties that are in use within this work.

A CFT can be classified through its central charge, an operator that commutes with all the other symmetry operators in the theory. The central charge itself is obtained via the commutator of two components of the stress-energy tensor. From this one can infer the importance of the stress-energy tensor in CFT as it forms the fundamental building block of the theory [81]. The other noteworthy topic of CFTs is the study of the Virasoro algebra representations which define states of the system. The energy-momentum tensor itself is intimately related with Virasoro generators. This summarises the background information needed to understand the two important properties of CFTs used in this work. As an important aside, CFTs must have no mass in the theory as a mass terms break conformal invariance.

In a 1D CFT one can construct an infinite set of commuting charges based on integrals over polynomials of the energy-momentum tensor of the theory. Due to the energy-momentum tensor relation to Virasoro generators, this can be used to construct an infinite set of commuting charges. Since an infinite set of commuting charges is related to integrability, the presence of these charges in a CFT creates a fascinating link between CFTs and integrability. Importantly this allows one to make use of integrability related technology within CFTs. Charges of this type are often referred to as Korteweg-de-Vries (KdV) charges of the conformal field theory [82]. From [83], these charges are explicitly defined as;

$$Q_p = \int_0^{2\pi} \frac{du}{2\pi} \mathcal{T}_p(u), \quad (2.1)$$

where  $\mathcal{T}_p(u)$  are appropriately regularised polynomials in the energy-momentum tensor  $\mathcal{T}$  and its derivatives. The exact form of these charges are displayed in [83], however for

the purposes of this work it is sufficient to state that in general  $\mathcal{T}_p(u) \sim \mathcal{T}^p(u)$  which implies  $Q_p \sim \mathcal{T}^p(u)$ .

The second fundamental property that is necessary for my purposes is the existence of *chiral separation* in a 1D CFT. Fundamentally this property means there are two independent types of emergent quanta in the system, ‘left-moving’ and ‘right-moving’. This is a very surprising property as in general CFTs can be strongly interacting. Chiral separation results from the existence of translational invariance (leading to conservation of energy and momentum), Lorentz invariance and scale invariance present in a CFT [84]. To show this consider the  $2 \times 2$  energy-momentum tensor,  $\mathcal{T}$ , of a 1D CFT,

$$\mathcal{T} = \begin{pmatrix} q_1 & q_2 \\ j_1 & j_2 \end{pmatrix}, \quad (2.2)$$

where  $q_1$  and  $q_2$  are the energy and momentum density while  $j_1$  and  $j_2$  are their corresponding currents. Conservation of energy and momentum implies,  $\partial_\mu \mathcal{T}^{\mu\nu} = 0$  which provides two conservation equations,

$$\begin{aligned} \partial_0 q_1 + \partial_1 j_1 &= 0 \\ \partial_0 q_2 + \partial_1 j_2 &= 0, \end{aligned} \quad (2.3)$$

where if one identifies  $\mu = \{t, x\}$  then the above are simply conservation equations of the type from (1.34). Lorentz invariance implies  $\mathcal{T}^{\mu\nu} = \mathcal{T}^{\nu\mu}$  whilst scale invariance implies  $\mathcal{T}^\mu_\mu = 0$ , i.e. traceless. Making use of these two symmetries the equations of (2.3) can be written as,

$$\begin{aligned} \partial_0 q_1 + \partial_1 q_2 &= 0 \\ \partial_0 q_2 + \partial_1 q_1 &= 0. \end{aligned} \quad (2.4)$$

At this point consider the following change of variables: a ‘total charge density’,  $T = (q_1 + q_2)/2$  and a difference  $\bar{T} = (q_1 - q_2)/2$  which physically corresponds to a momentum charge. Also change  $\partial_z = -(1/2)(\partial_0 - \partial_1)$  and  $\partial_{\bar{z}} = (1/2)(\partial_0 + \partial_1)$ . In

this notation,

$$\partial_{\bar{z}} T = 0, \quad \text{and} \quad \partial_z \bar{T} = 0, \quad (2.5)$$

which defines two independent equations that are understood to represent a chiral factorization. As a direct consequence of this time evolution for these charge is defined as follows [84],

$$T(x, t) = T(x - t), \quad \text{and} \quad \bar{T}(x, t) = \bar{T}(x + t). \quad (2.6)$$

This shows the 1D CFT can be re-written as two independent systems moving in opposite directions.

## 2.2 SCGF for transport of KdV charges

The main purpose of this chapter is to obtain the SCGF for the transport of some KdV charge  $Q_p$  in an NESS. The distribution for such quantities is not known in the literature and having access to these quantities may prove to be of importance. In the process I obtain a new way of calculating the SCGF that is also applicable to free, massive quantum field theories which is shown in appendix A.1.

This method, dubbed bootstrapping, requires knowledge of the steady state current of the transported quantity and requires the system to obey chiral factorization i.e. the system should be comprised of two independent quanta, generically these are left and right moving. Finally, it requires the fluctuation relation, specifically the Gallavotti-Cohen type, to hold in the transport of the quantity. Based on these three aspects one can obtain the SCGF.

In this section and the remainder of the chapter, the NESS are assumed to be constructed via the partitioning protocol introduced in section 1.1.

### 2.2.1 Current and fluctuation relations for KdV charges

In this section I present an expression for the steady state current of a general KdV charge,  $Q_p$  of a CFT arising from the partitioning protocol. Similarly, I show the required form of fluctuations relation if they are assumed to apply in the transport of these charges. These two expressions will allow for the derivation of the full SCGF of transported KdV

charges.

From [85, 86] the steady state current in a CFT is known to be expressed by

$$\langle j \rangle = \frac{c\pi}{12} \left( \frac{1}{\beta_l^2} - \frac{1}{\beta_r^2} \right), \quad (2.7)$$

where  $\beta_l$  and  $\beta_r$  are the inverse temperatures of the partitions in the partitioning protocol. In order to obtain the current of an arbitrary KdV charge, I use dimensional analysis. This is possible as recall from the previous section that  $Q_p \sim \mathcal{T}^p(u)$ , thus  $p$  defines the multiples of the energy-momentum tensor used to construct it. Then dimensionally  $[Q_p] = [Q]^p$  where  $[Q]$  is dimensions of energy. The NESS state arising from the partitioning protocol is known to be a maximal entropy state where, in the presence of an infinite set of conserved charges, this is defined by a GGE (see section 1.4.2). Thus, in the NESS there exists a density matrix,  $\rho_{\text{steady}} \sim e^{\Sigma \beta^{(p)} Q_p}$ . Since the argument of the exponential must be dimensionless this identifies  $[Q_p] = [\beta^{(p)}]^{-1}$ . From this distribution one can also conclude  $[\beta^{(p)}] = [\beta]^p$  with  $\beta$  the inverse temperature as usual (using natural units). In natural units one knows  $[t] = [\beta]$ . Now, consider the current of a general charge, dimensionally  $[j_p] = [Q_p][t]^{-1}$ . Using the above information  $[Q_p][t]^{-1} = [\beta^{(p)}]^{-1}[\beta^{(p)}]^{-1/p}$ . Finally, in order to obtain an expression for the current I note that the chiral separation of a CFT is expected to hold for all excitations, including those associated with the KdV charges. Thus, with the results of the dimensional analysis combined with the requirement of chiral separation the steady state current corresponding to  $Q_p$  is,

$$\langle j_p \rangle = C \left( (\beta_l^{(p)})^{-1-1/p} + (\beta_r^{(p)})^{-1-1/p} \right), \quad (2.8)$$

where  $C$  is some constant of proportionality. This completes the generalisation of the steady state current for a KdV charge.

Recall from (1.30), in the partitioning protocol it is known that the Galavotti-Cohen relation is given by,

$$F(\lambda) = F(\beta_r - \beta_l - \lambda), \quad (2.9)$$

where  $F(\lambda)$  is the SCGF of the energy current. I make the assumption that FRs hold independently for all KdV charges and find an expression for FRs that are satisfied by the individual KdV charges. From (1.4), the SCGF encodes the scaled cumulants, specifically at first order it provides the steady state current. Thus,  $F(\lambda) \sim \lambda j + \mathcal{O}(\lambda^2)$ . In the case of the SCGF of a general conserved charge  $Q_p$  as before it is then expected that  $[F_p(\lambda)] = [\lambda][\beta^{(p)}]^{-1-1/p}$ . By definition of the SCGF  $[F_p(\lambda)] = [t]^{-1}$  no matter which charge this is applied to. Thus  $[F_p(\lambda)] = [\beta^{(p)}]^{-1/p} = [\lambda][\beta^{(p)}]^{-1-1/p} \implies [\lambda] = [\beta^{(p)}]$ . Putting this together,

$$F_p(\lambda) = F_p(\beta_r^{(p)} - \beta_l^{(p)} - \lambda). \quad (2.10)$$

Using (2.8) and (2.10), I obtain an exact expression for the SCGF.

### 2.2.2 Bootstrapping the SCGF of transported KdV charges

In conjunction with the above two expressions, (2.8) and (2.10) one uses the CFTs chirality separation which was already assumed in order to obtain (2.8). This symmetry is readily written in terms of the SCGF as

$$F_p(\lambda) = f_p(\lambda, \beta_r^{(p)}) + f_p(-\lambda, \beta_l^{(p)}), \quad (2.11)$$

for some function  $f_p$ . Clearly the chiral splitting in this form directly implies the current will split into left and right moving parts. This, along with (2.8) and (2.10) are used to determine an expression for  $F(\lambda)$ . This method has been called the Bootstrapping method as one obtains the full SCGF from three foundational identities and concepts of the theory. Reference [44] presented a form of Bootstrapping for the case of the SCGF for energy transfer in a 1D CFT, what follows is a generalised form of this argument.

I simplify notation for the derivation by defining  $\beta^{(p)} \equiv \tilde{\beta}$ . Since expansion of  $F(\lambda)$  holds for each of the two terms in (2.11) separately,  $f_p(\lambda, \tilde{\beta}) = \lambda j_p(\lambda, \tilde{\beta}) + \mathcal{O}(\lambda^2)$  where  $j_p$  is the corresponding term in (2.8). Using this I write  $f_p$  as a function of a

dimensionless quantity,

$$\begin{aligned} f_p(\lambda, \beta^{(p)}) &= C \frac{\lambda}{\tilde{\beta}^{1+1/p}} + \mathcal{O}(\lambda^2) \\ &= C \frac{1}{\lambda^{1/p}} \frac{\lambda^{1+1/p}}{\tilde{\beta}^{1+1/p}} + \mathcal{O}(\lambda^2). \end{aligned} \quad (2.12)$$

With this I define some function  $g[w]$  such that,

$$f_p(\lambda, \tilde{\beta}) = C \frac{1}{\lambda^{1/p}} g \left[ \frac{\lambda}{\tilde{\beta}} \right] \quad (2.13)$$

$$\text{where, } g[w] = w^{1+1/p} + w^{2+1/p} + \mathcal{O}(w^{3+1/p}). \quad (2.14)$$

Inserting the above back into (2.11) to obtain  $F_p(\lambda)$ , using the resulting expression in (2.10) and writing in terms of dimensionless variables gives:

$$\begin{aligned} & \frac{1}{\lambda^{1/p} \left( \frac{\tilde{\beta}_r}{\lambda} - \frac{\tilde{\beta}_l}{\lambda} - 1 \right)^{1/p}} \left( g \left[ \frac{\frac{\tilde{\beta}_r}{\lambda} - \frac{\tilde{\beta}_l}{\lambda} - 1}{\frac{\tilde{\beta}_r}{\lambda}} \right] + (-1)^{1/p} g \left[ \frac{-1 \left( \frac{\tilde{\beta}_r}{\lambda} - \frac{\tilde{\beta}_l}{\lambda} - 1 \right)}{\frac{\tilde{\beta}_l}{\lambda}} \right] \right) \\ &= \frac{1}{\lambda^{1/p}} \left( g \left[ \frac{\lambda}{\tilde{\beta}_r} \right] + (-1)^{1/p} g \left[ -\frac{\lambda}{\tilde{\beta}_l} \right] \right). \end{aligned} \quad (2.15)$$

To simplify the above expression I perform a change in variables:  $\frac{\tilde{\beta}_r}{\lambda} = \frac{1}{w} + h$ ,  $\frac{\tilde{\beta}_l}{\lambda} = \frac{1}{w} - 1$ . Now I expand in  $h$ , where for the left-hand side of the above expression I use (2.14), and the right-hand side I use the Taylor expansion. Then matching the left and right at  $\mathcal{O}(h^{1+1/p})$  produces a differential equation for  $g[w]$ ,

$$\frac{dg}{dw} = -w^{1/p-1} - \frac{1}{w^2} \left( \frac{w}{1-w} \right)^{1+1/p}. \quad (2.16)$$

Integrating both sides gives  $g[w]$ . Then, recalling (2.13) it is easy to obtain  $(1/\lambda^{1/p})g[\lambda/\tilde{\beta}]$  and insert into (2.11) to finally find the SCGF of a KdV charge of a CFT,

$$F_p(\lambda) = Cp \left( -\frac{1}{\tilde{\beta}_l^{1/p}} + \frac{1}{(\tilde{\beta}_l - \lambda)^{1/p}} - \frac{1}{\tilde{\beta}_r^{1/p}} + \frac{1}{(\tilde{\beta}_r + \lambda)^{1/p}} \right). \quad (2.17)$$

This is an unpublished but completely new result. The result matches those found for

energy transport in CFTs, i.e.  $p = 1$ . In appendix A.1 I show how Bootstrapping can be used to obtain results in non-interacting massive theories. This result shows that the SCGF for the transport of KdV charges is sensitive to  $\tilde{\beta}_r$  and  $\tilde{\beta}_l$ . Specifically if  $\tilde{\beta}_{r/l} < 1$  then as  $p$  increases  $F_p$  becomes less sensitive to the temperature and actually the currents and all other scaled cumulant become smaller. In this instance the energy current and its fluctuations dominate the system.

## 2.3 Classical interpretation of KdV charge transport fluctuations

Equation (2.17) can be recast it into a more illuminating form based on a result in [44]. In [84] the SCGF that is equivalent to (2.17) with  $p = 1$  is re-written as a sum of two independent Poisson processes. It is known that Poisson processes is a signature of particles behaving in a classical way, this implies energy transport within critical points have a fundamentally classical nature. First I show how to find a Poisson expression of the more general result of (2.17) and then give a physical interpretation of this.

Assume that a Poisson form of the SCGF exists i.e.  $F(\lambda) = \int dq w(q) (e^{\lambda q} - 1)$  where  $w(q)$  is the Poisson rate. Now by taking a  $\lambda$ -derivative on both sides and setting  $\lambda \rightarrow i\lambda$  one obtains,

$$\left. \frac{dF(\lambda)}{d\lambda} \right|_{\lambda=i\lambda} = \int dq q w(q) e^{i\lambda q}. \quad (2.18)$$

Clearly  $qw(q)$  can be interpreted as the inverse Fourier transform of  $dF(\lambda)/d\lambda|_{\lambda=i\lambda}$ . From this one finds,

$$w(q) = \frac{1}{q} \int_{-\infty}^{\infty} \frac{d\lambda}{2\pi} \left. \frac{dF(\lambda)}{d\lambda} \right|_{\lambda=i\lambda} e^{i\lambda q}, \quad (2.19)$$

For the SCGF to have a valid Poisson form the weights, defined by the above equation, must be real and positive. For the weights to be real  $\left. \frac{dF(\lambda)}{d\lambda} \right|_{\lambda=i\lambda}$  must be a Hermitian function. Inserting (2.17) into (2.19) and using the Mathematica symbolic calculation software [87], the weights can be shown to be,

$$w(q) = \Gamma(1 + 1/p) e^{-\beta_{l/r} q} q^{\frac{1}{p}-1}. \quad (2.20)$$



Then, by change of variables  $q \rightarrow \varepsilon^p$ , (2.17) is written as a sum of Poisson processes,

$$F(\lambda) = C\Gamma(1 + 1/p) \int_0^\infty \frac{d\varepsilon}{2\pi} \left[ e^{-\varepsilon^p \beta_r^{(p)}} \left[ e^{\varepsilon^p \lambda} - 1 \right] + e^{-\varepsilon^p \beta_l^{(p)}} \left[ e^{-\varepsilon^p \lambda} - 1 \right] \right]. \quad (2.21)$$

where  $\varepsilon$  is understood to be an amount of energy carried by a classical particle,  $p$  represents powers of  $\varepsilon$ , and  $\Gamma$  is the gamma-function. Thus one interprets the KdV current in the system coming from two sets of classical particles (left and right) carrying energy  $\varepsilon^p$  being driven by a Poisson process with a Poisson rate of  $e^{-\varepsilon^p \beta_{l/r}^{(p)}}$ .

The exact classical nature of this result can be illuminated by starting with two independent equilibrium gasses comprised of free particles. I consider these to be Bosons, but the following argument is equivalent if made for Fermions. Well known statistical mechanics results show that the Landau potential, or thermodynamic potential, in the continuum limit is given by [88]:

$$\Omega = \int \frac{d\eta}{2\pi} d(\eta) \log \left( 1 - e^{-\beta\eta} \right), \quad (2.22)$$

where  $\beta$  is the inverse temperature of the thermalised system,  $\eta$  is the energy and  $d(\eta)$  is the density of states. Usually, in order to obtain energy cumulants one takes  $\beta$  derivatives of the above where the  $n^{\text{th}}$  derivative corresponds to the  $n^{\text{th}}$  moment. To make a closer comparison to (2.21) I introduce a parameter  $\lambda$  such that  $\lambda$ -derivatives produce the same cumulants. This can be written as follows:

$$\Omega = \int \frac{d\eta}{2\pi} d(\eta) \left[ \log \left( 1 - e^{-\beta\eta} \right) - \log \left( 1 - e^{(-\beta-\lambda)\eta} \right) \right], \quad (2.23)$$

where the first term is required to ensure normalization, i.e.  $\Omega(\lambda = 0) = 0$ . Now consider the sum of two such independent, equilibrium gasses at inverse temperatures  $\beta_r$  and  $\beta_l$ . In analogy to the chiral factorization I consider the currents of each of the system to be moving in opposite directions. As these are independent systems, the free energy of this combined system is simply

$$F(\lambda) = \int \frac{d\eta}{2\pi} d(\eta) \left[ \log \left( 1 - e^{-\beta_l \eta} \right) - \log \left( 1 - e^{(-\beta_l - \lambda)\eta} \right) + \log \left( 1 - e^{-\beta_r \eta} \right) - \log \left( 1 - e^{(-\beta_r + \lambda)\eta} \right) \right], \quad (2.24)$$

where opposite signs in-front of  $\lambda$  ensures that on taking the first derivative, one obtains two independent currents of opposite sign. Now comes the important step. In the semi-classical limit, the Bose-Einstein distribution is given by the Maxwell distribution,

$$\frac{1}{e^{\beta\eta} - 1} \rightarrow e^{-\beta\eta}. \quad (2.25)$$

This is a result of the low-density limit of a quantum gas. In the low density limit the quantum particles don't meet very often and thus quantum effects are suppressed. The density is defined by the occupation function, specifically the average number of particles in a given microstate  $k$  is given by  $1/(e^{\beta\eta_k} - 1)$ . For this expression to be small,  $e^{-\beta\eta} \rightarrow 0$  or (2.25). Applying the limit  $e^{-\beta\eta} \rightarrow 0$  to (2.24),

$$F(\lambda) = \int_0^\infty \frac{d\eta}{2\pi} d(\eta) \left[ e^{-\eta\beta_r} \left[ e^{\eta\lambda} - 1 \right] + e^{-\eta\beta_l} \left[ e^{-\eta\lambda} - 1 \right] \right]. \quad (2.26)$$

Then using a density of states  $d(\eta) = (C\Gamma(1 + 1/p)/p)\eta^{1/p-1}$  and changing  $\eta \rightarrow \varepsilon^p$ , one obtains exactly (2.21). Note that the notation of  $\beta_{l/r}$  must also change, where it is to be understood that the correct charge is coupled to the correct Lagrange multiplier. Thus, I have found the system that a non-equilibrium CFT is equivalent to, the sum of two systems in equilibrium with a specific choice of density of states. Physically this is consistent as from the Chiral symmetry of a CFT, left moving particles can be treated as independent of the right-moving particles and in this case the non-equilibrium nature of this system generated by a partitioning protocol is the sum of the two equilibrium partitions we started with.

In appendix A.2 I show that fluctuations of energy transport in a 1D CFT i.e. (2.26) with  $p = 1$ , can be written as the sum of an infinite number of random walkers on a ring. This shows this quantum result can be obtained from an explicit classical stochastic dynamical system, unfortunately this doesn't hold for  $p > 1$ .

## 2.4 Extended fluctuation relation introduced

In this section I show (2.17) satisfies the so-called extended fluctuation relation (EFR), a stronger form of the Gallovotti-Cohen relation, that holds under certain assumptions. This relation is defined for system in an NESS produced via the partitioning protocol. I

present this in a form that may seem overly complex but is necessary when the EFR is re-addressed in section 3.4 where there will exist multiple conserved charges. The EFR is defined by [66],

$$F(\lambda) = \int_0^\lambda d\lambda' \langle j \rangle_{\{(\beta_l^\bullet - \lambda' \delta_{i^*}^\bullet, \beta_r^\bullet + \lambda' \delta_{i^*}^\bullet)\}}, \quad (2.27)$$

where  $\beta_{r/l}^\bullet$  are column vectors of  $\beta_l$  and  $\beta_r$ , the inverse temperatures of the partitions in the partitioning protocol,  $\delta_{i^*}^\bullet$  is the  $i^*$  row of the identity matrix and  $i^*$  represents the  $i^*$  charge in the case where multiple conserved charges are present and  $j$  is the current. This relation provides an important relationship between the full SCGF and the current, specifically knowledge of the current can in principle be used to generate information about the full SCGF. This was shown to hold for CFTs whenever there is “pure transmission” i.e. there are no impurities in the system. In work done in section 3.4, I show exactly under what conditions the EFRs will appear, and more importantly, when they won't. It will be shown that the EFRs are only expected to hold in the case of a ‘free’ hydrodynamic system, where this meaning of ‘free’ will be discussed (see section 3.4).

The result found in (2.17) is easily shown to satisfy (2.27). The EFR in the case of only one charge present in the system predicts,

$$F(\lambda) = \int_0^\lambda d\lambda' \langle j \rangle_{\{(\beta_l - \lambda', \beta_r + \lambda')\}}. \quad (2.28)$$

In order to show this is true for (2.17), I start with (2.8),

$$\langle j \rangle_{|\beta_l \rightarrow \beta_l - \lambda', \beta_r \rightarrow \beta_r + \lambda'} = C \left( (\beta_l^{(p)} - \lambda)^{-1-1/p} + (\beta_r^{(p)} + \lambda)^{-1-1/p} \right). \quad (2.29)$$

Integrating this

$$\begin{aligned} & \int_0^\lambda d\lambda' \langle j \rangle_{|\beta_l \rightarrow \beta_l - \lambda', \beta_r \rightarrow \beta_r + \lambda'} \\ &= Cp \left( -\frac{1}{\beta_l^{(p)1/p}} + \frac{1}{(\beta_l^{(p)} - \lambda)^{1/p}} - \frac{1}{\beta_r^{(p)1/p}} + \frac{1}{(\beta_r^{(p)} + \lambda)^{1/p}} \right) = F_p(\lambda). \end{aligned} \quad (2.30)$$

Thus, proving the EFR holds in case.

Before the work in [51], which is presented in section 3.4, there was a fairly general

argument given in [84] for the presence of the EFR which rests on the following three assumptions:

1. The total energy moving through the connection between the two subsystems is small compared to the total energy in the system.
2. The flow in the steady state region is constant in time.
3. The system separates into independent left and right moving parts i.e. satisfies chiral separation.

With these three points, [84] shows the joint SCGF of KdV currents  $F(\{\lambda_i\})$  meets the following condition:

$$\partial_{\lambda_k} F(\{\lambda_i\}) = \frac{\text{Tr} \left( j_{(k)}(0) e^{-\sum_i \bar{\beta}^{(i)} H^{(i)} + (\lambda_i + \delta^{(i)}/2) P^{(i)}} \right)}{\text{Tr} \left( e^{-\sum_i \bar{\beta}^{(i)} H^{(i)} + (\lambda_i + \delta^{(i)}/2) P^{(i)}} \right)}, \quad (2.31)$$

with

$$\bar{\beta}^{(i)} \equiv \frac{\beta_l^{(i)} + \beta_r^{(i)}}{2}, \quad \delta^{(i)} \equiv \beta_r^{(i)} - \beta_l^{(i)}. \quad (2.32)$$

$H^{(i)}$  and  $P^{(i)}$  are generalised Hamiltonian and momentum operators which are related to the KdV charges of the system,  $\beta^{(i)}$  are corresponding Lagrange multipliers, and  $\lambda_i$  are the conjugate parameters associated with each higher order charge. As the  $H^{(i)}$  and  $P^{(i)}$  are related to the KdV charges, they are also equivalent to multiples of the energy-momentum tensor.  $j_{(k)}(0)$  is the current operator corresponding to the  $k^{\text{th}}$  conserved charge.

Since,

$$\langle j_k \rangle = \frac{\text{Tr} \left( j_{(k)}(0) e^{-\sum_i \bar{\beta}^{(i)} H^{(i)} + (\delta^{(i)}/2) P^{(i)}} \right)}{\text{Tr} \left( e^{-\sum_i \bar{\beta}^{(i)} H^{(i)} + (\delta^{(i)}/2) P^{(i)}} \right)}, \quad (2.33)$$

the EFR is obtained as

$$\partial_{\lambda_k} F(\{\lambda_i\}) = j_{ss}^{(k)} \Big|_{\beta_l^{(i)} \rightarrow \beta_l^{(i)} - \lambda_i, \beta_r^{(i)} \rightarrow \beta_r^{(i)} + \lambda_i}. \quad (2.34)$$

The assumptions required for finding this expression means it is a fairly broad result expected to hold for 1D critical points as well as free field theories. Physically the EFR shows that one can bias the hydrodynamic state by only linear shifts of the Lagrange parameters in the initial baths of the partitioning protocol, in order to generate transport cumulants. These results were confirmed to hold in various free particle models beyond 1D CFT [40–42]

In general, the approach of obtaining the SCGF via bootstrapping proved difficult in the presence of interactions of a general integrable model, specifically the lack of chiral symmetry means this method becomes intractable. However, in the next chapter I explain an approach that is far more general, the central result of this thesis. What is interesting is as a result of this general approach the EFR appearance and validity is easily explained. This understanding will result in the hypothesis that the presence of EFR can be used as a proxy for a hydrodynamic free theory.

## Chapter 3

# Ballistic fluctuation formalism

In this chapter I present the Ballistic Fluctuation Formalism, a completely new framework that provides a general approach to calculating the SCGF for ballistic currents in hydrodynamic system based on macroscopic, hydrodynamic quantities. This chapter is based on original research I have done contained in [51].

This chapter uses the Macroscopic Fluctuation Theory as the inspiration for a more hydrodynamic-focussed approach. A very brief overview of the MFT can be found in appendix B. As has been discussed above, fluctuations of transported quantities scaled by time are encoded by the SCGF. Thus, it is natural to calculate such quantities in the hydrodynamic limit. The ballistic fluctuation formalism defined here is applicable to systems in maximal entropy states with dynamics defined by Euler hydrodynamics as introduced in section 1.5. This formalism builds from identities found in linear fluctuating hydrodynamics, an approach for describing maximal entropy states arising from the long time limit of Euler hydrodynamics which was developed in [49, 50].

The primary results of the Ballistic Fluctuation Formalism are the flow-equation, which defines how a hydrodynamic state should be altered to incorporate information about the SCGF, and an equation which provides the relationship between the current of interest in the altered state and the corresponding SCGF.

In this chapter I begin with a detailed discussion of maximal entropy states and then introduce identities from linear fluctuating hydrodynamics which are used to obtain the defining equations of the Ballistic Fluctuation Formalism. With the formal aspects in place, I show how this framework is used through an application to obtain the energy transport SCGF in a 1D CFT. I then derive the extended fluctuation relation (intro-

duced in section 2.4), present a discussion on the presence of dynamical phase transitions predicted by the Ballistic Fluctuation Formalism and obtain analytical solutions of the SCGF that works under certain conditions.

### 3.1 Maximal entropy states and fluctuating hydrodynamics

In this section I will discuss in detail the states of interest in the Ballistic Fluctuation Formalism (BFF), the maximal entropy states. I then introduce a dynamical equation for the field-field correlator and a general relationship between the field-field correlator and the current-current correlator. Both these expressions can be found in a body of work known as linear fluctuating hydrodynamics [49,50]. The BFF makes use of one and two-point correlators of fields and currents to obtain the SCGF which leads to the necessity of the identities discussed here. This section assumes the existence of multiple conserved quantities at the Euler scale which means it naturally builds on the introductory work of section 1.5, which I will refer back to.

#### 3.1.1 Maximal entropy states

The BFF is applicable to maximal entropy states (MESs). Sections 1.4.2 and 1.5 have already introduced these states as Gibbs-like states in the sense that they are defined by a density matrix,

$$\rho \propto e^{\sum \beta^i Q_i}, \quad (3.1)$$

with  $Q_i$  locally conserved charges in the system and  $\beta^i$  the corresponding Lagrange multipliers; note that the  $i$  is an index and not an exponent as will be the case throughout the remainder of this work unless otherwise specified. In this section I expand on some important aspects of these states.

Although MESs are often associated with equilibrium states in the case where there exist local conserved charges that are irreversible in time, such as momentum, these describe NESSs. Such quantities are transported ballistically, hence the name of the framework. Despite seemingly simplistic, these states may exhibit rich non-equilibrium behaviour such as long-range correlations where correlations are caused by the pres-

ence of quasi-local charges. Recall from section 1.4.2 that quasi-local charges may be required in order to fully describe a MES. Maximal entropy states are, by definition, homogeneous and stationary which will be of vital importance going forward in this chapter.

The BFF prescribes an approach for obtaining the SCGF related to transport of a conserved quantity within an MES where transport is the total ‘amount’ of charge to cross a reference point. In the BFF one assumes the MES arises from the long-time dynamics of a system governed by Euler hydrodynamics. Physically the MES of interest is a fluid cell that contains the reference point and has become so large during the dynamics that this is the only state that needs to be considered. Thus, in the long-time limit, the transport is considered to be completely contained within a single fluid cell defined by a Gibbs-like state constructed of local and (sometimes) quasi-local charges with Lagrange parameters  $\beta^i$ .

Of particular importance in this work, the partitioning protocol is known to produce an MES around the juncture between the two partitions in the long-time limit of the system. In CFTs and integrable models this has been explicitly constructed where states are shown to support ballistic transport [84, 89].

### 3.1.2 Euler dynamics for field correlator

Correlations play an important role in the BFF. As such I first obtain an equation of motion that governs the correlation function of fields in an MES. Such correlations are defined by,

$$S_{ij}(x, t) \equiv \langle q_i(x, t) q_j(0, 0) \rangle_{\underline{\beta}}, \quad (3.2)$$

where  $S_{ij}$  can be understood as a matrix and  $q_i$  is a conserved charge of the system that satisfies an Euler hydrodynamic equation as was presented in section 1.5 and expectation values are with respect to the vector of all  $\beta^i$ , denoted  $\underline{\beta}$ , in a maximal entropy state (MES). In this section I follow [79, 90].

In order to obtain the dynamics of  $S_{ij}(x, t)$  in the MES, I consider a state slightly perturbed such that it becomes an inhomogeneous state where the expectation value is



given by,

$$\langle q(x,t) \rangle_{\underline{\beta} + \underline{\tilde{\beta}}} = \frac{\text{Tr} \left( e^{-\sum_j (\beta^j Q_j + \int dz \tilde{\beta}^j(z) q_j(z,0))} q(x,t) \right)}{\text{Tr} \left( e^{-\sum_j (\beta^j Q_j + \int dz \tilde{\beta}^j(z) q_j(z,0))} \right)}. \quad (3.3)$$

In order to obtain an MES one sets  $\tilde{\beta} = 0$ . In this state it is clear that taking derivatives with respect to  $\tilde{\beta}^i$  pulls down factors of  $q$  which generates connected field correlations. Assuming that  $\tilde{\beta}^i \approx 0$  means this is interpreted as a linear expansion around a homogeneous state. This leads to,

$$-\frac{\delta}{\delta \tilde{\beta}^j(x)} \langle q_i(y,t) \rangle_{\underline{\beta} + \underline{\tilde{\beta}}} = \langle q_i(x,t) q_j(0,0) \rangle_{\underline{\beta} + \underline{\tilde{\beta}}} = S_{ij}^{(\tilde{\beta})}(x,t). \quad (3.4)$$

To obtain a dynamic equation for  $S_{ij}(x,t)$  I derive such an equation for  $S_{ij}^{(\tilde{\beta})}(x,t)$  then consider  $\underline{\tilde{\beta}} = 0$ . Recall the definition of the flux Jacobian from (1.39),

$$A_i^j = \frac{\partial \langle j_i \rangle}{\partial \langle q_j \rangle}, \quad (3.5)$$

where at this point I consider averages with respect to  $(\underline{\beta} + \underline{\tilde{\beta}})$ . Then from the Euler hydrodynamic equations of (1.40) one takes a  $\tilde{\beta}^j$  derivative and using the chain rule with the definition of  $A_i^j$ ,

$$\partial_t S_{ij}^{(\tilde{\beta})}(x,t) + \partial_x \sum_k A_i^k(x,t) S_{kj}^{(\tilde{\beta})}(x,t) = 0. \quad (3.6)$$

Now in order to recover the equivalent expression for  $S_{ij}(x,t)$ , I set  $\underline{\tilde{\beta}} = 0$  resulting in homogeneous and stationary states by definition of the MES. In particular this means expectation values become,

$$\langle q_i(x,t) \rangle_{\underline{\beta}} = \frac{\text{Tr} \left( e^{-\sum_k \beta^k Q_k} q_i(x,t) \right)}{\text{Tr} \left( e^{-\sum_k \beta^k Q_k} \right)}. \quad (3.7)$$

Now consider the expectation of local densities in the MES,  $q_i = \langle q_i(0,0) \rangle_{\underline{\beta}}$ . These are independent of space and time by homogeneity and stationarity of the MES. This implies there exists a mapping from  $\underline{\beta} \mapsto q$ . Similarly the local current  $j_i = \langle j_i(0,0) \rangle_{\underline{\beta}}$

is space-time independent but furthermore, due to the mapping  $\underline{\beta} \mapsto \mathbf{q}$ ,  $j_i$  can be written as a function of  $\mathbf{q}$ . One then defines the model-dependent function  $\mathcal{F}$  such that  $j_i = \mathcal{F}(\mathbf{q}_\bullet)$  where  $\bullet$  represents the set of all  $i$ . This can be seen as explicitly defining the function in the first term of the hydrodynamic expansion, see (1.37). Thus, the model at hand, specifically the structure of the MES, defines the way the  $j$  depends on  $\mathbf{q}$  but note this is not space-time dependent. Thus in the MES, the flux Jacobian  $A_i^j$  is space-time independent. Referring back to (3.6), in the MES state  $S_{ij}^{(\underline{\beta})} \rightarrow S_{ij}$  and  $A_i^j$  is space-time independent resulting in the following equation of motion for the correlations in an MES state,

$$\partial_t S_{ij}(x, t) + \sum_k A_i^k \partial_x S_{kj}(x, t) = 0. \quad (3.8)$$

This defines the Euler equations for the field-field correlation matrix  $S_{ij}$ . The other important aspect of (3.8) is the initial condition. For this consider the static covariance matrix defined by,

$$\begin{aligned} -\frac{\partial}{\partial \beta^i} \langle q_j(x, t) \rangle_{\underline{\beta}} &= \int dy \langle q_i(y, 0) q_j(x, t) \rangle_{\underline{\beta}} \\ &= \int dy S_{ij}(y, 0) \\ &\equiv C_{ij}, \end{aligned} \quad (3.9)$$

where I used  $Q_i = \int dy q(y)$  and the fact that  $\langle q_j(x, t) \rangle_{\underline{\beta}} = \langle q_j(0, 0) \rangle_{\underline{\beta}}$  due to homogeneity and stationarity. This encodes the initial system correlations which is used as the initial condition of (3.8) since trivially  $S_{ij}(x, 0) = \delta(x) C_{ij}$  (seen by integrating on both sides). This is physically sensible as one expects the initial time correlations to be a  $\delta$ -function as two points can't be correlated before any dynamics takes place in the system.

Physically, taking  $\beta$  derivatives in (3.4) is equivalent to determining the response of the system to local disturbances. It is these types of disturbances that generate dynamical correlations, thus (3.8) is interpreted as the dynamics of correlations attributed to local disturbances in the MES. Expanding on this, in systems with ballistic transport the dynamics are defined by the Euler equations.

A further important aspect of  $S_{ij}$  is that  $S_{ij}(x-x', t-t') = \langle q_i(x, t) q_j(x', t') \rangle_{\underline{\beta}}$  which is true as in the MES, states are homogenous and stationary. Thus the only aspect of importance is relative distance in space-time [50].

### 3.1.3 Sum rules

Now consider current-current correlations defined, analogously to  $S_{ij}$  above as,

$$\Gamma_{ij}(x, t) \equiv \langle j_i(x, t) j_j(0, 0) \rangle_{\underline{\beta}}. \quad (3.10)$$

where, again due to homogeneity and stationarity of hydrodynamic states,  $\Gamma_{ij}(x-x', t-t') = \langle j_i(x, t) j_j(x', t') \rangle_{\underline{\beta}}$ . It will turn out to be vital to know how  $\Gamma_{ij}(x, t)$  is related to  $S_{ij}(x, t)$ . I present a particular form of this relationship known as the sum rules. The sum rules will provide the basis from which to derive the flow-equation. This section is based on work in [49, 90].

One starts from the integral form of the conservation equation,

$$q_i(x, t) - q_i(x, 0) = -\partial_x \int_0^t ds j_i(x, s). \quad (3.11)$$

Multiply this by itself on both sides and take the expectation value in the MES i.e.

$$\langle (q_i(x, t) - q_i(x, 0))(q_j(x', t) - q_j(x', 0)) \rangle_{\underline{\beta}} = \int_0^t ds' \int_0^t ds \partial_x \partial_{x'} \langle j_i(x, s) j_j(x', s') \rangle_{\underline{\beta}}. \quad (3.12)$$

Then introduce a general function  $f(x)$  and a term  $\delta(x')$  and integrate such that

$$\begin{aligned} & \int_{-\infty}^{\infty} dx \int_{-\infty}^{\infty} dx' f(x) \delta(x') \langle (q_i(x, t) - q_i(x, 0))(q_j(x', t) - q_j(x', 0)) \rangle_{\underline{\beta}} \\ &= \int_0^t ds' \int_0^t ds \int_{-\infty}^{\infty} dx \int_{-\infty}^{\infty} dx' f(x) \delta(x') \partial_x \partial_{x'} \langle j_i(x, s) j_j(x', s') \rangle_{\underline{\beta}}. \end{aligned} \quad (3.13)$$

I will deal with the left- and right-hand sides of the equation separately. On the left-hand side (lhs) it is simple to take the  $x'$  integral. Then recall  $S_{ij}(x-x', t-t') = \langle q_i(x, t) q_j(x', t') \rangle_{\underline{\beta}}$  which means,

$$lhs = \int_{-\infty}^{\infty} dx f(x) (2S_{ij}(x, 0) - S_{ij}(x, t) - S_{ij}(x, -t)). \quad (3.14)$$

Since the initial condition of (3.8) is  $S_{ij}(x, 0) = \delta(x)C_{ij}$ ,

$$lhs = 2f(0)C_{ij} - \int_{-\infty}^{\infty} dx (S_{ij}(x, t) + S_{ij}(x, -t)). \quad (3.15)$$

The right hand side (rhs) of (3.13) is slightly more involved. First perform the  $x'$  integration,

$$rhs = \int_0^t ds' \int_0^t ds \int_{-\infty}^{\infty} dx f(x) \partial_x \partial_{x'} \langle j_i(x, s) j_j(x', s') \rangle_{\underline{\beta}} |_{x'=0}. \quad (3.16)$$

Recall  $\Gamma_{ij}(x - x', s - s') \equiv \langle j_i(x, s) j_j(x', s') \rangle_{\underline{\beta}}$  and  $\partial_x \Gamma_{ij}(x - x', s - s') = -\partial_{x'} \Gamma_{ij}(x - x', s - s')$  resulting in,

$$rhs = - \int_0^t ds' \int_0^t ds \int_{-\infty}^{\infty} dx f(x) \partial_x \partial_x \Gamma_{ij}(x, s - s'). \quad (3.17)$$

Using integration by parts twice, again assuming  $\Gamma_{ij}(x, t) \rightarrow 0$  when  $x \rightarrow \pm\infty$ ,

$$rhs = - \int_{-\infty}^{\infty} dx f''(x) \int_0^t ds' \int_0^t ds \Gamma_{ij}(x, s - s'). \quad (3.18)$$

Then consider  $t \rightarrow \infty$  and  $q = s - s'$  and undertaking the required integrals,

$$rhs = - \lim_{t \rightarrow \infty} t \int_{-\infty}^{\infty} dx f''(x) \int_0^t dq \Gamma_{ij}(x, q). \quad (3.19)$$

Finally, this produces the general form of the sum rules,

$$\begin{aligned} & \lim_{t \rightarrow \infty} \int_{-\infty}^{\infty} dx f(x) (S_{ij}(x, t) + S_{ij}(x, -t)) - 2f(0)C_{ij} \\ &= \lim_{t \rightarrow \infty} t \int_{-\infty}^{\infty} dx f''(x) \int_0^t dq \Gamma_{ij}(x, q). \end{aligned} \quad (3.20)$$

Of particular interest in this work is the case where  $f(x) = |x|$  leaving  $f''(x) = 2\delta(x)$ . Then since conserved charges commute by definition,  $S_{ij}(x, -t) = S_{ji}(-x, t)$ . Then, when integrating over  $x$  and taking the large  $t$  limit [78],

$$\int_0^{\infty} dt \Gamma_{ij}(0, t) = \lim_{t \rightarrow \infty} \frac{1}{t} \int_{-\infty}^{\infty} dx |x| S_{ij}(x, t). \quad (3.21)$$

With these two expressions in place I move on to the exposition of the BFF equations.

## 3.2 Equations and assumptions of ballistic fluctuation formalism

In this section I provide the three foundational concepts and the equations that form the basis of the BFF. First, I show how the hydrodynamic state can be biased such that the state variables depend on  $\lambda$ , the conjugate parameter in the SCGF. The second expression is the flow equation, this equation defines the dependence of hydrodynamic variables on  $\lambda$ . Finally, the third expression will show how the current, defined in the  $\lambda$  biased state, is related to the corresponding SCGF. The results of this section very closely follow the results we presented in our publication [51, section 3].

### 3.2.1 Assumptions and biasing the state

The BFF holds under three specific circumstances. The most important property needed for the BFF to apply is the system must be in an MES which supports ballistic transport though some time-irreversible conserved charge. The second important property is states support sufficient clustering of correlations in the system, i.e. multi-point connected correlation functions of local fields, in particular of local currents, vanish at large space and time separations, in a way that makes them integrable. Although the spacial clustering is generically expected in an MES it is not guaranteed for time separations although it is reasonable to expect this. I discuss what happens if this clustering breaks down in section 3.5 bellow. The final requirement is based on the fact that I have only considered hydrodynamics in 1D, thus the results that follow apply to systems whose transport takes place in 1D. This is not to say that this framework only applies to 1D system as I will apply the BFF to a  $d$ -dimensional Conformal Field Theory in chapter 5. With these assumptions stated I now move on to the foundational observation of the BFF, that the conjugate parameter  $\lambda$  of a SCGF,  $F(\lambda)$ , can be absorbed into a hydrodynamic state of the system in a way that allows one to generate connected field correlations based only on the new state.

To begin I modify the measure for the state  $\langle \cdots \rangle_{\underline{\beta}}$  by a time-integrated local current

$j(0, t)$  of the charge  $Q$  at the origin. That is,

$$\langle \mathcal{O}(x, t) \rangle^{(\lambda)} = \frac{\langle e^{\frac{\lambda}{2} \int_{-\infty}^{\infty} dt j(0, t)} \mathcal{O}(x, t) e^{\frac{\lambda}{2} \int_{-\infty}^{\infty} dt j(0, t)} \rangle_{\underline{\beta}}}{\langle e^{\lambda \int_{-\infty}^{\infty} dt j(0, t)} \rangle_{\underline{\beta}}}, \quad (3.22)$$

where by definition  $\langle \mathcal{O}(x, t) \rangle^{(0)} = \langle \mathcal{O}(x, t) \rangle_{\underline{\beta}}$ . The insertion is symmetrised in order to guarantee that averages of Hermitian observables are real numbers in the quantum case. The importance of this insertion is gleaned by understanding that  $\lambda$ -derivatives will bring down factors of  $j$ ,

$$\frac{d}{d\lambda} \langle \mathcal{O} \rangle^{(\lambda)} = \int_{-\infty}^{\infty} dt \langle j(0, t) \mathcal{O} \rangle^{(\lambda), c}, \quad (3.23)$$

where the  $c$  refers to the connected symmetrised correlation function. With this one can construct correlations involving the total of a transported quantity. This can only be considered as a well-defined, formal expansion in  $\lambda$  if connected correlation functions vanish fast enough at large time separation - i.e. under the assumption that clustering is sufficiently fast.

As a loose physical interpretation, the insertion above allows one to ‘bias’ the dynamics by changing the weights of trajectories in order to make rare events ‘typical’ which allows one to gain access to the probabilities of such events. The biasing by a time-integrated current has been used widely in the study of large deviations in stochastic dynamics or open quantum systems. In fact it is very similar to the generalised (classical or quantum) Doob transformation [91, 92].

The key observation about the newly resulting state is it remains homogeneous and stationary, i.e. a well-defined MES. Since an MES is defined by its Lagrange multipliers, it becomes possible to obtain a function  $\underline{\beta}(\lambda)$  with  $\underline{\beta}(0) = \underline{\beta}$ , where the precise functional form will be defined via the flow equations found in the next section. The stationarity of the state is clear as the time dependence is integrated out. The homogeneity is understood through the fact that  $j(x, t)$  is part of a conservation law. Thus,  $\int_{-\infty}^{\infty} dt j(0, t) = \int_{-\infty}^{\infty} dt j(x, t)$  for any  $x$ , where the resulting state is homogeneous. Thus this biased state is itself an MES i.e. there exists  $\underline{\beta}(\lambda)$  with  $\underline{\beta}(0) = \underline{\beta}$  and

$$\langle \mathcal{O} \rangle^{(\lambda)} = \langle \mathcal{O} \rangle_{\underline{\beta}(\lambda)} = \langle \mathcal{O} \rangle(\lambda). \quad (3.24)$$

This is the crucial observation of the method.

### 3.2.2 Flow equation

The flow equation is a differential equation that defines the functional form of the  $\lambda$ -dependence of a state. This can be defined either at the level of the Euler variables i.e.  $\langle q \rangle_{\underline{\beta}}$  or on the state variables,  $\underline{\beta}$ , explicitly. Both forms are useful in different contexts as will be seen in proceeding chapters.

#### Euler-variable flow equation

To obtain the flow equation on the level of Euler-scale variable one begins with the Euler equation defined for the matrix  $S_{ij}(x, t)$ , (3.8). In what follows,  $S$ ,  $A$  and  $C$  without the sub/superscript  $i, j$  must be understood as a matrix object. To solve this equation consider the Fourier transform  $S(x, t) = \int_{-\infty}^{\infty} dk e^{-ikx} \tilde{S}(k, t)$ . Then the Euler equation on  $\tilde{S}(k, t)$  becomes,

$$\partial_t \tilde{S}(k, t) - ikA\tilde{S}(k, t) = 0. \quad (3.25)$$

As  $A$  and  $\tilde{S}$  are matrices, special care must be taken in solving the above. By considering  $\tilde{S}(k, t)$  column by column, it is easy to see that the solution for column  $i^*$  of this differential equation is simply  $M\tilde{S}_{i^*}(k, t) = e^{ikt\underline{v}^{\text{eff}}} M\tilde{S}_{i^*}(k, 0)$  where  $M$  is the matrix that diagonalises  $A$  and  $\underline{v}^{\text{eff}}$  is the diagonal matrix comprised of the eigenvalues of  $A$ . Clearly, when one considers the full  $\tilde{S}$  matrix the solution is,

$$\tilde{S}(k, t) = M^{-1} e^{ikt\underline{v}^{\text{eff}}} M\tilde{S}(k, 0). \quad (3.26)$$

Since the initial condition is given above from above as  $S(x, 0) = C\delta(x)$ ,  $\tilde{S}(k, 0) = C$ . Consider the inverse Fourier transform and use the fact that the eigenvalues and eigenvectors of  $A$  are not dependent on  $k$ . Doing this,

$$\begin{aligned} S(x, t) &= \int_{-\infty}^{\infty} dk e^{-ikx} M^{-1} e^{ikt\underline{v}^{\text{eff}}} M\tilde{S}(k, 0) \\ &= M^{-1} \int_{-\infty}^{\infty} dk e^{-ik(t\underline{v}^{\text{eff}} - x)} MC \\ &= M^{-1} \delta(t\underline{v}^{\text{eff}} - x) MC, \end{aligned} \quad (3.27)$$

where the  $\delta$ -function constrains each of the eigenvalues individually.

With this expression for  $S(x, t)$  one can use the results of the sum rule with  $f(x) = |x|$ , i.e. (3.21) to obtain

$$\int_0^\infty dt \Gamma(0, t) = \lim_{t \rightarrow \infty} \frac{1}{t} \int dx |x| M^{-1} \delta(t \underline{v}^{\text{eff}} - x) MC. \quad (3.28)$$

Taking care of the matrices it is clear that,

$$\begin{aligned} \int_0^\infty dt \Gamma(0, t) &= \lim_{t \rightarrow \infty} \frac{1}{t} M^{-1} \left| t \underline{v}^{\text{eff}} \right| MC \\ &= |A| C, \end{aligned} \quad (3.29)$$

where, by definition,  $|A| = M^{-1} \left| \underline{v}^{\text{eff}} \right| M$ .

Consider  $\int_0^\infty dt \Gamma_{i^*i}(0, t)$  and  $\langle j_i \rangle_{\underline{\beta}(\lambda)} \equiv j_i(\lambda)$  where  $i^*$  here refers to a fixed index related to the charge of interest. The  $i^*$  index is effectively carried by the  $\lambda$  through its coupling to the transported charge. By definition of the  $\lambda$ -dependent state,

$$\int_0^\infty dt \Gamma_{i^*i}(0, t) = \partial_\lambda \langle j_i \rangle_{\underline{\beta}(\lambda)} = \partial_\lambda j_i(\lambda). \quad (3.30)$$

Then using chain rule with the definition of  $A_i^j = \partial j_i / \partial q_j$ , where  $\langle q_i \rangle_{\underline{\beta}} = q_i$  and explicitly inserting the  $\lambda$ -dependence back in,

$$\partial_\lambda q_i(\lambda) = \sum_j \text{sgn}(A(\lambda))_{i^*}^j C_{ji}(\lambda), \quad (3.31)$$

where  $\text{sgn}(A) \equiv M^{-1} \text{sgn}(\underline{v}^{\text{eff}}) M$ . This is the flow equation for  $q_i(\lambda)$ . Solving this differential equation defines how  $q$  depends on  $\lambda$ . This equation can be used to find a differential equations that defines the function  $\beta^i(\lambda)$ , this is done in the next section.

### State-variable flow equation

Begin by recognising the Euler scale variables as a function of the state variables one can derive a flow equation that is applicable on the level of the state variables. First recall from (3.9),  $C_{ij} = -\partial q_j / \partial \beta^i$ . Then using the chain rule for the first equality and (3.31)



with the definition of  $C_{ij}$  in the second equality,

$$\partial_\lambda q_i = \sum_j \frac{\partial q_i}{\partial \beta^j} \frac{\partial \beta^j}{\partial \lambda} = - \sum_j \text{sgn}(A(\lambda))_i^j \frac{\partial q_i}{\partial \beta^j}, \quad (3.32)$$

which simplifies to the flow equation for the state variables,

$$\frac{\partial \beta^i(\lambda)}{\partial \lambda} = - \text{sgn}(A(\lambda))_{i^*}^i, \quad (3.33)$$

where, again,  $i^*$  refers to the index associated with the current of interest which is implicitly defined by the choice of  $\lambda$ . This differential equation defines the functional form of  $\beta^j(\lambda)$ .

### Characteristic velocity and interpretation of the flow equation

At this stage I highlight the role that the flux Jacobian plays as an effective velocity. Once again I solve (3.8), however in this case I make use of the method of characteristics. To make the expression amenable to this method, I diagonalise  $A$  where  $A = M \underline{v}^{\text{eff}} M^{-1}$  and  $\underline{v}^{\text{eff}}$  is a diagonal matrix with  $v_i^{\text{eff}}$  on the diagonal. With this, (3.8) can be written as,

$$\partial_t S + \underline{v}^{\text{eff}} \partial_x S = 0, \quad (3.34)$$

where  $S \equiv M^{-1} \mathbf{S}$ . I now use the method of characteristics, a common method for solving these types of equations. Since  $\underline{v}^{\text{eff}}$ , by definition, is diagonal the above expression is equivalent to  $\partial_t S_i^j + v_i^{\text{eff}} \partial_x S_i^j = 0$ . One now assumes that there exists some parameter  $u$  such that  $S_i^j$  can be written as  $S_i^j(x(u), t(u))$  and that  $\partial_u S_i^j(x(u), t(u)) = 0$ . Then using the chain rule,

$$\partial_u S_i^j(x(u), t(u)) = \frac{\partial t}{\partial u} \frac{\partial S_i^j}{\partial t} + \frac{\partial x}{\partial u} \frac{\partial S_i^j}{\partial x} = 0, \quad (3.35)$$

which identifies  $\partial t / \partial u = 1$  and  $\partial x / \partial u = v_i^{\text{eff}}$ . The first equation can be solved which identifies  $u = t$  up to a constant. Using this in the second expression,  $\frac{dx}{dt} = v_i^{\text{eff}}$  for  $S_i^j$ . In words  $v_i^{\text{eff}}$  represents the characteristic velocity in the system. The  $\delta$ -function in (3.27) actually enforces this requirement but provides a stronger constraint that this velocity is constant - a fact that is consistent with the space-time independence of  $A_i^j$  in the MES.

This justifies the choice of  $v^{\text{eff}}$  to define the eigenvalues of  $A_i^j$  since the characteristic velocity in a system is known to represent an effective velocity and in these systems this effective velocity is constant. It is known that the characteristic velocity actually represents the velocity of perturbations in the system [93] which means  $A$  is encoding the velocity of perturbations in the system.

### 3.2.3 Fundamental equation

The final piece of the BFF is to use the  $\lambda$ -dependent state defined by the flow equation to determine  $F(\lambda)$ . Taking the  $\lambda$ -derivative of the SCGF, then shifting in the time integration region allowed by stationarity of the state and after symmetrisation produces the following,

$$\frac{dF(\lambda)}{d\lambda} = \lim_{t \rightarrow \infty} \frac{1}{t} \int_{-t/2}^{t/2} ds \frac{\langle e^{\frac{\lambda}{2} \int_{-t/2}^{t/2} dr j(0,r)} j(0,s) e^{\frac{\lambda}{2} \int_{-t/2}^{t/2} dr j(0,r)} \rangle_{\underline{\beta}}}{\langle e^{\lambda \int_{-t/2}^{t/2} dr j(0,r)} \rangle_{\underline{\beta}}}. \quad (3.36)$$

Now assume that as  $t \rightarrow \infty$  the main contribution to the  $s$  integral happens in the bulk and away from the boundaries  $s = \pm t/2$ . This is equivalent to assuming that correlations decay at very large times, the assumption of clustering. Then as the BFF is applied to stationary states, the main contribution to the time integral is in the bulk. Thus, the integrand isn't dependent on time which means,

$$\begin{aligned} \frac{dF(\lambda)}{d\lambda} &= \lim_{t \rightarrow \infty} \frac{1}{t} \int_{-t/2}^{t/2} ds \frac{\langle e^{\frac{\lambda}{2} \int_{-\infty}^{\infty} dr j(0,r)} j(0,s) e^{\frac{\lambda}{2} \int_{-\infty}^{\infty} dr j(0,r)} \rangle_{\underline{\beta}}}{\langle e^{\lambda \int_{-\infty}^{\infty} dr j(0,r)} \rangle_{\underline{\beta}}} \\ &= \frac{\langle e^{\frac{\lambda}{2} \int_{-\infty}^{\infty} dr j(0,r)} j(0,0) e^{\frac{\lambda}{2} \int_{-\infty}^{\infty} dr j(0,r)} \rangle_{\underline{\beta}}}{\langle e^{\lambda \int_{-\infty}^{\infty} dr j(0,r)} \rangle_{\underline{\beta}}} \lim_{t \rightarrow \infty} \frac{1}{t} \int_{-t/2}^{t/2} ds \\ &= \langle j(0,0) \rangle_{\underline{\beta}(\lambda)}, \end{aligned} \quad (3.37)$$

where (3.22) is used for the last equality. Recall  $\langle j \rangle_{\underline{\beta}(\lambda)} \equiv j(\lambda)$  then integrating on  $\lambda$  with the condition  $F(0) = 0$  which is required by normalization of  $F$ ,

$$F(\lambda) = \int_0^\lambda d\lambda' j(\lambda'). \quad (3.38)$$

This expression is a natural generalisation of the relationship between  $F(\lambda)$  and the cumulants of (1.4). This equation, called the fundamental equation of the BFF, provides the link between  $\lambda$ -biased states and the full SCGF. The fundamental equation can be seen as providing a re-summation of the expansion of (1.4) where all the information of the system is contained within a modified current term. As it is defined here it is only expected to hold for MES states and strongly relies on clustering to work.

This concludes the BFF structure. In summary states were biased by the time-integrated current of interest. These states are shown to satisfy a differential equation known as the flow equation. Then the fundamental equation of BFF provides an expression for the re-summation to all orders of  $\lambda$  within a modified current term defined by a state that satisfies the flow equation. In the next three chapters I show how this framework is applied to a classical stochastic system (chapter 4), a higher dimensional system (chapter 5) and finally obtain important new and fundamental results for interacting integrable models (chapter 6). However, before then I will revisit a 1D CFT as introduced in chapter 2 in order to provide a simple example of the use-case of the BFF.

### 3.3 Application of ballistic fluctuation formalism to 1D CFT

In this section I show how to use the BFF in a trivial example that was already introduced in the previous chapter. In this case I will show how to obtain the SCGF for the energy current of a 1D CFT. First I construct and solve the flow equation, in this case it is best to consider the flow equation on the state variables i.e. (3.33). From here using (3.38) will allow for the trivial calculation of the SCGF.

Recall from section 2.1 that the 1D CFT has two charges  $q_1, q_2$  and associated currents  $j_1, j_2$ . It was also shown that, due to Lorentz invariance and scale invariance,  $q_1 = j_2$  and  $q_2 = j_1$ . With this it is trivial to find the flux Jacobian matrix  $A_i^j = \partial j_i / \partial q_j$  such that,

$$A = \begin{pmatrix} 0 & 1 \\ 1 & 0 \end{pmatrix}. \quad (3.39)$$

The eigenvalues of this are  $-1$  and  $1$ . This means  $\text{sgn}(A) = A$ .

Now the state variables are needed. Since there are two independent charge densities  $q_1$  and  $q_2$  the MES is defined by two Lagrange multipliers such that,

$$\rho_{\text{local}} = e^{-\beta^1 \int dx q_1 + \beta^2 \int dx q_2}, \quad (3.40)$$

where the signs are chosen by convention since  $q_1$  refers to the energy density and  $q_2$  refers to the momentum density. Now consider (3.33) for the energy flow, this corresponds to choosing  $i^* = 1$  and thus the first row of A such that,

$$\partial_\lambda \begin{pmatrix} \beta^1 & \beta^2 \end{pmatrix} = \begin{pmatrix} 0 & -1 \end{pmatrix}. \quad (3.41)$$

Thus

$$\beta^1(\lambda) = \beta^1, \quad \text{and} \quad \beta^2(\lambda) = -\lambda + \beta^2 \quad (3.42)$$

where I have used  $\beta^1(0) \equiv \beta^1$  and  $\beta^2(0) \equiv \beta^2$ . In principle one can now use (3.38), however this requires the explicit dependence of the current on  $\beta^1$  and  $\beta^2$ . In order to obtain a result it is best to recall from section 2.1 that there exists a chiral symmetry defined by the charges  $T = (q_1 + q_2)/2$  and  $\bar{T} = (q_1 - q_2)/2$ . By rewriting the density matrix,

$$\rho_{\text{local}} = e^{-\beta_r \int dx T + \beta_l \int dx \bar{T}}, \quad (3.43)$$

where  $-\beta_r = (\beta^1 + \beta^2)/2$  and  $\beta_l = (\beta^2 - \beta^1)/2$ . The reason for the subscripts is due to the time evolution of  $T$  and  $\bar{T}$  from (2.6) these charges are understood to describe separate left and right movers in the system. If the steady state of interest is obtained by the partitioning protocol it is easy to understand that the Lagrange multipliers are associated with the initial bath temperatures. Then converting (3.42) into these variables,

$$\beta_r(\lambda) = \beta_r + \lambda, \quad \text{and} \quad \beta_l(\lambda) = \beta_l - \lambda. \quad (3.44)$$

The form of the energy current in the partitioning protocol is known as was displayed in

(2.7). With this one can directly insert into (3.38) to obtain

$$F(\lambda) = \frac{c\pi}{12} \left( -\frac{1}{\beta_r} + \frac{1}{\beta_r + \lambda} - \frac{1}{\beta_l} + \frac{1}{\beta_l - \lambda} \right), \quad (3.45)$$

exactly that of (2.17) at  $p = 1$  as required. Thus, as a first trivial check the BFF is capable of producing known results for a 1D CFT. Interestingly (3.44) exactly defines the extended fluctuation relation. This leads to the next section where I show how the BFF provides the exact circumstances under which the extended fluctuation relations are expected.

### 3.4 Extended fluctuation relation revisited

This section closely follows my work in [51, section 3.3].

I recall the form of the extended fluctuation relation (EFR) from (2.27) for ease of reference,

$$F(\lambda) = \int_0^\lambda d\lambda' \langle j \rangle_{\{(\beta_l^\bullet - \lambda \delta_{i^*}^\bullet, \beta_r^\bullet + \lambda \delta_{i^*}^\bullet)\}}, \quad (3.46)$$

where  $\beta_l$  and  $\beta_r$  are the inverse temperatures of the partitions in the partitioning protocol. I show that a system with a flux Jacobian,  $A_i^j$ , that is independent of the state variables in an MES produced by the partitioning protocol results in the EFR being satisfied. The exact scale of applicability of the EFRs was not known until our work of [51].

Consider the case where the flux Jacobian is independent of the state variables  $\{\beta^i(x, t)\}$ , which is known to be true for non-interacting models and 1D CFT as presented in the previous section. Such a scenario results in linear Euler hydrodynamic equations, since  $A_i^j$  is independent of  $q$ , and leads to the idea that this case may be considered a hydrodynamic system without interactions. In such cases, it is a simple matter to solve the flow (3.33):

$$\beta^i(\lambda) = \beta^i - \lambda \operatorname{sgn}(A)_{i^*}^i. \quad (3.47)$$

That is, the flow corresponds to a shift of the Lagrange parameters proportional to  $\lambda$  (notice consistency with (3.42)). In particular, from the fundamental BFF equation (3.38),

$$F(\lambda) = \int_0^\lambda d\lambda' \langle j \rangle_{\{\beta^\bullet - \lambda' \operatorname{sgn}(A)_{i^*}^\bullet\}}. \quad (3.48)$$

In order to confirm the EFR I now show how this applies to a system in the partitioning protocol.

In the case where  $A_i^j$  is independent of the state it was shown above that the Euler hydrodynamic equations become linear. This allows for a solution to these equations in the case of the partitioning protocol, and the evaluation of the steady state in the region around the connection point. I begin by finding an Euler equation for the state variables  $\beta$ . Since  $\langle q \rangle_{\underline{\beta}} = q(\underline{\beta})$ , then using chain rule on the Euler equation, (1.40), and the fact that  $A_i^j$  is independent of  $\underline{\beta}$  to write:

$$\partial_t \beta^i(x, t) + \sum_j \partial_x \beta^j(x, t) A_j^i = 0. \quad (3.49)$$

As was done in above sections, diagonalise  $A_j^i$  through  $\sum_i A_j^i M_{ik} = v_k^{\text{eff}} M_{jk}$ . This results in,

$$\partial_t n_k(x, t) + v_k^{\text{eff}} \partial_x n_k(x, t) = 0. \quad (3.50)$$

where,

$$n_k = \sum_i \beta^i M_{ik}, \quad (3.51)$$

The states  $n_k$  are known as the normal modes of the system. These are states in a special co-ordinate system that diagonalise the Flux Jacobian and render the hydrodynamics simpler. With these modes it is easier to solve the hydrodynamic equation on the level of the state variables.

Since I am interested in the solution to the Euler equations under the partitioning protocol, the initial conditions are given by the two distinct equilibrium states, one on the left, one on the right defined by independent Lagrange multipliers defining inverse temperature. Thus,

$$\beta^i(x, 0) = \begin{cases} \beta_l^i & (x < 0) \\ \beta_r^i & (x > 0). \end{cases} \quad (3.52)$$

Then on the Euler scale, both the initial condition in the partitioning protocol and the Euler equation are invariant under the scaling  $(x, t) \mapsto (vx, vt)$  which means the solution to the partitioning protocol problem must have this symmetry as well. Thus, all functions of space time are functions of  $\xi = x/t$  only. Changing variables to  $\xi$  and recognising

that since  $n_k$  is a function of  $\beta$ , it is now a function of  $\beta_l, \beta_r$ ,

$$(\xi - v_k^{\text{eff}}) \partial_\xi n_k(\xi; \underline{\beta}_l, \underline{\beta}_r) = 0. \quad (3.53)$$

The solution is simple to obtain

$$n_k(\xi; \underline{\beta}_l, \underline{\beta}_r) = \begin{cases} n_{k;l} & (\xi < v_k^{\text{eff}}) \\ n_{k;r} & (\xi > v_k^{\text{eff}}) \end{cases}, \quad (3.54)$$

where  $n_{k;l}$  and  $n_{k;r}$  are the normal modes in the states specified by the Lagrange parameters  $\underline{\beta}_l$  and  $\underline{\beta}_r$ , respectively. In the partitioning protocol the point of interest is the contact point, where  $x = 0$ , this translates to the ray  $\xi = 0$ . For ease of notation, I denote  $n_k(0; \underline{\beta}_l, \underline{\beta}_r) = n_k(\underline{\beta}_l, \underline{\beta}_r)$ . Now consider the solution to the flow equation, (3.47), and again diagonalise  $A_i^j$  using the normal modes, (3.51), this results in,

$$n_k(\underline{\beta}_l, \underline{\beta}_r; \lambda) = n_k(\underline{\beta}_l, \underline{\beta}_r) - \lambda \text{sgn}(v_k^{\text{eff}}) M_{i^*k}. \quad (3.55)$$

Finally, using (3.54) in the above,

$$n_k(\underline{\beta}_l, \underline{\beta}_r; \lambda) = \begin{cases} n_{k;l} + \lambda M_{i^*k} & (0 < v_k^{\text{eff}}) \\ n_{k;r} - \lambda M_{i^*k} & (0 > v_k^{\text{eff}}) \end{cases} = n_k(\beta_l^\bullet - \lambda \delta_{i^*}^\bullet, \beta_r^\bullet + \lambda \delta_{i^*}^\bullet), \quad (3.56)$$

where  $\bullet$  refers to the set of all possible indices. Then simply by observing the argument of  $n_k$  above and considering (3.47) one finds,

$$\beta^i(\beta_l^\bullet, \beta_r^\bullet) - \lambda \text{sgn}(A)_{i^*}^i = \beta^i(\beta_l^\bullet - \lambda \delta_{i^*}^\bullet, \beta_r^\bullet + \lambda \delta_{i^*}^\bullet). \quad (3.57)$$

This combined with (3.48), is the fully general statement of the EFR. The EFR describes fluctuations that can be obtained through a linear bias of the initial states described by  $\beta_l$  and  $\beta_r$ . Since all fluctuations are effectively described by only the initial states, the EFR implies initial-state fluctuations are not affected during transport. This leads to the interpretation that the EFR holds for hydrodynamic systems that do not interact and is a direct consequence of  $A_i^j$  being state independent. This further shows that the BFF fully agrees with known results, and that, effectively, it generalises the EFR to linear Euler

hydrodynamics.

### 3.5 Co-propagating modes and dynamical phase transitions

This section closely follows my work in [51, section 3.5].

At certain mode velocities the BFF predicts anomalous behaviour in the SCGF that may indicate the existence of dynamical phase transitions in the system. These transition points seem to be as a result of the breaking of clustering in the system.

Recall that normal modes of the system are those that diagonalise  $A_i^j$  and thus are modes that move with velocity  $v^{\text{eff}}$ . Further, recall the previous section where it was shown that at Euler scale,  $q(x, t) = q(\xi)$  with  $\xi = x/t$ . I will refer to  $\xi$  as a ray.

The BFF considers transport of some conserved quantity through  $x = 0$  which corresponds to the ray  $\xi = 0$ . The formalism indicates that when modes travel along the ray  $\xi = 0$  one obtains dynamical phase transitions as introduced in section 1.2.2. In [94–99] a dynamical phase transition is found to occur when there is a change in the behaviour of fluctuations for a dynamical quantity through a modification of some state parameter. To observe this behaviour in the BFF I consider the current-cumulants gained from the  $\lambda$ -biased states. By definition, each  $\lambda$ -derivative of these states brings down a factor  $\int dy j(y, 0)$  resulting in  $\partial_\lambda^n j$  producing the  $n^{\text{th}}$  cumulant. In order to obtain these cumulants one requires derivatives of the right-hand-side of the flow equation. For instance calculation of the third moment requires the  $\lambda$ -derivative of  $\text{sgn}(v^{\text{eff}}(\lambda))$  - where normal modes are considered since  $A_i^j$  has been diagonalised. This calculation is valid except when  $v^{\text{eff}}(\lambda) = 0$  since this requires the gradient of the sign-function at its discontinuity. Moreover the results obtained for  $c_3$  will be different if  $v^{\text{eff}}(\lambda)$  is positive versus if it is negative. This is exactly the type of behaviour one expects from a phase transition as a change in the state parameter  $\lambda$  causes a change in  $v^{\text{eff}}$  resulting in appreciably different behaviour in system fluctuations.

The cause of this phase transition may be due to the breaking of one of the fundamental requirements for the BFF, that of sufficient clustering. Consider (3.27), from which it is clear that if the system has a mode travelling along the ray i.e.  $\xi = v^{\text{eff}}$ , then one has a  $\delta$ -function evaluated at 0 and  $S_{ij}$  diverges. Since  $S_{ij}$  is the field-field correlation



a divergence in this object may be interpreted as correlations not clustering fast enough. In the BFF transport is usually considered along the ray  $\xi = 0$  and it is when a mode travels along this ray that one observes anomalous behaviour in the system fluctuations.

Physically this picture can be explained. In the Euler scaling limit there is no diffusion of modes, thus  $v^{\text{eff}}$  can be considered the effective velocity of the ballistic propagation of normal modes of a fluid, a physical example of which is pressure waves in air i.e. sound waves. With this understanding, it is clear that physically there may exist ballistically propagating normal modes that create very strong correlations along their paths. In fact, such concepts are known in general and are sometimes referred to as “sound peaks”, or “heat peaks”. Interestingly, and importantly for later developments, such strong correlations also occur naturally in rarefaction waves, the waves following a shock wave [100]: there, the state at ray  $\xi$  is such that  $v_j^{\text{eff}} = \xi$  for some  $j$ . From here on I call any modes that propagate along a ray as a “co-propagating mode”.

One subtle point is worth mentioning, from results obtained in later chapters, it seems as though in order for a phase transition to occur, the co-propagating mode should be “isolated”. It is easiest to define isolated as the opposite of a non-isolated mode. A non-isolated mode is a mode that is one of a continuum of effective velocities, that are smoothly populated and coupled to the transport of the charge of interest. In the case of non-isolated modes, one doesn’t obtain a divergence as there is a smoothing. For instance, as is seen in the case of integrable models discussed in chapter 6, one sums over all modes through an integral, this integral can be used to resolve the discontinuities resulting from the sign function. However there may still be situations where isolated effective velocities may be present in integrable systems, for instance for spin transport in the XXZ spin chain [101], and it might be possible to study transport of charges that couple to a single quasi-particle velocity.

This observation of co-propagating modes may make a connection with nonlinear fluctuating hydrodynamics [49, 50, 102]. Nonlinear fluctuating hydrodynamics can be used to describe the growth of correlations that occur for co-propagating modes, as well as correlations in rarefactions waves. In these models, hydrodynamic equations with an added noise term are considered. At first order expansion of these hydrodynamic equations one usually observes a specific type of behaviour (Gaussian fluctuations) however,

if there exists a co-propagating mode there is a complete change in the type of fluctuations as this first order term vanishes and fluctuations are driven by the second order in the expansion (in this case fluctuations belong to the KPZ class). Although BFF does not confirm the KPZ class of fluctuations predicted by non-linear fluctuating hydrodynamics it certainly is in agreement that there is a fundamental change in behaviour along the co-propagating modes.

### 3.6 Normal mode decomposition of SCGF

This section closely follows my work in [51, Appendix C].

This section is important and it indicates one of the few general results known about  $F(\lambda)$ . In certain cases, even beyond free models, one can obtain an explicit expression for  $F(\lambda)$ . This occurs when the integral in (3.38) is performed in terms of the normal modes of the Euler hydrodynamics of the model.

It was stated above that normal modes are defined by (3.51) and diagonalise the flux Jacobian  $A$ . This definition of the normal modes is equivalent to the following,

$$\underline{v}^{\text{eff}} = \frac{\partial \underline{\beta}}{\partial \underline{n}} A \frac{\partial \underline{n}}{\partial \underline{\beta}}, \quad (3.58)$$

found by taking a derivative with respect to  $\underline{\beta}$  on both sides of the first equation in (3.51) and placed into the second expression.

One starts with a function that can be used to generate currents, the equivalent of a specific free energy for currents [89],

$$j_i = -\frac{\partial g}{\partial \beta^i}, \quad (3.59)$$

where  $g$  is the generating functional. If  $g$  can be written as a sum of independent functions of the normal modes, then one obtains an analytical expression for  $F(\lambda)$ . Specifically, if

$$g = \sum_i G_i(n_i). \quad (3.60)$$

with  $G_i$  some function. This property remains poorly understood and is only known on a case by case basis, for example generalised hydrodynamics, which is discussed in section 6.1.2, has this property. On the other hand I will show CFTs with more than one

dimension do not have this property, as discussed in section 5.4.

When (3.60) is satisfied, the SCGF is given by

$$F(\lambda) = \sum_i \left( \text{sgn}(v_i^{\text{eff}}(\lambda)) \left( G_i(n_i(\lambda)) - G_i(n_i(0)) \right) - \int_0^\lambda d\lambda' \delta(v_i^{\text{eff}}(\lambda')) \partial_{\lambda'} v_i^{\text{eff}}(\lambda') \left( G_i(n_i(\lambda')) - G_i(n_i(0)) \right) \right) \quad (3.61)$$

This result matches the result I will present in chapter 6 for generalised hydrodynamics. The proof of (3.61) is obtained by treating the above as an ansatz and showing the derivative of this SCGF produces a current via (3.59) thus satisfying the fundamental equation in BFF, (3.38), and is correctly normalised.

The  $\lambda$ -derivative of (3.61) requires  $\partial_\lambda G_i(n_i(\lambda))$ . To begin I use chain rule to obtain,

$$\partial_\lambda G_i(n_i(\lambda)) = \sum_j \frac{\partial n_j}{\partial \lambda} \frac{\partial G_i(n_i)}{\partial n_j}. \quad (3.62)$$

From (3.60) it is clear that  $\partial G_i(n_i)/\partial n_j = (\partial g/\partial n_j) \delta_i^j$  with Kronecker  $\delta$ -function. Then starting with the chain rule again and making use of (3.59), the flow equation and (3.58),

$$\begin{aligned} \partial_\lambda G_i(n_i(\lambda)) &= \frac{\partial n_i}{\partial \lambda} \frac{\partial g}{\partial n_i} \\ &= - \sum_{j,k} \frac{\partial n_i}{\partial \beta^k} \frac{\partial \beta^k}{\partial \lambda} \frac{\partial \beta^j}{\partial n_i} j_j \\ &= \sum_{j,k} \frac{\partial n_i}{\partial \beta^k} \text{sgn}(A^T)^k_{i^*} \frac{\partial \beta^j}{\partial n_i} j_j \\ &= \text{sgn}(v_i^{\text{eff}}) \frac{\partial n_i}{\partial \beta^{i^*}} \sum_j \frac{\partial \beta^j}{\partial n_i} j_j, \end{aligned} \quad (3.63)$$

where the second equality is found via the chain rule with (3.60) and (3.59), the third from using the flow equation and the fourth uses (3.58).

I now turn back to proving (3.61) is a valid expression. The derivative on the first line of (3.61) produces (3.63) while also producing a  $\delta$ -function term from the derivative of  $\text{sgn}(v_i^{\text{eff}})$ . Using the Leibniz integration rule, the term in the second line of (3.61) produces one term that exactly cancels the  $\delta$ -function term produced from the first line

and a term that results in  $\left(G_i(n_i(0)) - G_i(n_i(0))\right) = 0$ . Thus terms cancel except for the results of (3.63). Thus,

$$\partial_\lambda F(\lambda) = \sum_i \text{sgn}(v_i^{\text{eff}}) \partial_\lambda G_i(n_i(\lambda)) = \sum_{i,j} \frac{\partial n_i}{\partial \beta^{i*}} \frac{\partial \beta^j}{\partial n_i} j_j = j_{i^*}, \quad (3.64)$$

which correctly obtains the current but depends on the normal mode decomposition of (3.60). Importantly, it is also trivially true that  $F(0) = 0$ , ensuring the correct normalization exists in this result. This completes the proof. I now provide at least one condition that is required for the decomposition of (3.60).

### Decomposition of (3.60)

Although this is not a proof of all circumstances under which (3.60) is true, it provides at least one condition which should be satisfied. This will prove useful in chapter 5 where it will be shown that the decomposition of (3.60) fails on the grounds laid out in this section. Consider  $g$  in (3.59) as a function of the normal coordinates  $\underline{n}$ . Under certain assumptions,  $\partial g / \partial n_i$  is independent of  $n_j$  for  $j \neq i$ . This would imply the decomposition (3.60).

For this argument, consider the multi-parameter SCGF, i.e. a differentiable SCGF  $F(\underline{\lambda})$  for the transport of all charges  $Q_j$ , each associated to  $\lambda_j$ . Then assume there is an associated multi-parameter flow defined by,

$$\frac{\partial \beta^i}{\partial \lambda_j} = -\text{sgn}(A)_j^i. \quad (3.65)$$

Clearly the results that follow rests on these assumptions. With the multi-flow, (3.65), and combining with  $\partial_\lambda F(\lambda) = j(\lambda)$ , (3.38), then assuming the matrix  $\partial \underline{\beta} / \partial \underline{\lambda}$  is invertible,

$$\frac{\partial F}{\partial \underline{\beta}} \text{sgn}(A^T) = \frac{\partial g}{\partial \underline{\beta}}, \quad (3.66)$$

where  $\partial_{\underline{\beta}} F$  and  $\partial_{\underline{\beta}} g$  are line vectors. Then changing variables,

$$\frac{\partial F}{\partial \underline{n}} \frac{\partial \underline{n}}{\partial \underline{\beta}} \text{sgn}(A^T) \frac{\partial \underline{\beta}}{\partial \underline{n}} = \frac{\partial g}{\partial \underline{n}}, \quad (3.67)$$

and using (3.58) this gives

$$\frac{\partial F}{\partial \underline{n}} = \frac{\partial g}{\partial \underline{n}} \text{sgn}(v^{\text{eff}}). \quad (3.68)$$

Differentiability of  $F$  at the points where  $\text{sgn}(v^{\text{eff}})$  changes are ill-defined due to co-propagating modes. However, away from these points, it is natural to assume that  $F$  is differentiable. Consider therefore taking in (3.68) another derivative with respect to the normal modes, away from the points where the effective velocity changes sign,  $\text{sgn}(v_j^{\text{eff}})$  has zero derivative and,

$$\frac{\partial^2 F}{\partial n_i \partial n_j} = \frac{\partial^2 g}{\partial n_i \partial n_j} \text{sgn}(v_j^{\text{eff}}). \quad (3.69)$$

Since the left-hand side is symmetric by differentiability of  $F$ ,

$$\frac{\partial^2 g}{\partial n_i \partial n_j} (\text{sgn}(v_i^{\text{eff}}) - \text{sgn}(v_j^{\text{eff}})) = 0. \quad (3.70)$$

With  $i \neq j$ , in states where the signs of  $v_i^{\text{eff}}$  and  $v_j^{\text{eff}}$  are different, this implies

$$\frac{\partial^2 g}{\partial n_i \partial n_j} = 0. \quad (3.71)$$

Suppose that for each  $i > j$ , there exists a neighbourhood of states such that  $\text{sgn}(v_i^{\text{eff}}) \neq \text{sgn}(v_j^{\text{eff}})$ . Then (3.71) will hold in all these neighbourhoods, for the corresponding  $(i, j)$ . Suppose also that for all  $j$  and all  $i$ , the function  $\partial g / \partial n_j$  is analytic in  $n_i$ , then by analytic continuation, one would have (3.71) for all  $\underline{n}$ , and therefore (3.60).

## Chapter 4

# Fluctuations in the $\ell$ -TASEP

In this chapter I present the results of using the BFF in the classical lattice gas system, the Totally Asymmetric Exclusion Process with particles of length  $\ell$  lattice units. This is a generalisation of the well-known Totally Asymmetric Exclusion Process (TASEP) where  $\ell = 1$ . The TASEP has been important in the study of non-equilibrium systems as it provides a relatively simple model which contains time-irreversible dynamics. The successful application of the BFF in this system indicates the powerful unifying description provided by the BFF.

Specifically, in this chapter, I provide a new result of the SCGF for particle current transport in the case  $\ell > 1$  while simultaneously exploring aspects of the BFF. Possibly the most important outcome of this chapter is the successful application of the BFF to a system that contains stochastic dynamics and the relation between the BFF and phase transitions. The contents of this chapter form the basis of original but as of now unpublished work.

I will begin with an overview of the  $\ell$ -TASEP, then calculate the SCGF for particle current in the  $\ell$ -TASEP. Finally, I discuss the implications on the BFF for the results obtained.

### 4.1 $\ell$ -TASEP

The Totally Asymmetric Exclusion Process (TASEP) is one of the paradigmatic models for non-equilibrium systems as it is a simple model that produces non-trivial currents, the hallmark of a non-equilibrium state. When  $\ell = 1$ , the  $\ell$ -TASEP is equivalent to the usual TASEP. The  $\ell$ -TASEP was originally introduced in [53] in order to model the biological

process of ribosomes moving from codon to codon along an m-RNA template, reading off genetic information and thereby generating the protein step by step. In this section I provide an overview of the  $\ell$ -TASEP.

#### 4.1.1 $\ell$ -TASEP primer

The  $\ell$ -TASEP is a 1D lattice gas comprised of particles of length  $\ell$  where  $\ell$  refers to the number of lattice sites covered by a single particle, hence at  $\ell = 1$  the TASEP is recovered. These particles can only hop to sites that are unoccupied by other particles, this gives rise to the name exclusion interaction. Assuming a hop is allowed to occur (i.e. to an empty site) then a hop to the right occurs with a rate  $p = 1$  and in the  $\ell$ -TASEP particles cannot move to the left. One can consider two different types of boundary conditions, periodic or open. In the periodic case one can think of the lattice as a ring where system dynamics are defined by the initial density of particles. In the open case the system is defined by feeding and exit rates to the lattice where particles enter the system on the left with rate  $\alpha$  (assuming there are  $\ell$  free lattice sites) and exit on the right with rate  $\beta$ , see figure 4.1 for the open case. Importantly, the current statistics in the periodic system are equivalent to those in the bulk of the open system when the system is very large,  $L \rightarrow \infty$ . This equivalence arises due to the relation between the entry rate and exit rate and the initial density of the system - this relation is discussed in more detail in the next section. Specifically, the particle transport in the middle of a large system (far away from boundaries) will be shown to depend on the system initial density. Then assuming a large enough system this transport is the same whether this initial density is constructed via  $\alpha$  and  $\beta$  or is simply the initial state of the system, as is the case in the periodic case. The results of this chapter can be generalised to the  $\ell$ -ASEP where  $p > q$ <sup>1</sup>, which allows for particles to move to the left and for other boundary rates, but this only increases the complexity without a corresponding increase in understanding so I confine discussion to the  $\ell$ -TASEP [103].

Recall the BFF predicts transport in a system governed by the Euler-scale hydrodynamics. Fortunately, the  $\ell$ -TASEP has been studied in this limit with Euler hydrodynamic equations [104–106].

---

<sup>1</sup>Specifically the weakly-asymmetric exclusion process with  $p \approx q$  cannot be treated by the BFF due to strong diffusive effects.

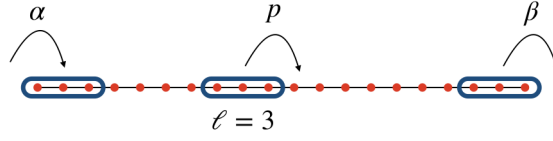


**Figure 4.1:** Depiction of open  $\ell$ -TASEP with  $\ell = 3$ . Describes a system of particles of length  $\ell$  hopping to the right with rate  $p$ . The particles can't overlap so no hop will take place if adjacent site is occupied. The particles enter the system with rate  $\alpha$  on the left and exit with rate  $\beta$  on the right. In the TASEP considered I use  $p = 1$ .

In the  $\ell$ -TASEP the density of particles is the conserved charge in the hydrodynamic limit where, to be clear, density is the fraction of particles per lattice unit,  $N/L$ . In order to maintain consistency with convention, instead of using  $q$  for the conserved charge, I will use the notation  $\rho$ . The steady state current will still be referred to as  $j$ . A vast simplification in the  $\ell$ -TASEP is there exists only one conserved charge,  $\rho$ , which means objects like the flux Jacobian  $A_i^j$  and the static correlation matrix  $C_{ij}$  from the previous section become numbers and the Euler equations are,

$$\partial_t \rho(x, t) + A \partial_x \rho(x, t) = 0, \quad \text{with } j(x, t) = j(\rho(x, t)). \quad (4.1)$$

Finally, in order to apply the BFF, I make the assumption that in the long time limit the system is in an MES which allows for the application of the BFF results in this context.

#### 4.1.2 Phases in the $\ell$ -TASEP

An important property of the  $\ell$ -TASEP in the hydrodynamic limit is the existence of three distinct phases, the high density, low density and maximal current phases. The phase diagram in the open system is determined by the feeding and exit rates, see fig. 4.2. In the closed system the phases are defined purely in terms of the initial density. Focusing on the open system allows for a deeper understanding of the formation of phases in the system where this provides greater insights when applying the BFF.

The low density phase is defined by a lower feeding rate  $\alpha$  and larger exit rate  $\beta$  such that the feeding rate dominates the picture since particles are able to leave the system quicker than they enter, corresponding to a lower density. When the feeding rate is high and the exit rate is low more particles are entering the system than leaving it, and the system is defined by the exit rate which results in higher system density. The



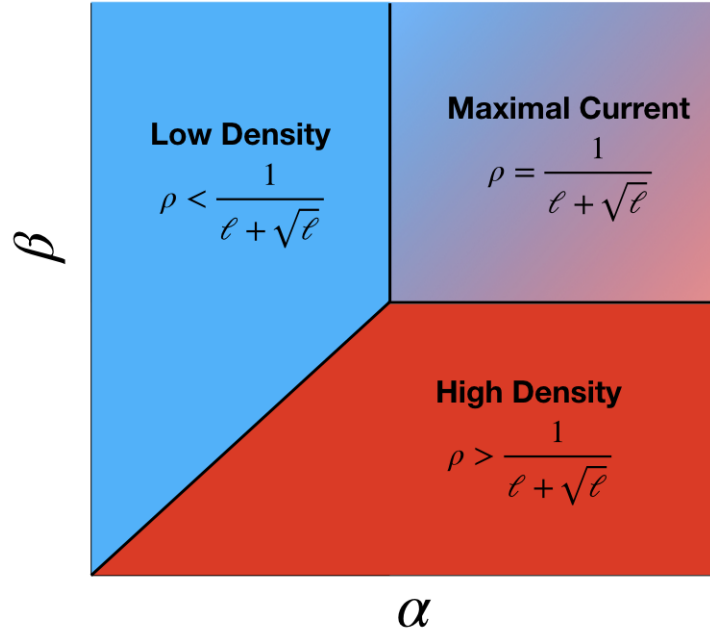


**Figure 4.2:** Phase diagram for the open boundary  $\ell$ -TASEP for the bulk of the system.

maximal current phase is an anomalous phase where the system obtains its maximum possible current [93]. It will be shown that the BFF is incapable of providing insights into the maximal current phase as the maximal current phase corresponds to the presence of co-propagating modes.

### 4.1.3 Mapping to zero range process

For the BFF to be applied one needs to either find or derive the Euler hydrodynamic description of the system, with particular importance attached to finding the equations of state i.e. the functional dependence of  $j$  on  $q$  or in this case  $\rho$ . The equations of state allow for the use of the BFF fundamental equation (3.38) as I obtain  $\rho(\lambda)$  from the flow equation (3.31). Hydrodynamic equations for the  $\ell$ -TASEP have been obtained via a mapping to the zero-range process (ZRP). The ZRP is a different lattice gas system originally introduced in [107] as a model system for interacting random walks. In this process any number of particles can occupy a single lattice site and hopping rates of a particle are only affected by the particle density on the occupied site [108, 109]. The hydrodynamic description of the  $\ell$ -TASEP involves mapping the  $\ell$ -sized particles to holes in the ZRP, I provide details of the ZRP and its mapping to the  $\ell$ -TASEP in

appendices C.1 and C.2 respectively. This mapping allows one to use the stationary product measure of the ZRP to derive its hydrodynamics equations. Due to the presence of site correlations in the  $\ell$ -TASEP there isn't a stationary product measure, however as the ZRP contains only zero-range interactions it has this property. Thus, by exploiting the existing mapping to the ZRP one can obtain the hydrodynamic description of the  $\ell$ -TASEP [104]. Since there exists a hydrodynamic description of the ZRP one can obtain a BFF description in this system too, I obtain a flow equation for the ZRP in appendix C.1.

## 4.2 SCGF for particle current in $\ell$ -TASEP

In this section I will make use of the BFF in order to determine the particle-current SCGF in the  $\ell$ -TASEP. At  $\ell = 1$  the current SCGF is known in the literature [110, 111]. In this chapter I show that using the BFF correctly reproduces the known result providing a further consistency check on the method, new results are then obtained for  $\ell > 1$ .

The BFF description requires two equations, the flow equation (3.31) and the BFF fundamental equation (3.38). The  $\ell$ -TASEP is naturally written in terms of  $\rho$  including the equations of state and the static-correlations  $C$ . Thus for the  $\ell$ -TASEP I obtain the flow equation on the density  $\rho$ , as opposed to the Lagrange parameters (3.33). In principle one should be able to perform this calculation using the Lagrange multiplier however it is not obvious how to express this.

### 4.2.1 BFF equations for $\ell$ -TASEP

In this section I present the known hydrodynamic quantities of the  $\ell$ -TASEP required for the BFF equations.

#### Macroscopic observables

The flow equation, (3.31) requires knowledge of both the static correlation function  $C$  and the flux Jacobian  $A$  which in this case are both simply numbers. The expression for  $C$  in the  $\ell$ -TASEP is known in terms of the system fugacity,  $z$ . Fugacity is defined by the system's non-equilibrium partition function  $Z$  [104],

$$Z = \sum_{n=0}^{N_{\max}} z^n Z_n, \quad (4.2)$$

where  $Z_n$  is the  $n$ -particle partition sum and the sum is over the possible number of particles in the system with  $N_{\max}$  representing the maximum number. Using the partition function and specifically the fugacity,

$$C = z \frac{\partial \rho}{\partial z}. \quad (4.3)$$

This quantity is also known as the compressibility of the system [104, 112]. Clearly the form of  $z(\rho)$  will be important and in appendix C.2 I report a derivation of the fugacity-density relationship from [106]. The result is presented here,

$$z = \frac{\rho(1 - (\ell - 1)\rho)^{\ell-1}}{(1 - \ell\rho)^\ell}. \quad (4.4)$$

Although these were derived for a system with periodic boundary conditions, as stated above, in the hydrodynamic limit the dynamics in the bulk of the open system is equivalent to the closed system which allows for the direct application of these results in the open system.

Recall that  $A = \partial j / \partial q$ , (3.5), thus in order to obtain  $A$ , the equations of state (functional form) of  $j(\rho)$  in the  $\ell$ -TASEP is required. This is also necessary for the fundamental equation, (3.38). Note again that  $A$  is now simply a number, not a matrix. In appendix C.2 I sketch the derivation of this expression from [104], the result of which gives,

$$j(\rho) = \frac{\rho(1 - \ell\rho)}{1 - (\ell - 1)\rho}, \quad (4.5)$$

where at  $\ell = 1$  the well-known steady-state current in the TASEP is recovered. Using this expression,

$$A = \frac{\partial j}{\partial \rho} = \frac{l\rho((l - 1)\rho - 2) + 1}{((l - 1)\rho - 1)^2}. \quad (4.6)$$

### The flow equation

Recall the flow equation defines the relationship between  $\rho$  and the conjugate-parameter  $\lambda$  of the SCGF. In this section I find the flow equation for  $\rho$  and provide solutions to this differential equation.

Starting with (3.31), insert (4.3) on the right-hand side, and use the chain rule on

the left-hand side in order to obtain,

$$\partial_\lambda z(\lambda) = \text{sgn}(A(\lambda))z(\lambda), \quad (4.7)$$

which can be understood as the flow equation for  $z$ . This shows there exists a simple relationship between  $z$  and  $\lambda$ , specifically depending on the sign of  $A$ ,  $z \propto e^{\pm\lambda}$ . Solving this to obtain an explicit expression for  $\rho(\lambda)$  requires knowing  $d\rho/d\lambda$  so either way the flow equation on  $\rho$  is required. Using the chain rule on (4.7) gives a flow equation for  $\rho$ ,

$$\partial_\lambda \rho(\lambda) = \left( \frac{\partial z}{\partial \rho} \right)^{-1} \text{sgn}(A(\lambda))z(\rho(\lambda)). \quad (4.8)$$

This equation can be solved using (4.4) and (4.6),

$$\chi^{-1}e^\lambda = \frac{\rho(1-(\ell-1)\rho)^{\ell-1}}{(1-\ell\rho)^\ell}, \quad \text{where } \rho < \frac{1}{\ell+\sqrt{\ell}} \quad (4.9)$$

$$\chi'e^{-\lambda} = \frac{\rho(1-(\ell-1)\rho)^{\ell-1}}{(1-\ell\rho)^\ell}, \quad \text{where } \rho > \frac{1}{\ell+\sqrt{\ell}} \quad (4.10)$$

where  $\chi$  and  $\chi'$  are constants to be fixed and the choice of using  $\chi^{-1}$  proves convenient later. The above expressions rely on the existence of a constraint on the particle density,  $\rho \leq \frac{1}{\ell}$  which comes from noticing  $\ell \times N < L$  where  $N$  is the number of particles and  $L$  is the length of the system. Interestingly there exist ill-defined results at the points where  $\rho = \frac{1}{\ell+\sqrt{\ell}}$ , which indicates a phase transition at these points. This phase transition may be related to co-propagating modes as introduced in section 3.5, this connection is elaborated on in section 4.3. Phase transitions at these points are known to exist in the  $\ell$ -TASEP, see fig. 4.2. Here (4.9) represents a low density phase and (4.10) a high density phase. As the BFF leaves  $\rho(\lambda)|_{\rho=1/(\ell+\sqrt{\ell})}$  ambiguous, it is not possible to obtain results in the maximal current phase and the following sections will concentrate on only the low and high density phases. This is discussed in more detail in section 4.3.

Armed with an expression for  $\rho(\lambda)$ , this can be inserted into (4.5) and used with (3.38) to obtain the current SCGF. Unfortunately, the above expressions can't be solved for  $\rho$  which means there isn't an analytic expression for the SCGF for general  $\ell$ , however using the flow equation it is possible to find general expressions for the cumulants.

### 4.2.2 Cumulants

Current scaled cumulants are found by taking  $\lambda$ -derivatives of (4.5) and setting  $\lambda = 0$  where  $\rho \rightarrow \rho(\lambda)$ , see (1.4). Analytical expressions are obtained by using (4.8) to express resulting  $\partial_\lambda \rho$  in terms of  $\rho$ . Doing this it is found in the low density phase:

$$c_2 = -\frac{1}{(\ell-1)\rho-1} \rho(\ell\rho-1)(\ell\rho((\ell-1)\rho-2)+1) \quad (4.11)$$

$$c_3 = \frac{1}{(\ell-1)\rho-1} \rho(\ell\rho(\ell\rho(\rho(\ell(\rho(3(\ell-1)^2\rho-13\ell+18)+22)-5\rho-18)-18)+2\rho(\rho+3)+7)-1). \quad (4.12)$$

Any cumulant can be calculated via this process and the high density phase clearly produces similar results. However, unlike the cumulants the full current SCGF requires an explicit form of  $\rho(\lambda)$  implying these results only exists on an  $\ell$  by  $\ell$  basis.

### 4.2.3 Current SCGF for $\ell = 1$ TASEP

In this section I show that the SCGF for  $\ell = 1$  calculated through the above method matches exactly the known result in the literature, confirming the approach laid out by BFF. The next section deals with  $\ell > 1$  where results do not exist in the literature.

In [113]  $\rho$ ,  $j(\rho)$  and  $C$  for an open TASEP are expressed in terms of  $\alpha$  and  $\beta$ , the boundary injection and exit rates introduced in section 4.1.1. In the low density phase, [113]:

$$j = \alpha(1-\alpha), \quad \rho = \alpha, \quad C = \alpha(1-\alpha), \quad (4.13)$$

where  $\rho < \frac{1}{2}$ . In the high density phase,  $\rho > \frac{1}{2}$ , the results are equivalent to the above with  $\alpha \rightarrow 1-\beta$ .

In both [110, 111] there exist expressions for the SCGF of currents in the low/high density phases of the open TASEP which provides a check for results at  $\ell = 1$ . In the low density phase this expression is,

$$F(\lambda) = (1-\alpha) \frac{(e^\lambda - 1)}{\alpha(e^\lambda - 1) + 1}, \quad (4.14)$$

with  $\alpha \rightarrow \beta$  in high density phase<sup>2</sup>. I now turn to the results of (4.9) to confirm they give the same result.

The low density phase of the TASEP corresponds to (4.9) at  $\ell = 1$ . Simplifying this result:  $\rho(\lambda) = \frac{1}{1+\chi e^{-\lambda}}$ . Inserting this into (4.5) at  $\ell = 1$  then integrating with respect to  $\lambda$  à la (3.38),

$$F(\lambda) = \frac{\chi}{\chi+1} \frac{e^\lambda - 1}{e^\lambda + \chi}. \quad (4.15)$$

To determine  $\chi$  one solves  $\rho(0) = \rho = \alpha$ . This leads to  $\chi = \frac{1-\alpha}{\alpha}$ . Inserting this correct expression for  $\chi$  the literature result (4.14) is obtained.

There is an important caveat, these results only hold when  $\rho(\lambda) < \frac{1}{2}$ , leading to the constraint:  $\rho(\lambda) = \frac{1}{1+\chi e^{-\lambda}} < \frac{1}{2} \Rightarrow \lambda < \log \chi$ . This is not explicitly stated in the literature; however, it is implied.

Thus, the correct current SCGF is obtained in the TASEP using the BFF. This validates the assumption that the BFF will work in the case of stochastic dynamics. This is an important result as it exposes the range of applicability of the BFF. Furthermore it provides a far more trivial approach than used in [110, 111] for obtaining  $F(\lambda)$ , where the original calculations for the TASEP are far more complex than the BFF approach.

#### 4.2.4 SCGF of current for $\ell > 1$ TASEP

I now obtain the first results for the SCGF of current in  $\ell > 1$   $\ell$ -TASEP. In this section an analytical expression is obtained for the SCGF at  $\ell = 2$ . In general, the analytic solutions require solving polynomials of order  $\ell$ , thus for  $\ell > 2$  only numerical solutions are provided for a few chosen  $\ell > 2$ .

[106] shows the phase transition between the high and low density phases takes place at  $\rho = \frac{1}{\ell+\sqrt{\ell}}$ , exactly the phases transition defined by (4.9) and (4.10). Without loss of generality I focus on the low density phase. As I am concerned with results in the open system, I express  $\rho$  in terms of the boundary term  $\alpha$  ( $\beta$  is used in the high density phase). Specialising results from [106] to a homogeneous  $\ell$ -TASEP, in the low density

---

<sup>2</sup>There is an interesting symmetry in the system where cumulants of the currents are symmetrical under  $\alpha \rightarrow \beta$  where the density is not.

phase;

$$\rho = \frac{\alpha}{\alpha(\ell-1)+1}, \quad (4.16)$$

which matches (4.13) at  $\ell = 1$ . This allows for the expression of the results in terms of  $\alpha$ .

As the focus is the low density phase, consider (4.9) where  $\alpha$  is found by setting  $\lambda = 0$  on the left to find that:

$$\chi = \frac{(1-\alpha)^\ell}{\alpha}. \quad (4.17)$$

Inverting (4.9) leads to  $\rho(\lambda)$  which is only possible on an  $\ell$  by  $\ell$  basis. At increasing values of  $\ell$ , this becomes increasingly difficult as it amounts to finding the roots of a polynomial of order  $\ell$ , thus an analytical result for the SCGF is found only for  $\ell = 2$ . It is possible to obtain numerical solutions for  $F(\lambda)$  for arbitrary  $\ell$  where I will consider the specific choices of  $\ell = 5, 7$  as examples.

### Solution for $\ell = 2$ low density phase

A simple analytical expression is obtained for the current SCGF when  $\ell = 2$ . Solving (4.9) for  $\rho$ ,

$$\rho(\lambda) = \frac{1}{2} \left( 1 - \sqrt{\frac{\chi}{\chi - 4e^\lambda}} \right), \quad (4.18)$$

where  $\chi = \frac{(1-\alpha)^2}{\alpha}$  from (4.17).

Then inserting the above expression into (4.5) (with  $\ell = 2$ ) and integrating via (3.38) to find the low density phase current SCGF at  $\ell = 2$ :

$$F(\lambda)|_{\ell=2} = -\frac{(\alpha-1)e^{-\lambda} \left( -\sqrt{\alpha^2 + \alpha(4e^\lambda - 2)} + 1 + \alpha(2e^\lambda - 1) + 1 \right)}{2\alpha}. \quad (4.19)$$

### Numerical solutions for $\ell = 2, 5, 7$

In general, to obtain the SCGF at any  $\ell$  requires a numerical solution. This is obtained by solving for the roots of (4.9) numerically and inserting the resulting expression into (4.5).

These in turn are numerically integrated to obtain plots of the SCGF for any  $\ell$ . A few comparative example of this process are found in fig. 4.3. The figure shows the SCGFs obtained are convex as expected. One notices the SCGF seems to have an asymptotic tail, as opposed to a parabolic shape that will be seen in the next two chapters. This poses no issues although it does imply the Gallavotti-Cohen relation may not hold in the case of the TASEP as this will appear as a symmetry in these plots.

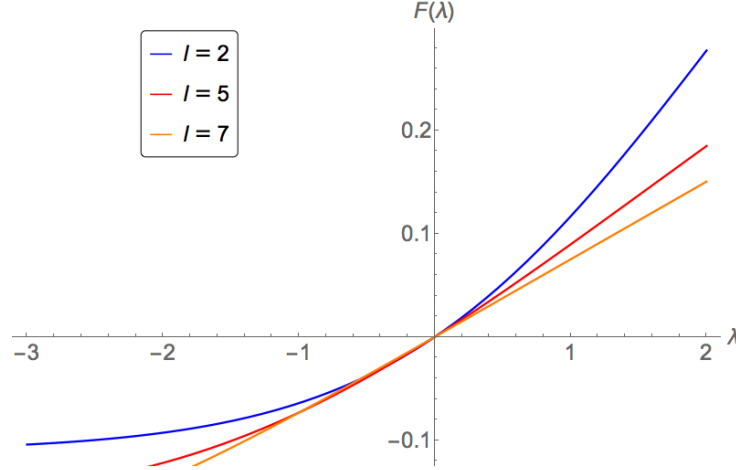


**Figure 4.3:** The numerically calculated SCGF for the particle transport in the  $\ell$ -TASEP where  $\ell = 2, 5$  and  $7$ . One can see the required convex shape of the SCGF is present in these plots.

### 4.3 Insights into the ballistic fluctuation formalism

Phase transitions are an important phenomenon in the TASEP ( $\ell=1$ ) where the appearance of low, high and maximal current phases are explained through reference to the collective velocity; this describes the velocity of a perturbation in the system [93]. The collective velocity is known to be expressed by  $v_{\text{coll}} = 1 - 2\rho$ . Now consider first the low density phase where  $\rho < 1/2$ . Imagine a small positive perturbation in the feeding rate  $\alpha$  with  $\beta$  large but kept constant, from the discussion in 4.1.2 this will lead to a small increase in density. This disturbance will propagate through the system from left to right and can also be defined by the sign of  $v_{\text{coll}}$ . Consider increasing  $\alpha$  such that the disturbance increases the density to  $\rho = 1/2$ , the collective velocity suddenly vanishes at this value and further increases of  $\alpha$ , for large fixed  $\beta$ , actually lead to negative collective velocities such that any perturbation in  $\alpha$  travels back towards the source of the disturbance. This point is when the system has entered the maximal current phase



and the system is ‘stuck’ at  $\rho = 1/2$ . An equivalent argument is made for  $\beta$  with low constant  $\alpha$ . This highlights the importance of understanding the sign of the collective velocity in phases transitions of this type.

The importance of this discussion in the context of the BFF is the collective velocity is defined by  $\partial_\rho j$ , precisely the flux Jacobian,  $A$  where at  $\ell = 1$ ,  $A = 1 - 2\rho$ , see (4.6). Thus, in the case of the TASEP, the flux Jacobian plays the role of the collective velocity, or the velocity of a perturbation in the system. This was actually made clear in section 3.2.2 where the eigenvalues of the flux Jacobian are identified as the characteristic velocity, this is equivalent to the velocity of perturbations. Since the collective velocity is known to play a role in phase transitions, so does the flux Jacobian. In fact, this was already pointed out in section 3.5 where one may now understand that the sign of the flux Jacobian marks the point where the velocity of perturbations change direction in the system. This leads to the expectation that the BFF will pick up dynamical phase transitions related to the direction of system perturbations where co-propagating modes (see section 3.5) mark the boundaries between phases. In a system such as a lattice gas the only system parameters are defined by the hopping, injection and exit rates and as such the arguments of section 4.1.2 and the previous paragraph seem to imply all phase transitions are defined by the direction of system perturbations. However, in general there may be a multitude of causes of phase transitions and it is not yet known if the BFF would reliably observe these, further analysis is necessary to understand this.

With the above discussion in mind the flow equation can be interpreted as a statement of linear response [20] where the flow equation is an attempt to bias the density  $\rho$  in order to explore large fluctuations of the state defined by large fluctuations in the current. In some sense we ‘disturb’ the system in this act of biasing and ‘watch’ what happens to the perturbations.

Throughout this chapter the maximal current phase was set aside. The reason is the BFF framework, by construction, is only defined by one parameter, the density  $\rho$ . The maximal current phase occurs when the density is exactly as  $\rho = 1/(\ell + \sqrt{\ell})$ , precisely the point where the framework becomes ambiguous (see (4.9) and (4.10)). In effect this is a phase where the direction of a disturbance is not the primary determining factor for the biasing and according to [93] is related to shock wave velocities, which again relates

to rarefaction waves. The maximal current phase provides an explicit example of the physics in a rarefaction wave regime. I have already suggested that behaviour of this sort may indicate a breaking required clustering for the BFF rendering inapplicable in section 3.5.

## Chapter 5

# Fluctuations in $d$ -dimensional CFT

In this chapter I present the results of using the BFF on a higher dimensional CFT. This is mostly comprised of work published alongside chapter 3 in [51] although section 5.3 introduces new unpublished results. This chapter indicates the power of the BFF by its application to a quantum system. Furthermore, it elucidates how to use the BFF in higher dimensional systems.

There are many quantum systems which admit ballistic transport where higher-dimensional relativistic CFT is particularly interesting. This system makes predictions for quantum systems tuned to quantum critical points at small but non-zero temperatures which are of great interest in physics. Results are well known for  $d = 1$ , and this system has already been considered in sections 2.1 and 3.3. However, in dimensions higher than one, very few results are available. As in the 1D case,  $d$ -dimensional conformal field theories contain many symmetries which produce equations of state leading to conformal hydrodynamics. This means the BFF is immediately applicable for these systems in an MES.

Here I present the important example of energy transport in conformal hydrodynamics of arbitrary dimension, obtaining explicitly the flow equation on the state, expressions for the cumulants  $c_2$ ,  $c_3$  and  $c_4$ , and numerically evaluating the SCGF  $F(\lambda)$ . Before the publication of [51], these were unknown results<sup>1</sup>. I also present the results for this system when the steady state is constructed via the partitioning protocol, this leads to numerical evidence for the existence of the Gallavotti-Cohen fluctuation relation. The

---

<sup>1</sup>The cumulant  $c_2$  follows from the current-current sum rule introduced in section 3.1.3 which was based on known results from [49]; however it was never worked out explicitly in conformal hydrodynamics.

results of this chapter build on from work done in [58, 114, 115].

## 5.1 Reduction to a one-dimensional hydrodynamic problem

In this chapter I focus on conformal field theory (CFT) in  $d > 1$  dimensions of space. The results of this section and the remainder of the chapter closely follow my work in [51, section 4].

In this system the energy-momentum tensor  $\mathcal{T}^{\mu\nu}$  can be used to summarize the symmetries that define the hydrodynamic equations. These properties are the same as those of the 1D CFT introduced in section 2.1 where,  $\mathcal{T}^{\mu\nu}$  satisfies  $\mathcal{T}^{\mu\nu} = \mathcal{T}^{\nu\mu}$  (Lorentz invariance),  $\mathcal{T}^\mu_\mu = 0$  (scale invariance) and  $\partial_\mu \mathcal{T}^{\mu\nu} = 0$  (conservation of energy and momentum). Further, assume the system is not integrable, which is true in general when excluding free field theory. In this case the maximal entropy states for the hydrodynamics of the system are defined by boosted thermal states [114] and it is in this state that the BFF is applied. In order to apply the BFF I assume transport takes place only in 1 direction, the direction  $x^1$  (with  $x^0$  the time coordinate), with the associated momentum operator  $P = \int d^d x \mathcal{T}^{01}(x)$ . In this case, the space of thermal states boosted in  $x^1$  can be represented by density matrices [114],

$$e^{-\beta^1 H - \beta^2 P} = e^{-\beta_{\text{rest}}(\cosh \theta H - \sinh \theta P)}, \quad (5.1)$$

and corresponding state denoted by  $\langle \cdots \rangle_{\beta_1, \beta_2}^{(d)}$ . Here  $H = \int d^d x \mathcal{T}^{00}(x)$  is the Hamiltonian, the rest-frame temperature is  $T_{\text{rest}} = \beta_{\text{rest}}^{-1}$ , and the Lorentz boost is of rapidity  $\theta$ . By Lorentz invariance and scale invariance the expectation values of energy-momentum components take the form [84]

$$\langle \mathcal{T}^{\mu\nu}(x, t) \rangle_{\beta_1, \beta_2}^{(d)} = a T_{\text{rest}}^{d+1} ((d+1) u^\mu u^\nu + \eta^{\mu\nu}), \quad \eta^{\mu\nu} = \text{diag}(-1, 1, 1 \dots 1) \quad (5.2)$$

where  $u^\mu = (\cosh \theta, \sinh \theta, 0, \dots, 0)^\mu$  and  $a$  is a model-dependent positive constant.

In order to make use of the BFF, the system must be made effectively one-dimensional. This can be done by integration over the directions transverse to  $x^1$  in other words I need to isolate the transport direction. Consider grouping the directions

transverse to  $x_1$  by defining the transverse space  $S_\perp$  of the  $d - 1$  hyper dimensional area  $V_\perp$ . Clearly this transverse space has coordinates given by  $x^\perp = (x^2, \dots, x^d)$ . In order to properly isolate the effect of the transverse dimensions I assume the transverse space is periodic in all its coordinates with equal periods, with state  $\langle \dots \rangle_{\beta_1, \beta_2}^{(d, V_\perp)}$  where the density matrix is of the form (5.1). Then in order for this to be consistent with  $\langle \mathcal{T}^{\mu\nu}(x, t) \rangle_{\beta_1, \beta_2}^{(d)}$  of (5.2) I require,

$$\lim_{V_\perp \rightarrow \infty} \langle \mathcal{T}^{\mu\nu}(x, t) \rangle_{\beta_1, \beta_2}^{(d, V_\perp)} = \langle \mathcal{T}^{\mu\nu}(x, t) \rangle_{\beta_1, \beta_2}^{(d)}. \quad (5.3)$$

Using this the one-dimensional densities can be defined as,

$$\begin{aligned} q_1^{(V_\perp)}(x, t) &= \int_{S_\perp} d^{d-1}x^\perp \mathcal{T}^{00}(x, x^\perp, t) \\ j_1^{(V_\perp)}(x, t) = q_2^{(V_\perp)}(x, t) &= \int_{S_\perp} d^{d-1}x^\perp \mathcal{T}^{01}(x, x^\perp, t) \\ j_2^{(V_\perp)}(x, t) &= \int_{S_\perp} d^{d-1}x^\perp \mathcal{T}^{11}(x, x^\perp, t) \end{aligned} \quad (5.4)$$

where the equality  $j_1^{(V_\perp)}(x, t) = q_2^{(V_\perp)}(x, t)$  is due to Lorentz invariance and which implies  $\mathcal{T}^{01}(x, x^\perp, t) = \mathcal{T}^{10}(x, x^\perp, t)$ . Since this system conserves energy and momentum,  $\partial_\mu \langle \mathcal{T}^{\mu\nu}(x, t) \rangle_{\beta_1, \beta_2}^{(d)} = 0$  which implies the conservation equations hold such that,

$$\partial_t q_i^{(V_\perp)}(x, t) + \partial_x j_i^{(V_\perp)}(x, t) = 0, \quad i = 1, 2. \quad (5.5)$$

In this picture correlation functions cluster sufficiently fast at large longitudinal distances. Therefore, this is an effectively one-dimensional system, with two conserved charges, and assuming that the transverse direction does not give rise to additional thermodynamic degrees of freedom, one-dimensional Euler hydrodynamics apply. One can now discuss the SCGF for the energy current  $j_1^{(V_\perp)}$  within the BFF framework. However the integrations in (5.4) leads to unnecessary extra terms of  $V_\perp$ , thus it is convenient to divide the SCGF by  $V_\perp$  leaving,

$$F(\lambda) = \lim_{t \rightarrow \infty} (tV_\perp)^{-1} \log \langle e^{\lambda \int_0^t ds \int_{S_\perp} d^{d-1}x^\perp \mathcal{T}^{01}(t, 0, x^\perp)} \rangle_{\beta_1, \beta_2}^{(d, V_\perp)}. \quad (5.6)$$

By clustering in  $d + 1$ -dimensional space-time, all cumulants generated by  $F(\lambda)$

have a finite limit as  $V_\perp \rightarrow \infty$ , which means the goal is to obtain

$$\lim_{V_\perp \rightarrow \infty} F(\lambda). \quad (5.7)$$

To find this in the BFF is equivalent to the expression from the fundamental BFF equation, (3.38) divided by  $V_\perp$ , with states satisfying the flow equation (3.33). It is then sufficient to know the following large- $V_\perp$  limits of conserved densities and currents:

$$\begin{aligned} q_i &\equiv \lim_{V_\perp \rightarrow \infty} V_\perp^{-1} \langle q_i^{(V_\perp)}(x, t) \rangle_{\beta_1, \beta_2}^{(d, V_\perp)} \\ j_i &\equiv \lim_{V_\perp \rightarrow \infty} V_\perp^{-1} \langle j_i^{(V_\perp)}(x, t) \rangle_{\beta_1, \beta_2}^{(d, V_\perp)}, \end{aligned} \quad (5.8)$$

and to solve for the flow (3.33) with the flux Jacobian given by

$$A_i^j = \frac{\partial j_i}{\partial q_j}. \quad (5.9)$$

Using (5.3) as well as homogeneity in the transverse direction, the limits in (5.8) are given exactly by the expression on the right-hand side of (5.2) for  $\mu, \nu \in \{0, 1\}$ . Thus the problem of evaluating (5.7) has been reduced to a one-dimensional hydrodynamic problem.

## 5.2 Exact SCGF and cumulants

I now use the flow equation, (3.33), and the fundamental equation, (3.38), to obtain expressions for the first four cumulants and a numerical expression for the SCGF of energy transport in a  $d$ -dimensional CFT. In order to proceed I first recall the structure of the conserved charges imposed by the system symmetries which also provides an equation of state. I use the equation of state to obtain the flux Jacobian which is used to obtain the flow equation. From the flow equation the required results follow.

Using (5.2) the components of the reduced  $d$ -dimensional energy-momentum tensor

are,

$$q_1 = aT_{\text{rest}}^{d+1}(d \cosh^2 \theta + \sinh^2 \theta) \quad (5.10)$$

$$j_1 = q_2 = a(d+1)T_{\text{rest}}^{d+1} \cosh \theta \sinh \theta \quad (5.11)$$

$$j_2 = aT_{\text{rest}}^{d+1}(\cosh^2 \theta + d \sinh^2 \theta). \quad (5.12)$$

Using the above, it's is easy to determine the flux Jacobian,  $A$  as,

$$A = \frac{\partial j}{\partial q} = \frac{1}{d \cosh^2 \theta - \sinh^2 \theta} \begin{pmatrix} 0 & d \cosh^2 \theta - \sinh^2 \theta \\ \cosh^2 \theta - d \sinh^2 \theta & (d-1) \sinh 2\theta \end{pmatrix}. \quad (5.13)$$

Interestingly, at  $d > 1$ , the flux Jacobian is not state-independent as it is at  $d = 1$ , which implies the extended fluctuation relation (section 3.4) does not hold in higher-dimensional CFT as is true in the case  $d = 1$  (section 2.4). This provides an important result as it invalidates the conjecture made in [114] for the SCGF, which was based on the extended fluctuation relation. I also note that these relationships define the equations of state for the system, i.e. the relationship between the currents and their associated charges.

Since the flow equation requires  $\text{sgn}(A)$ , I now turn to calculating this. The matrix  $\text{sgn}(A)$  is obtained by diagonalising  $A$ , and taking the sign of the eigenvalues. The eigenvalues of  $A$  are:

$$v_{\pm}^{\text{eff}} = \frac{d-1}{2(d \cosh^2 \theta - \sinh^2 \theta)} (\sinh 2\theta \pm \alpha) \quad \text{where} \quad \alpha = \frac{2\sqrt{d}}{d-1} = 2 \frac{v_s}{1-v_s^2} \quad (5.14)$$

with the speed of sound of conformal hydrodynamics given by  $v_s = 1/\sqrt{d}$ . Clearly,  $\text{sgn}(v_{\pm}^{\text{eff}}) = \text{sgn}(\sinh 2\theta \pm \alpha) = \text{sgn}(\theta \pm \theta_s)$  with the sound rapidity  $\theta_s$  defined by  $\tanh \theta_s = v_s$ . Define  $\xi_1 = \text{sgn } v_+^{\text{eff}} + \text{sgn } v_-^{\text{eff}}$  and  $\xi_2 = \text{sgn } v_+^{\text{eff}} - \text{sgn } v_-^{\text{eff}}$  which results in,

$$\xi_1 = \begin{cases} 2 \text{sgn}(\theta), & |\theta| > \theta_s \\ 0, & |\theta| < \theta_s \end{cases}, \quad \xi_2 = \begin{cases} 0, & |\theta| > \theta_s \\ 2, & |\theta| < \theta_s. \end{cases} \quad (5.15)$$

That is,  $\xi_1$  is non-zero for supersonic rapidities and zero otherwise, and  $\xi_2$  is non-zero

for infrasonic rapidities and zero otherwise. This gives,

$$\text{sgn } A = \frac{1}{2\alpha} \begin{pmatrix} \xi_1 \alpha - \xi_2 \sinh 2\theta & 2\xi_2(\cosh^2 \theta + \gamma) \\ -2\xi_2(\sinh^2 \theta - \gamma) & \xi_1 \alpha + \xi_2 \sinh 2\theta \end{pmatrix}, \quad (5.16)$$

where

$$\gamma = \frac{1}{d-1} = \frac{v_s^2}{1-v_s^2}. \quad (5.17)$$

In order to obtain the flow equation for energy transport one fixes  $i_* = 1$  in (3.33) and lets the Lagrange multipliers become  $\lambda$  dependent. Then using  $\beta_1 = \beta_{\text{rest}} \cosh \theta$  and  $\beta_2 = -\beta_{\text{rest}} \sinh \theta$  one obtains the flow equations,

$$\begin{aligned} \partial_\lambda \beta_{\text{rest}}(\lambda) &= -\frac{1}{2\sqrt{d}} \left( \xi_2(\lambda) \sinh(\theta(\lambda)) + \sqrt{d} \xi_1(\lambda) \cosh(\theta(\lambda)) \right) \\ \partial_\lambda \theta(\lambda) &= \frac{1}{2\beta_{\text{rest}}(\lambda)} \left( \xi_1(\lambda) \sinh(\theta(\lambda)) + \sqrt{d} \xi_2(\lambda) \cosh(\theta(\lambda)) \right). \end{aligned} \quad (5.18)$$

With the flow equation in place it is now possible to obtain the SCGF according to the fundamental equation of the BFF, (3.38), by integrating the  $\lambda$ -dependent current of (5.11)

$$j_1(\lambda) = a \frac{d+1}{2} T_{\text{rest}}^{d+1}(\lambda) \sinh 2\theta(\lambda). \quad (5.19)$$

Before producing the SCGF, it is important that analytical expressions for the cumulants are simply obtained by taking derivatives with respect to  $\lambda$  and setting  $\lambda = 0$  exactly as was done in section 4.2. These expressions for the cumulants were unknown before our work [51]. The derivatives may be readily evaluated:

$$\begin{aligned} \partial_\lambda j_1(\lambda) &= a(d+1) T_{\text{rest}}^{d+1}(\lambda) \left( \frac{d+1}{2} \sinh 2\theta(\lambda) \partial_\lambda \log T_{\text{rest}}(\lambda) \right. \\ &\quad \left. + \cosh 2\theta(\lambda) \partial_\lambda \theta(\lambda) \right). \end{aligned} \quad (5.20)$$

Reading off the required identities from (5.18), setting  $\lambda = 0$  and using the explicit form



of  $\xi_{1/2}$  given by (5.15), the second cumulant is obtained;

$$c_2 = \frac{a(d+1)T_{\text{rest}}^{d+2}}{2\sqrt{d}} \times \begin{cases} \sqrt{d} \sinh|\theta| ((d+3) \cosh(2\theta) + d+1), & |\theta| > \theta_s \\ \cosh(\theta) ((3d+1) \cosh(2\theta) - (d+1)), & |\theta| < \theta_s \end{cases} \quad (5.21)$$

where  $\theta = \theta(0)$  and  $\beta_{\text{rest}} = \beta_{\text{rest}}(0)$ . This process easily generates cumulants of  $n^{\text{th}}$  order. As an example, using the Mathematica symbolic calculation software [87],  $c_3$  is found to be,

$$c_3 = \frac{a(d+1)T_{\text{rest}}^{d+3}}{4d} \times \begin{cases} d(d+3) \sinh(2\theta) ((d+5) \cosh(2\theta) + d-1), & |\theta| > \theta_s \\ 2(2d+1) \sinh(2\theta) ((3d+1) \cosh(2\theta) + d-1), & |\theta| < \theta_s. \end{cases} \quad (5.22)$$

and  $c_4$ :

$$c_4 = \frac{a(d+1)T_{\text{rest}}^{d+4}}{8d^{3/2}} \times \begin{cases} d^{3/2}(d+3) \sinh|\theta| ((d+5)(d+7) \cosh(4\theta) \\ + 4(d+1)(d+5) \cosh(2\theta) + 3(d+1)(d+3)), & |\theta| > \theta_s \\ 2(2d+1) \cosh(\theta) ((3d+1)(5d+3) \cosh(4\theta) \\ - 4(5d+3) \cosh(2\theta) + (d+3)^2). & |\theta| < \theta_s. \end{cases} \quad (5.23)$$

Unfortunately it turns out that obtaining an analytical expression for  $F(\lambda)$  is not possible. However, it can be obtained by numerically solving (5.18) to find  $\beta_{\text{rest}}(\lambda)$  and  $\theta(\lambda)$ , then inserting these expressions into (5.19), and numerically integrating to obtain  $F(\lambda)$ . The results for doing this for  $d=2$  and  $d=3$  are displayed in Fig. 5.1. The resulting functions are convex, as they should by the general theory of LDT, see section 1.2.2. From these plots it is possible to verify that the Gallavotti-Cohen fluctuation relation holds which is further explored in the next section.

Once again, the phenomenon discussed in subsection 3.5 can be explicitly seen here. Consider a thermal state boosted to the sound rapidity,  $\theta = \pm\theta_s$ . In this case, as a consequence of the discontinuities in  $\xi_{1,2}$  in (5.15), the derivatives of  $\beta_{\text{rest}}(\lambda)$  and  $\theta(\lambda)$  with respect to  $\lambda$  have discontinuities at  $\lambda = 0$ . This implies that the third derivative of  $F(\lambda)$  is ill-defined at  $\lambda = 0$ . That is, the BFF cannot obtain the scaled cumulants  $c_n$

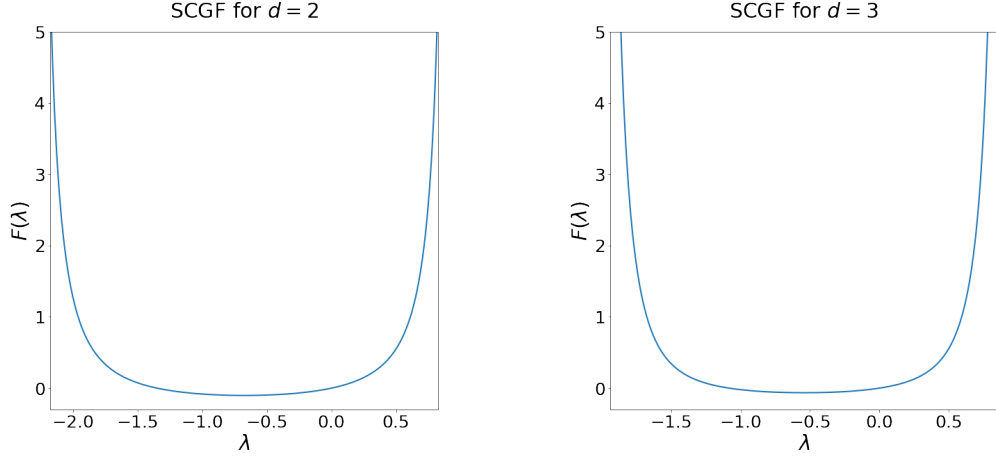


**Figure 5.1:** Figure showing numerical solutions for the SCGF of energy transport for a CFT in 2D (left) and 3D (right). Using  $\beta_{\text{rest}}(\lambda = 0) = 1.73145$ ,  $\theta(\lambda = 0) = 0.55$ . The resulting curves are convex as expected and indicate a symmetry.

for  $n \geq 3$  at the speed of sound in the system. Physically, this may be understood since when an object moves in a medium exactly at the speed of sound, there is a build-up of waves. At the macroscopic scale, this appears to increase correlations in the system to such an extent that it modifies the scaling of higher-order cumulants with time, thus we may expect a breaking of the clustering required for the BFF. Furthermore, there appears to be a dynamical phase transition at the speed of sound as on both sides of this phase transition point, the cumulants take different forms, as is clear from (5.21) and (5.22).

### 5.3 Fluctuation relations in $d$ -dimensional CFT

This section introduces original but as yet unpublished work. When considering the plots in fig. 5.1, there is a clear symmetry which is shown to be consistent with the Gallavotti-Cohen fluctuation relation. Recall from section 1.3.3 that the FR in a NESS emerging from the partitioning protocol is expected to satisfy,

$$F(\lambda) = F(-\lambda - (\beta_l - \beta_r)). \quad (5.24)$$

In order to analyse the FR, I assume the NESS in the previous section was generated by the partitioning protocol which means I need to understand how  $\beta_{\text{rest}}$  and  $\theta$  are related

to  $\beta_l$  and  $\beta_r$ . In [115] it is shown that,

$$\beta_l = \beta_{\text{rest}} \left( \frac{1-v}{v+1} \right)^{\frac{1}{2\sqrt{d}}} \quad (5.25)$$

$$\beta_r = \beta_{\text{rest}} \left( \frac{(d^2+1)v^2 + (d+1)v\sqrt{(d-1)^2v^2 + 4d} + 2d}{2d(1-v^2)} \right)^{\frac{1}{d+1}}, \quad (5.26)$$

where  $v = \tanh(\theta)$ . Thus, the results of the previous section can be translated to the case where the NESS is defined by a partitioning protocol. I show below that the results obtained through the BFF do satisfy the FR as well as confirming the validity of (5.25). However, it is shown that for boosts beyond the system speed of sound, the relationship (5.25) breaks down.

If the FR holds, (5.24), the expected symmetry point in  $F(\lambda)$  is at  $\lambda = (\beta_l - \beta_r)/2$ . When  $d = 1$  the FR is known to hold, and in this case the SCGF is known analytically (see (2.17) at  $p = 1$ ). I begin by confirming the correct results are obtained for  $d = 1$  through the machinery above. Based on the choice,  $\beta_{\text{rest}} = \beta_{\text{rest}}(\lambda = 0) = 1.73145$  and  $\theta = \theta(\lambda = 0) = 0.55$  by using (5.25) this results in  $\beta_l = 1$  and  $\beta_r = 3$ . Checking with the numeric expression for  $d = 1$  obtained via the process of the previous section, the symmetry point is numerically calculated to be at  $\lambda = -1.00104$ . The FR predicts a symmetry at  $\lambda = -1$ , thus, results match the known analytical result perfectly.

Using the same values  $\beta_{\text{rest}}(\lambda = 0) = 1.73145$  and  $\theta(\lambda = 0) = 0.55$ , I obtain results for various values of  $d$ . At  $d = 2$ , using (5.25), I find  $\beta_l = 1.17$  and  $\beta_r = 2.55$  with the expected symmetry point at  $\lambda = -0.68$ , while for  $d = 3$ ,  $\beta_l = 1.26$  and  $\beta_r = 2.37$  with the expected symmetry point at  $\lambda = -0.55$ . Fig. 5.2 shows this information graphically and using the reflection of the left side of the curve, provides numerical evidence that the FR is satisfied by my solution above. The results for  $d = 4$  also satisfy the expected FR. However, at  $d = 5$  there is an issue, the symmetry point predicted using (5.25) produces the wrong result, see fig. 5.2. This leads to an interesting insight. Recall that the signs of eigenvalues of  $A$  are dependent on  $\theta$  with respect to the speed of sound. Specifically, there will be different behaviour when  $|\theta| > |\theta_s|$  where for  $d = 5$ ,  $\theta_s = 0.48$ . When  $\theta = 0.55$  the system is boosted by a rapidity larger than the speed of sound which causes a change in behaviour, a phase transition. Repeating the results for  $\theta = 0.45$  at  $d = 5$  results in the correct value for the symmetry point thereby showing it isn't an issue at

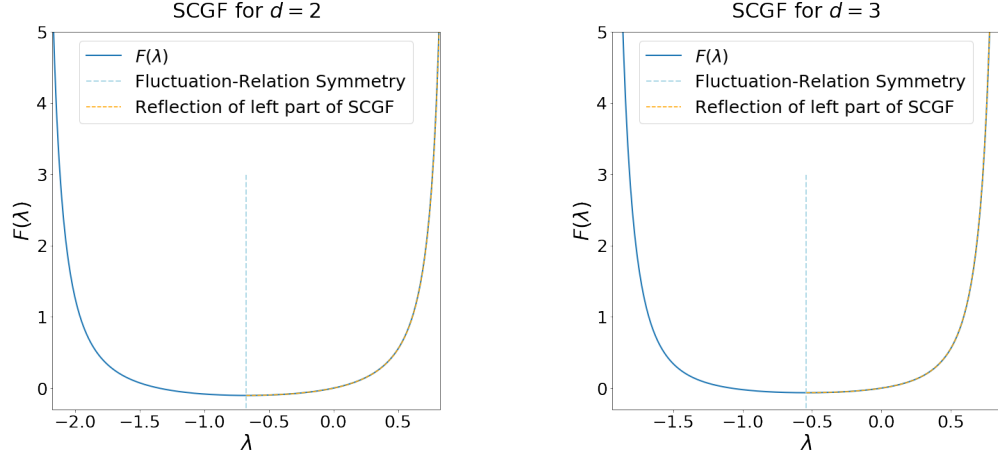


**Figure 5.2:** Plots showing the 2D and 3D CFT SCGF for energy transport. Figures are produced using  $\beta_{\text{rest}} = 1.73145$ ,  $\theta = 0.55$ . The dotted line in the middle is the expected centre from the FR while the reflection of the left part of the curve is superimposed on the right-hand side of the curve. The closeness in match indicates that, numerically, the FR holds in these systems and provides further confirmation that (5.25) is the correct.

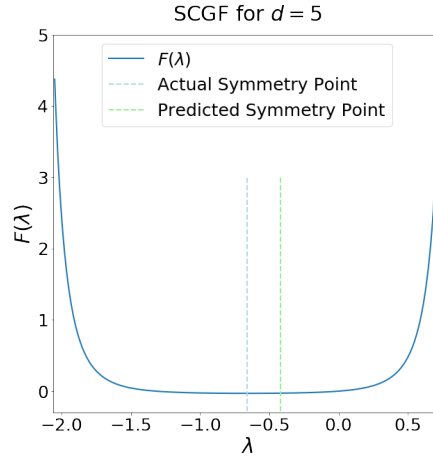


**Figure 5.3:** 5D plot of SCGF for energy transport with  $\beta_{\text{rest}} = 1.73145$ ,  $\theta = 0.55$ . The two dotted lines indicate that the FR expected from application of (5.25) is not correct. This is because (5.25) doesn't hold when boosted beyond the speed of sound.

$d = 5$  but rather is related to the rapidity used. This shows that boosts larger than the speed of sound result in a different relationship with the effective left and right bath temperatures. In fact this was predicted by [115] where it was known these expressions don't hold for large boosts. This is proposed to be related to the fact that moving faster than the system's speed of sound has placed the system in the rarefaction wave - the region of low relative pressure that follows a shock wave.

## 5.4 Normal mode decomposition of $d$ -dimensional CFT

Recall from section 3.6 that in some cases it is possible to obtain an analytical form of the SCGF in terms of normal modes of the system. In this section I find the normal modes for this system. It will be shown that (3.60) does not hold i.e. the generating functional for currents is not a sum of independent functions of the normal modes and (3.61) is not valid in this instance.

In (3.58), I presented the definition of the normal modes that diagonalise the flux Jacobian,  $A$ . For ease this is reproduced here,

$$\underline{v}^{\text{eff}} = \frac{\partial \underline{\beta}}{\partial \underline{n}} A \frac{\partial \underline{n}}{\partial \underline{\beta}}. \quad (5.27)$$

As I have already diagonalised  $A$  above, it is a simple matter to find the correct normal modes in this system. It was found that the following combinations of the rest-frame temperature  $T_{\text{rest}}$  and the boost  $\theta$  form normal modes:

$$n_+ = T_{\text{rest}} e^{\frac{\theta}{\sqrt{d}}}, \quad n_- = T_{\text{rest}} e^{-\frac{\theta}{\sqrt{d}}} \quad (5.28)$$

with effective velocities  $v_{\pm}^{\text{eff}}$ , respectively, as given in (5.14). These results are easily confirmed by showing they diagonalise  $A$ .

Recall also (3.59), a function that can be used to generate currents and reproduced here for ease of reference,

$$j_i = -\frac{\partial g}{\partial \beta^i}. \quad (5.29)$$

It is also possible to find a form for  $g$  in the case of the  $d$ -dimensional CFT. One can check that the currents  $j_1$  and  $j_2$  as given in (5.11) and (5.12) are generated as per (5.29) by the function

$$g = -T_{\text{rest}}^d \sinh \theta. \quad (5.30)$$

There is no independent combination of the expressions in (5.28) that result in (5.30). It was stated in section 3.6 that if  $g$  can be written as a sum of independent functions of the normal modes, then one obtains an analytical expression for  $F(\lambda)$ . The reason no such functions exist in this system is it violates the multi-parameter property

introduced in section 3.6.

### Multi-parameter property not satisfied

It turns out that the different currents present in the  $d$ -dimensional CFT are not independent of each other. This is important as it means the ‘multi-parameter’ property is not satisfied and a neat analytical expression for the SCGF based on section 3.6 cannot be found. This section produces the proof of this inter-dependence of the currents.

One starts by showing if currents are independent then there should exist a joint SCGF  $F(\lambda_1, \lambda_2)$  which leads to a multi-flow equation:

$$\frac{\partial \beta^i}{\partial \lambda_j} = -\text{sgn}(A)_i^j. \quad (5.31)$$

Assuming the currents are independent of each other is equivalent to requiring

$$\frac{\partial}{\partial \lambda_k} \frac{\partial}{\partial \lambda_j} \beta_i(\{\lambda_n\}) = \frac{\partial}{\partial \lambda_j} \frac{\partial}{\partial \lambda_k} \beta_i(\{\lambda_n\}). \quad (5.32)$$

Then using the above multi-flow equation along with the chain rule,

$$\sum_l \text{sgn}(A)_{kl} \frac{\partial}{\partial \beta^l} \text{sgn}(A)_i^j = \sum_l \text{sgn}(A)_{jl} \frac{\partial}{\partial \beta^l} \text{sgn}(A)_i^k. \quad (5.33)$$

So if  $\text{sgn}(A)_i^j$  satisfies this for all  $i, j, k$  then the currents can be considered independent of each other.

In order to check this in the case of the  $d$ -dimensional CFT, I use  $\beta_1 = \beta_{\text{rest}} \cosh(\theta)$  and  $\beta_2 = -\beta_{\text{rest}} \sinh(\theta)$  which allows for the use of the form of  $\text{sgn} A$  as defined in (5.16). With this it is easy to check the condition in (5.33) through the various combinations of  $i, j, k$  and it is found that the currents are indeed not independent.

## Chapter 6

# Ballistic fluctuation formalism applied to integrable models

This chapter presents the application of the BFF to integrable models where I obtain an explicit expression for the SCGF of a transported conserved charge. This result is applicable to any integrable model, classical or quantum, that has a thermodynamic Bethe ansatz description and is the primary focus of work submitted for publication [54]. The figures of section 6.5 are the results of original but unpublished work from the application of this general result.

As was discussed in section 1.4.1, integrable models play an important role in understanding quantum systems. Having a complete description of the fluctuations in such models provides a foundation for the grander goal of understanding fluctuations in general quantum systems and as a stand-alone result would be of great value. However, this result has the added value of underlining the importance of the BFF. In preceding chapters I have already used the BFF to unify results from classical lattice models and quantum systems described by a CFT, proving the BFF to be wide ranging theory for non-equilibrium states. This chapter adds the incredibly diverse class of integrable models to this growing cannon of the BFF.

In this chapter I make use of generalised hydrodynamics - a form of hydrodynamics applied to integrable models described in terms of thermodynamic Bethe ansatz quantities. Both these concepts are introduced in section 6.1 below. The main outcome, a fully general SCGF for transport, is derived in the following section making use of the BFF equations. I apply the general result to the hard rod gas, a classical integrable

model, and the important quantum integrable model, the Lieb-Liniger gas. In the final section of this chapter I present numerical evidence that  $F(\lambda)$  obtained here satisfies the fluctuation relation of the Gallavotti-Cohen type introduced in section 1.3.3.

For the purposes of this chapter I am interested in the fluctuations of the total transfer of some particular charge  $Q_{i^*}$  in the integrable model. Although the results apply to any of the charges, for concreteness applications will consider energy and particle transport. Furthermore I will consider the transport in an NESS generated by a partitioning protocol (see section 1.1). Thus, I am interested in fluctuations of the total current passing through the juncture of the two partitions of the partitioning protocol,

$$J^{(t)} = \int_0^t ds j_{i^*}(0, s), \quad (6.1)$$

where  $i^*$  refers the charge of interest, i.e. particle or energy current and the juncture is taken to be at  $x = 0$ . Importantly the LDT, (1.1) is expected to hold for this quantity.

## 6.1 TBA and generalised hydrodynamics

Recall from section 1.4.1 that integrable models can be either classical or quantum and contain a set of infinite conserved charges. In order to apply the BFF to integrable models one needs a hydrodynamic description of them. In this section I introduce generalised hydrodynamics - a hydrodynamic description of integrable models. This is understood in terms of objects from the thermodynamic Bethe ansatz - stemming from the Bethe ansatz used to solve integrable models. Although initially built for quantum models, later work showed that generalised hydrodynamics should be applicable to some classical systems as the hydrodynamic equations found correspond to those of a classical soliton gas [116]. In particular this justifies the application of later results to the classical hard rod gas in section 6.4.

### 6.1.1 Thermodynamic Bethe ansatz

As the name implies, the *Thermodynamic Bethe Ansatz (TBA)* is the application of the Bethe ansatz used in integrable systems but in the thermodynamic limit [117]. In the thermodynamic limit, in the presence of an infinite number of conserved charges, the system's density matrix is given by a Generalised Gibbs Ensemble (GGE), as introduced



in section 1.4.2. The TBA has been formulated as a quasi-particle description of the GGE where the system can be understood as comprised of quasi-particles where system properties arise from the density and free energy of the particles [118, 119]. The TBA is a substantial topic of research so I only present the details directly needed in this section. The necessary ideas of the TBA can be naturally broken down into two parts, the first part is a brief description of the quasi-particles, the second is the thermodynamics related to these quasi-particles.

### Quasi-particles

The quasi-particles in the TBA depend on a spectral parameter  $\theta$ . It is possible for a single system to have multiple types of quasi-particle however in this work I only consider systems with one particle type. The spectral parameter can be thought of as the particle's 'velocity' for Galilean systems which again is the only type considered in this work. In relativistic systems the spectral parameter effectively takes on the role of rapidity.

A conserved charge  $Q_i$  in the system is carried by the quasi-particles such that  $Q_i|\theta_1, \theta_2, \dots\rangle = \left(\sum_k h^{(i)}(\theta_k)\right)|\theta_1, \theta_2, \dots\rangle$ . Here  $h_i$  can be identified as the 'amount' of the charge carried by an individual quasi-particle.

The quasi-particles also have their own energy and momentum. In Galilean systems this is simply  $(1/2)m\theta^2$  and  $m\theta$  respectively. For this work I only consider the case  $m = 1$ .

### Thermodynamics of quasi-particles

The TBA is concerned with thermodynamic properties of the above described quasi-particles. Thus, the TBA defines a series of expressions that are closely related to standard thermodynamic objects. In particular there exists a particle density  $\rho_p$ , a state density  $\rho_s$ , a pseudo energy  $\mathcal{E}$ , an occupation function  $n$  and a free energy function  $F$ .

The TBA description of a system is fairly general and for the purposes of this thesis, a specific model can be defined via two characteristics. The first characteristic is the quasi-particle type i.e. boson, fermion, classical or radiative mode which is found through the full TBA analysis of the system of interest [79]. The second characteristic is a term describing particle-particle interactions, the differential scattering phase  $\varphi(\theta, \alpha)$  where  $\theta$  and  $\alpha$  are the spectral parameters for the two particles of interest. Re-

call from section 1.4.1 that integrable models in 1D have the interesting property that  $n$ -particle interactions can be broken down into products of two particle interactions. In the TBA, these interactions are defined only by associated interactions between two quasi-particles. Both the particle type and form of  $\varphi$  are found through a full TBA analysis of the system. For the purposes of the GHD below and the BFF that follows these properties can be treated as input from literature and as such are not, in general, proven within this thesis. However, I do provide a brief overview of the TBA applied to the Lieb-Liniger model in appendix D.1.

One of the primary results of the TBA is the pseudo energy:

$$\varepsilon(\theta) = \sum_i \beta^i h_i(\theta) + \int \frac{d\alpha}{2\pi} \varphi(\theta, \alpha) F(\varepsilon(\alpha)), \quad (6.2)$$

where  $\beta^i$  is the Lagrange multiplier corresponding to conserved charge  $Q_i$  from the GGE; and  $h_i$  is the part of the conserved charge carried by the quasi-particles and the free energy  $F$  is given by

$$F(\varepsilon) = \begin{cases} -\log(1 + e^{-\varepsilon}) & \text{Fermion} \\ \log(1 - e^{-\varepsilon}) & \text{Boson} \\ -e^{-\varepsilon} & \text{Classical} \\ 1/\varepsilon & \text{Radiative modes.} \end{cases} \quad (6.3)$$

To get a feel for this pseudo energy it is best to turn to the occupation function. This is defined by:

$$n(\theta) = \frac{dF(\varepsilon)}{d\varepsilon} \Big|_{\varepsilon=\varepsilon(\theta)} = \begin{cases} \frac{1}{e^{\varepsilon(\theta)} + 1} & \text{Fermion} \\ \frac{1}{e^{\varepsilon(\theta)} - 1} & \text{Boson} \\ e^{-\varepsilon(\theta)} & \text{Classical} \\ -1/\varepsilon(\theta)^2 & \text{Radiative modes.} \end{cases} \quad (6.4)$$

Comparing the above expressions to the well-known Fermi and Bose-Einstein statistics provides the interpretation for the pseudo energy and the associated quantities. The pseudo energy is associated with the usual energy of a single particle state with the La-

grange multiplier included. However, the pseudo energy is also adjusted by interactions with other particles, as can be seen by the presence of  $\varphi$  in (6.2).

The density of states is related to the particle density and the momentum of the quasi-particle through the following relationship:

$$2\pi\rho_s(\theta) = p'(\theta) + \int d\alpha \varphi(\theta - \alpha)\rho_p(\alpha), \quad (6.5)$$

where  $p'$  is the derivative of the momentum with respect to  $\theta$  and  $\rho_p$  is the particle density. This is direct from the TBA and a derivation in the case of the Lieb-Liniger model is presented in appendix D.1. To provide some physical intuition, recall that the velocity space density of states for an electron gas in a 1D system is a constant. In the case with Galilean particles,  $p'$  is constant. Thus the density of states in integrable models is related to the 1D density of states but modified by particle interactions represented by  $\varphi(\theta - \alpha)$ .

The expression above relating the state and particle density is further connected to the other usual thermodynamic quantities through the occupation function,  $n(\theta)$ , which in addition to (6.4) can be obtained through,  $n(\theta) = \rho_p(\theta)/\rho_s(\theta)$ . Then using the second relation one obtains an expression for particle density,  $\rho_p$ , in terms of the occupation function,  $n$ ,

$$\rho_p(\theta) = n(\theta)(p')^{\text{dr}}(\theta), \text{ where } (\cdot)^{\text{dr}} = (\cdot) + \int \frac{d\alpha}{2\pi} \varphi(\theta - \alpha)n(\alpha)(\cdot)^{\text{dr}}(\alpha). \quad (6.6)$$

This definition also introduces the dressing operator. This is a very important operator which encodes how a given observable is altered by the presence of interactions. This will be primarily used to dress the  $h_i$ , the charge carried by the quasi-particles.

These are all the necessary TBA ingredients that are used to define the GHD description.

### 6.1.2 Generalised hydrodynamics main results

*Generalised hydrodynamics (GHD)* was developed in [89, 120] in order to describe non-equilibrium integrable systems. GHD generalises the Euler hydrodynamics of section 1.5 to integrable models where one needs to take into account the infinite set of conserved charges. These charges are introduced through the GGE since the maximal en-

tropy states of local fluid cells in the hydrodynamic picture are assumed to be defined by a GGE. Thus, from section 1.5, consider  $\underline{\beta}$  to be an infinite sized vector of Lagrange multipliers. To take advantage of techniques built for integrable systems the GHD makes use of the fact that a system described by a GGE state can be understood in terms of the thermodynamics of quasi-particles through the TBA. Thus, GHD provides a hydrodynamic description of integrable systems in terms of the quasi-particles of TBA.

The defining equation of GHD are the Euler equations of (1.40)<sup>1</sup>. In order understand these in terms of the quasi-particles one starts with the definition of  $q_i(x, t)$  and  $j_i(x, t)$  in terms of quasi-particles,

$$q_i(x, t) = \frac{\text{Tr} \rho_{GGE}(x, t) q_i}{\text{Tr} \rho_{GGE}(x, t)} = \int d\theta h_i(\theta) \rho_p(x, t; \theta) \quad (6.7)$$

$$j_i(x, t) = \frac{\text{Tr} \rho_{GGE}(x, t) j_i}{\text{Tr} \rho_{GGE}(x, t)} = \int d\theta h_i(\theta) \rho_p(x, t; \theta) v^{\text{eff}}(x, t; \theta), \quad (6.8)$$

where TBA quantities are introduced in the previous section and  $v^{\text{eff}}(x, t; \theta)$  is the group velocity of the quasi-particles as they move through the system. Where,  $v^{\text{eff}}(x, t; \theta) = (E')^{\text{dr}} / ((p')^{\text{dr}})$  and is thus related to  $\rho_p(x, t; \theta)$  through the dressing operator dependence on  $n(x, t; \theta)$  (see (6.6)) i.e. it depends on the GGE state. The first expression is a well-known expression from TBA and can be understood as an alternative definition of  $\rho_p$ . The second expression was first presented in [89, 120] and represents expectation values of the current expressed as a sum over quasi-particles carrying charge  $h^{(i)}$  moving at velocity  $v^{\text{eff}}$ . In order to understand the source of the  $(x, t)$  dependence recall that each fluid cell exists in an MES. This means the expectation value of each local observable is dependent only on the local MES which itself is defined by its set of  $\underline{\beta}$ . This leads to the observation that  $\langle q_i(x, t) \rangle_{\underline{\beta}} = \langle q_i(0, 0) \rangle_{\underline{\beta}(x, t)}$  i.e. in the Euler scale of the system the space-time dependence of expectation values can be defined by the local state which itself varies slowly in space-time. Thus the  $x, t$  dependence in (6.7) and (6.8) comes from the  $x, t$  dependence of  $\underline{\beta}(x, t)$  and enters through the definition of pseudo energy, (6.2) with (6.4). Thus the dynamics of  $\rho_p(x, t; \theta)$  govern the dynamics of the system. The equation of motion for  $\rho_p(x, t; \theta)$  is then found by inserting the previous expressions

---

<sup>1</sup>GHD has been extended to include dissipation i.e. a Navier-Stokes equation in [78], however this thesis will only consider the Euler scale equations.

into the Euler-hydrodynamic equations, (1.34) to find,

$$\partial_t \rho_p(\theta) + \partial_x (v^{\text{eff}}(\theta) \rho_p(\theta)). \quad (6.9)$$

However, there exists a better coordinate system than  $\rho_p(x, t; \theta)$ . Consider changing  $\rho_p \rightarrow n$  via (6.6). In this case one finds an important simplification. In order to see this consider the dressing transformation defined in (6.6) as an integral-operator (with measure  $d\theta/2\pi$ ) where  $(X)^{\text{dr}} = (1 - \varphi \mathcal{N})^{-1}(X)$  with  $\mathcal{N} \equiv n(\alpha) \delta(\theta - \alpha)$  and  $\varphi \equiv \varphi(\theta - \alpha)$ . Now define an inner product:  $a \cdot b = \int (d\theta/2\pi) a(\theta) b(\theta)$ . Then using the fact that  $v^{\text{eff}} \equiv (E')^{\text{dr}}/(p')^{\text{dr}}$  it is possible to write

$$q_i(x, t) = h_i \cdot \mathcal{N} (1 - \varphi \mathcal{N})^{-1} p' \quad (6.10)$$

$$j_i(x, t) = h_i \cdot \mathcal{N} (1 - \varphi \mathcal{N})^{-1} E'. \quad (6.11)$$

Inserting these expressions into the Euler-hydrodynamic equations (1.34), using  $\partial_{x,t} = (1 - \varphi \cdot \mathcal{N})^{-1} \partial_{x,t} \mathcal{N} (1 - \varphi \mathcal{N})^{-1}$  and using the fact that  $h_i$  is a complete basis to cancel out the  $h_i$ ,

$$\begin{aligned} & (1 - \varphi \mathcal{N})^{-1} \varphi \partial_t \mathcal{N} (p')^{\text{dr}} \\ & + (1 - \varphi \mathcal{N})^{-1} \varphi \partial_x \mathcal{N} (E')^{\text{dr}} = 0. \end{aligned} \quad (6.12)$$

where I used the definition of the dressing. Then cancelling terms appropriately and using  $v^{\text{eff}} = (E')^{\text{dr}}/(p')^{\text{dr}}$

$$\partial_t n(x, t; \theta) + v^{\text{eff}}(x, t; \theta) \partial_x n(x, t; \theta) = 0. \quad (6.13)$$

Thus changing from  $q(x, t) \rightarrow \rho_p \rightarrow n$  has diagonalised the flux Jacobian,  $A_i^{j2}$ . Recall from section 3.4 that modes that diagonalise the A matrix are called normal modes. Thus the occupation function  $n$  plays the role of normal modes in GHD and  $v^{\text{eff}}$  is the velocity of these normal modes.

In the Euler limit, the quasi-particles of the system actually have a natural interpretation as solitons [116]. With this in mind one can understand the GHD as being a

---

<sup>2</sup>Note that it diagonalises  $A_i^j(n)$  i.e.  $A_i^j$  as a function of the occupation function.

classical soliton limit of a quantum system. In section 2.3 I found a classical form for the energy transport SCGF in a CFT. Since massless bosons and fermions correspond to a CFT with central charge  $c = 1$  or  $c = 1/2$  respectively, it is not surprising to find some indication of a classical form with the GHD.

## 6.2 The SCGF of conserved quantity transport

This section is closely based on our work in [54, section 5.1] where I obtain a general expression for the SCGF of the transport for any conserved quantity in an integrable system using the BFF.

For the BFF I require the flow equation on the state variables  $\underline{\beta}$ , (3.33), and the BFF fundamental equation, (3.38), in the case of integrable models. For ease of reference I reproduce these equations here. Recall the flow equation is,

$$\frac{\partial \beta^i(\lambda)}{\partial \lambda} = -\text{sgn}(A(\lambda))_{i^*}^i, \quad (6.14)$$

where  $i^*$  refers to the index associated with the current of interest which is implicitly defined by the choice of  $\lambda$ . While the BFF fundamental equation is given by,

$$F(\lambda) = \int_0^\lambda d\lambda' j(\lambda'), \quad \text{where, } j(\lambda) \equiv \langle j \rangle_{\underline{\beta}(\lambda)}. \quad (6.15)$$

This clearly requires a hydrodynamic description of the integrable model which was introduced above as GHD, based on a TBA description. Furthermore, for the BFF to be applicable I assume that the system reaches an NESS generated by the partitioning protocol where the NESS is described by an MES. Then using the BFF I obtain an SCGF  $F(\lambda)$  for the flow of a conserved charge written in terms of TBA quantities. From this expression for  $F(\lambda)$ , *all cumulants can be obtained order by order* in terms of TBA quantities in the original state. Before our work in [54], this had not been done in general for interacting integrable models and, specifically for interacting quantum integrable models.

### 6.2.1 BFF equations for integrable models

Since the normal modes of GHD are  $n(\theta)$ , the TBA occupation function, I chose to present results in terms of  $n(\theta)$ . Then as  $n(\theta)$  is directly related to the pseudo energy  $\varepsilon$ ,

(6.4) which is built from  $\underline{\beta}$  via (6.2),  $\varepsilon$  also plays an important role. In order to make use of (6.15) the equations of state are needed combined with a flow equation on the state. In the case of GHD, the equations of state are expressed by (6.8). With this the BFF equations can be constructed for a general integrable model.

I consider  $\underline{\beta}$ , becoming  $\lambda$ -dependent by satisfying the flow equation (6.14). Thus, through (6.2) the pseudoenergy acquires a  $\lambda$ -dependence,  $\varepsilon(\theta; \lambda)$ . Recall that dressed functions depend on  $\varepsilon$  through  $n(\theta)$ , (6.6), which leads to all dressed functions gaining  $\lambda$ -dependence,  $h^{\text{dr}}(\theta; \lambda)$ . From (6.2), the pseudoenergy  $\varepsilon(\theta; \lambda)$  then satisfies

$$\varepsilon(\theta; \lambda) = \sum_i \beta^i(\lambda) h_i(\theta) + \int \frac{d\alpha}{2\pi} \varphi(\theta, \alpha) F(\varepsilon(\alpha; \lambda)). \quad (6.16)$$

Taking a  $\lambda$ -derivative and using the flow equation, (6.14), on the first term and  $\partial_\lambda F = \partial_\varepsilon F \partial_\lambda \varepsilon$  on the second term,

$$\partial_\lambda \varepsilon(\theta; \lambda) = - \sum_i \text{sgn}(A(\lambda))_i^i h_i(\theta) + \int \frac{d\alpha}{2\pi} \varphi(\theta, \alpha) n(\alpha; \lambda) \partial_\lambda \varepsilon(\alpha; \lambda). \quad (6.17)$$

Recall the definition of the dressing operator (6.6). With this one can see the equation above is equivalent to,

$$\partial_\lambda \varepsilon(\theta; \lambda) = - \sum_i \text{sgn}(A(\lambda))_i^i h_i^{\text{dr}}(\theta; \lambda). \quad (6.18)$$

In [90] it is shown that the dressing operator itself diagonalises  $A_i^j$ , this can be seen through the calculations that result in (6.13) which is used to show that  $h_i^{\text{dr}}$  diagonalises  $A_i^j$  with  $v^{\text{eff}}$ . Making use of this, the flow equation on the pseudoenergy is given by,

$$\partial_\lambda \varepsilon(\theta; \lambda) = - \text{sgn}(v^{\text{eff}}(\theta; \lambda)) h_i^{\text{dr}}(\theta; \lambda). \quad (6.19)$$

Then as the pseudoenergy fully characterises the GGE, this defines the  $\lambda$ -dependence of a general integrable model.

### 6.2.2 $F(\lambda)$ for integrable models

An expression for  $F(\lambda)$  can now be obtained using (6.15) and the solution of (6.19) in (6.8). I will show below that

$$F(\lambda) = - \int \frac{d\theta}{2\pi} E'(\theta) \left( \text{sgn}(v^{\text{eff}}(\theta; \lambda)) (F(\varepsilon(\theta; \lambda)) - F(\varepsilon(\theta; 0))) \right. \\ \left. - \int_0^\lambda d\lambda' \delta(v^{\text{eff}}(\theta; \lambda')) (\partial_{\lambda'} v^{\text{eff}}(\theta; \lambda')) (F(\varepsilon(\theta; \lambda')) - F(\varepsilon(\theta; 0))) \right), \quad (6.20)$$

In principle one can integrate (6.15), by parts in order to obtain  $F(\lambda)$ . However, it is easier to go the other way and show the derivative of (6.20) with respect to  $\lambda$ , in accordance with (6.15), is equal to  $\langle j_i \rangle$  from (6.8) and that  $F(\lambda)$  is correctly normalised, i.e.  $F(\lambda = 0) = 0$ .

Begin with the  $\lambda$ -derivative of the first line in the above expression. Clearly this results in two terms, the first comes from  $\partial_\lambda (\text{sgn}(v^{\text{eff}}(\theta; \lambda)))$  whilst the second comes from  $\partial_\lambda F(\varepsilon(\theta; \lambda))$ . The resulting expression from the second term can be obtained using (6.19) and (6.4), where this results in (6.8), with the  $\lambda$ -dependent state  $n(\theta; \lambda)$ . Thus, it is left to show that the remaining terms all cancel each other out.

Now consider the  $\lambda$ -derivative of the second line in (6.20). I make use of the Leibniz integral rule to perform this derivative. Performing this derivative results in two terms, the integrand evaluated at  $\lambda' = \lambda$  and  $\lambda' = 0$ . Then clearly, from  $F(\varepsilon(\theta; \lambda')) - F(\varepsilon(\theta; 0))$ , the integrand at  $\lambda' = 0$  is zero. The contribution of the integrand at  $\lambda' = \lambda$  is exactly the same as the first term produced by  $\lambda$ -derivative of the first line, i.e. the  $\partial_\lambda (\text{sgn}(v^{\text{eff}}(\theta; \lambda)))$  contribution. Thus, all the remaining terms are shown to have cancelled. Finally, this expression is correctly normalised by construction. This completes the proof since the  $\lambda$ -derivative of (6.20) results in  $\langle j_i \rangle$  from (6.8).

The result (6.20) is an exact general result for the SCGF in GGEs of arbitrary integrable models. The important contribution of this result is the inclusion of interactions which are contained within  $v^{\text{eff}}(\theta; \lambda)$  and  $\varepsilon(\theta; \lambda)$ . In order to obtain an expression (numerical or analytical if possible) for  $F(\lambda)$  one does the following: first solve the flow equation (6.19), most often numerically; secondly use the resulting pseudoenergy to evaluate the TBA quantities involved in (6.20), thirdly the spectral parameter is inte-



grated over.

This result can be applied to any model with known TBA, allowing one to obtain statistics of flows for a large range of interacting quantum models. Importantly, the result agrees with the Lesovik-Levitov formula for free-fermions as is shown in appendix D.2. In order to illustrate how to use this result, I apply (6.20) to obtain new results in the classical hard rod gas and the quantum Lieb-Liniger model in the next sections.

This result is equivalent to the type described in section 3.6 where the reason is as follows. In [89] it was shown that the generating function of the current is  $g = -\int d\theta E'(\theta)F(\varepsilon(\theta))$  in GHD. Since the infinite number of normal modes are defined by the occupation function  $n(\theta)$ , and  $\varepsilon$  and  $n$  are related via a one-to-one relationship via (6.4), the generating functional is clearly a sum of independent functions of the normal modes such that (3.60) is satisfied. Thus it is unsurprising that a result of the type predicted in section 3.6 is obtained. Although it is satisfying that this was obtained via independent means in this case.

## 6.3 Cumulants for transport

Before considering applications of this results to specific models, I present the scaled cumulants obtained from the expression (6.20). The first few cumulants provide important information about the shape of the distribution, and are the most accessible to numerical simulations and experiment; these are arguably the most important outcome of the expression for  $F(\lambda)$ .

The cumulants are obtained from (6.20) via  $c_k = \partial_\lambda^k F(\lambda)|_{\lambda=0}$ . The first cumulant is the average current, given in (6.8). For the second cumulant, omitting the  $\theta$ -dependence of the integrand for ease of notation,

$$c_2 = \int d\theta \rho_p |v^{\text{eff}}| (h_{i^*}^{\text{dr}})^2 f, \quad (6.21)$$

where  $\rho_p = n(p')^{\text{dr}}/(2\pi)$  is the quasiparticle density, and  $f = -d \log n / d\varepsilon$  is known as the statistical factor. The expression in (6.21) was already evaluated exactly in [90] by different methods, and follows as a consequence of current-current sum rules introduced in section 3.1.3. Equation (6.21) is in agreement with this, providing an important check on the result. The higher cumulants are new, and again omitting the explicit  $\theta$ -

dependence of the integrand are given by,

$$c_3 = \int d\theta \rho_p f |v^{\text{eff}}| h_{i*}^{\text{dr}} \left[ (h_{i*}^{\text{dr}})^2 \tilde{f} s + 3 \left( (h_{i*}^{\text{dr}})^2 f s \right)^{\text{dr}} \right], \quad (6.22)$$

where  $\tilde{f} = -(\text{d log } f / \text{d } \varepsilon + 2f)$  and  $s = \text{sgn}(v^{\text{eff}})$ . While the fourth cumulant is given as,

$$c_4 = \int d\theta \rho_p f v^{\text{eff}} \left\{ (h_{j*}^{\text{dr}})^4 s \hat{f} \tilde{f} + 3s((sf(h_{j*}^{\text{dr}})^2)^{\text{dr}})^2 + 4h_{j*}^{\text{dr}} s(f\tilde{f}(h_{j*}^{\text{dr}})^3)^{\text{dr}} \right. \\ \left. + 6\tilde{f}(h_{j*}^{\text{dr}})^2 (sf(h_{j*}^{\text{dr}})^2)^{\text{dr}} + 12h_{j*}^{\text{dr}} s(sf h_{j*}^{\text{dr}} (sf(h_{j*}^{\text{dr}})^2)^{\text{dr}})^{\text{dr}} \right\}, \quad (6.23)$$

where  $\hat{f} = -(\text{d log}(f\tilde{f}) / \text{d } \varepsilon + 3f)$ . In appendix D.3 I provide the details of the calculation of these cumulants.

In the next section I show a comparison of the exact results of the first four cumulants obtained from (6.20) applied to a classical integrable model, the Hard rod gas, to results gained from a Monte Carlo simulation. The agreement of these provides a further check on the results gained here.

## 6.4 Classical hard rod gas

In this section I use Monte Carlo simulations to verify the expressions for cumulants based on (6.20). This requires the specialisation of the above general expressions to the hard rod gas. This section is closely based on our work in [54, section 6].

The hard rod gas (HR) is a one-dimensional classical system of rods of length  $a$  interacting via elastic collisions. This means, on colliding the rods swap velocities. This is possibly the simplest interacting integrable model which provides an important testing ground for any techniques that apply to integrable systems as a whole. Furthermore, as it is a classical model it is fairly simple to generate Monte-Carlo simulations of the system, which I use to help confirm cumulant results.

The hydrodynamic description of the gas was obtained in [121] and shown to be consistent with a TBA description in [90]. Recall the TBA describes the system as comprised of quasi-particles where, in the case of the HR gas, the quasi-particles are velocity carrying tracers, i.e. when two rods collide and swap velocity it is equivalent to the quasi-particle hopping by the length of a rod. In the language of TBA quantities introduced above, the HR gas is defined by,  $F(\varepsilon) = -e^{-\varepsilon}$ ,  $n(\theta) = e^{-\varepsilon(\theta)}$ ,  $f(\theta) = 1$ , and

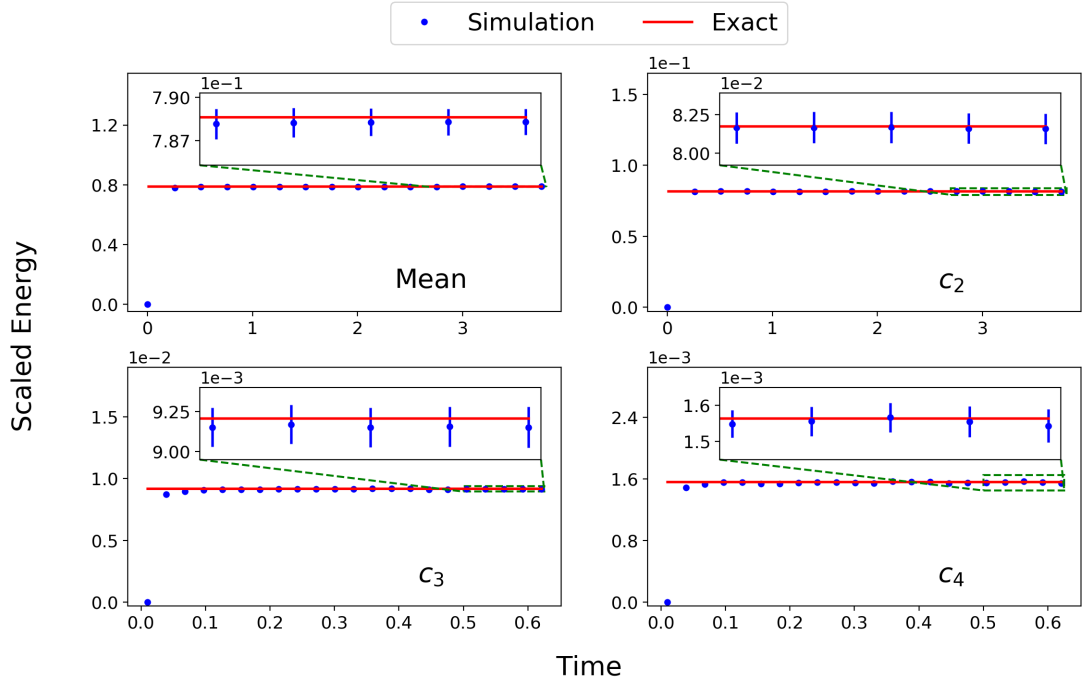


**Figure 6.1:** Insets highlight the agreement between theoretical predictions and Monte Carlo simulation of the first four energy flow cumulants in the hard rod gas. Theoretical predictions from (6.20) are the red lines, Monte Carlo results are the blue dots with error bars. The initial velocities of the rods are drawn from normal distributions, with mean 8 and variance 15, and mean  $-3$  and variance 10, for the left and right system halves, respectively. Other parameters are: rod length  $a = 0.56$ ;  $10^5$  particles;  $2 \times 10^7$  Monte Carlo samplings; initial system length  $10^5$ . Rod densities are fixed by the velocity variances in thermal distributions. The scaling parameter for the y-axis is  $\bar{v}^3/a$  where  $\bar{v}$  is the average rod speed. Error bars are found via bootstrap re-sampling using 3000 samples. Times plotted are chosen so as to reach the effective steady state before boundary effects arise; higher cumulants, which are affected by rarer events with faster moving rods, are sensitive to finite-size effects sooner.

the interactions are defined by  $\varphi(\theta, \alpha) = -a$  for rod length  $a$ . Notice the interaction term is constant, this is the basis of simplifications that occur in the HR gas as the dressing operator simplifies dramatically (see appendix D.5). The quasi-particles are Galilean which means energy and momentum are given by  $(1/2)\theta^2$  and  $\theta$  respectively (assuming mass,  $m = 1$ ).

In order to verify the expressions obtained for the cumulants in the previous section, I specialise these to the HR and compare the predictions of the first four cumulants of the energy flow with direct Monte Carlo simulations of the gas. In order to consider energy transport I consider the charge  $h_{i^*}(\theta) = \theta^2/2$  which is the amount of conserved charge, in this case energy, carried by the quasi-particles. Using the exact TBA description [122], I obtain the cumulants predicted in a NESS arising from the partitioning protocol with

initial left and right states that are thermal and boosted with different temperatures and boost velocities. See appendix D.5 for a derivation of thermal distributions in the HR; these are normal distributions, proportional to  $\exp(\beta(v - v_0)^2/2)$  where  $v_0$  describes the boost velocity and  $\beta$  the temperature of the bath. The calculation of the cumulants requires an expression for the occupation function  $n(\theta)$ , then using this I am able to obtain  $\rho_p$ , implement the dressing operator and thereby find  $v^{\text{eff}}$ . With these I have all the necessary ingredients to calculate the cumulants above. In order to obtain  $n(\theta)$  in the HR, it is possible to show at the interface of the partitioning protocol that [89, 122],

$$n(\theta) = n_l(\theta)\Theta(\theta - \theta^*) + n_r(\theta)\Theta(\theta^* - \theta), \quad (6.24)$$

where  $\theta^*$  is defined by  $v^{\text{eff}}(\theta^*) = 0$ ,  $\Theta$  is the Heaviside step function and  $n_{l(r)}(\theta)$  are the states defined by the initial left(right) distributions from the partitioning protocol which in this case are boosted thermal distributions defined in appendix D.5. I show this result in appendix D.4. To obtain  $\theta^*$  requires solving  $v^{\text{eff}}(\theta^*) = 0$  through an iterative procedure: start with a guess  $\theta_0^*$  (usually  $\theta_0^* = 0$  which is true in the free case) then calculate  $n_0(\theta)$  based on  $\theta_0^*$ . Since  $v^{\text{eff}}$  is a function of  $n(\theta)$ , through  $(E')^{\text{dr}}$  and  $(p')^{\text{dr}}$ , one solves  $v^{\text{eff}}(\theta_1^*) = 0$  using  $n_0$  to obtain  $\theta_1^*$ . This is repeated until converge is reached which is mostly within five iterations or less. In the HR, simplifications occur as the dressing functions take on a far simpler form based on the fact that  $\varphi(\theta)$  is constant. In general, one would need also to solve dressed quantities through an iterative procedure, but this is discussed in greater detail in the next section on the Lieb-Liniger gas.

The second half of the problem is to simulate the gas by running the (deterministic) HR dynamics from a sampled initial condition, where the initial left and right halves of the line are sampled with the prescribed left and right thermal boosted states. I add up the energy of the rods that pass through the centre of the system up to time  $t$ . This is done for multiple samples, from which I obtain the cumulants and then scale by time.

The Monte Carlo error bars are obtained via the bootstrap sampling method in which I re-sample data with replacement from the obtained data set and calculate ‘alternative’ values of the required cumulant [123]. The standard deviation of these values represents the associated uncertainty. Figure 6.1 shows cumulants of the steady state energy flow in the HR resulting from the Monte Carlo simulation, compared with results

predicted from the BFF results. It is clear that within error bars the prediction from (6.20) is successful. The appendix D.5 contains the details on theoretical cumulant calculations in the HR, and appendix D.6 provides details on the Monte Carlo numerical simulation. In this approach the initial partitions are not just put into contact but are thrust into each other. This is a highly non-trivial set-up and the accurate prediction displays the power of the results obtained here while providing strong evidence that (6.20) is correct.

The success of this simulation is not obvious. Recall that the BFF holds for an NESS in a MES. The complication is this Monte-Carlo simulation actually starts counting the energy transported at the initial time, when the system is certainly not in an MES. Thus, these results can only work because energy transport is dominated by the late time of the system to such an extent that the initial energy fluctuations are not contributing much. This is not expected to always be true and may be a unique property of the HR, although further investigation of this is required before more definitive statements can be made.

## 6.5 Quantum Lieb-Liniger gas

In this section I undertake a thorough investigation of the implications of (6.20) for the Lieb-Liniger gas within a NESS generated via the partitioning protocol. I provide an introduction to important details of this model, obtain values for the cumulants while varying the interaction strength and the temperature difference between initially thermalised partitions, and finally plot the SCGF which will lead to a discussion on fluctuation relations in the next section.

### 6.5.1 Primer on Lieb-Liniger and problem statement

The Lieb-Liniger gas (LL) is a 1D model of interacting bosons which interact via a repulsive  $\delta$ -interaction, meaning bosons only interact when they meet. This model is of vital importance within the integrability community as not only does it provide a simple testing ground for ideas related to quantum integrability, but experimental advances now allow unprecedented control under lab conditions. Specifically the review of [124] explains that there now exist experimental predictions related to quantum dynamics, thermalisation, solitons, fermionisation, YY thermodynamics, strong coupling, phase diagram, 3-body correlations and excited states of the LL gas. The Hamiltonian of the

LL is given by [125],

$$H = \int dx \left( \frac{1}{2m} \partial_x \psi^\dagger \partial_x \psi + c \psi^\dagger \psi^\dagger \psi \psi \right). \quad (6.25)$$

The LL has a well-known TBA formulation defined by the following TBA quantities:  $F(\epsilon) = -\log(1 + e^{-\epsilon})$ ,  $n(\theta) = 1/(1 + e^{\epsilon(\theta)})$ , and  $f = 1 - n$ , while interactions are defined by  $\varphi(\theta, \alpha) = 4c/((\theta - \alpha)^2 + 4c^2)$  where  $c$  is the coupling strength. Notice that the TBA quasi-particles are fermions. A summary of the derivation of TBA formulation for the LL gas is presented in appendix D.1.

There are two important limits for the LL in the TBA, the zero-interaction strength and infinite-interaction strength limits. In the limit  $c \rightarrow 0$ ,  $\varphi(\theta, \alpha) \rightarrow 2\pi\delta(\theta)$  and the LL is equivalent to a free boson model as expected. This result can be seen by solving for the pseudo energy, (6.2), in this limit and then inserting the result for the free energy of Fermionic TBA particles, (6.3) where this procedure results in the free energy simplifying to that of free Bosons. The limit  $c \rightarrow \infty$  is a free fermion model and is trivially true since in this limit  $\varphi(\theta, \alpha) \rightarrow 0$ .

One must take care about the coupling used since  $c$  is not a dimensionless quantity. The correct factor that defines coupling in the LL is  $c/n_0$  where  $n_0$  is the particle density and corresponds to  $q$  of (6.7) in the case where  $h_i(\theta) = 1$  [89, 125]. This is done to ensure that when one discusses large interactions, the correct scale is discussed.

Specialising expressions for cumulants and the integrable SCGF, (6.20) to this model, provides explicit predictions for all the large-scale cumulants for transport, including for the total number of particles transferred ( $h_i^*(\theta) = 1$ ) and the total energy ( $h_i^*(\theta) = \theta^2/2$ ) where states are defined by  $\beta_l$  and  $\beta_r$  of the partitioning protocol.

### 6.5.2 Cumulants in the Lieb-Liniger

As in the case of the hard rod gas, to make use of the expressions for the cumulants one needs to obtain an expression for  $n(\theta)$ . The procedure to obtain this is explained in the following paragraph. However, unlike in the HR gas, there is no closed solution for the dressing function, (6.6). Thus  $(E')^{\text{dr}}$  and  $(p')^{\text{dr}}$  must be obtained via an iterative solution through an extra step using  $n_1(\theta)$  as obtained before. These iterations also converge quickly and mostly within 5 iterations. The other complication comes from the terms  $n_l$

and  $n_r$  in (6.24) as they don't have a closed analytical form as in the HR case. In the case of the LL gas one calculates  $n_l$  ( $n_r$ ) using the  $\beta_l$  ( $\beta_r$ ) (from the partitioning protocol) in (6.2), solving iteratively for  $\varepsilon_l$  ( $\varepsilon_r$ ) and inserting this into (6.4).

In fig. 6.2 and fig. 6.3 I present a heat map of the values of all four cumulants of both integrated energy and particle transport respectively. In each plot the x-axis represents that variation of  $\beta_r$  of the partitioning protocol with fixed  $\beta_l = 0.5$  whilst the y-axis represents the variation of the dimensionless interaction constant. The interaction strength in these plots is dimensionless via  $c/n_0$  where  $n_0$  is the particle density, as discussed above. Since the dimensionless interaction strength depends on  $n_0$  which in turn depends on temperature, there exists a non-linear relationship between the dimensionless coupling and  $\beta_r$ . As the overall behaviour displayed in these plots is the same, I focus the explanation on fig. 6.2 which shows the cumulants in energy transport.

Notice that  $c_1$ , the current, increases with increasing  $\beta_r$ . Increasing  $\beta_r$  corresponds to an increasing temperature difference between the two partitions of the system leading to a greater driving force on the system. The larger driving results in a larger current flow. Now consider  $c_3$ , since  $c_3$  is a measure of the distribution's skewness this appropriately increases with the increasing difference in temperature. The opposite effect occurs for both the variance of energy transport and  $c_4$ . The reason is the increasing  $\beta_r$  is equivalent to lowering the temperature of the right partition. Thus, the left temperature, which was held constant, begins to dominate the system. This leads to an overall decrease in the strength of fluctuations as the stochasticity is driven largely from only one source. Since  $c_4$  is known to measure the 'tailedness' of the distribution, a decreasing  $c_4$  means one observes infrequent tail or outlier events - again consistent with this decreasing of stochasticity.

It is also clear that increasing of the coupling strength leads to a decrease in all four cumulants, which can be understood as the appearance of 'jams' in the system. To understand this, consider the case of zero interaction strength - these are non-interacting particles and as such move 'through' each other without anything impeding their movement. Then as the interacting strength is turned on the particles repel each other, this effect acts like a break on the system since particles slow down as they come across other particles. This slow down leads to 'jams' in the system in which particles are af-

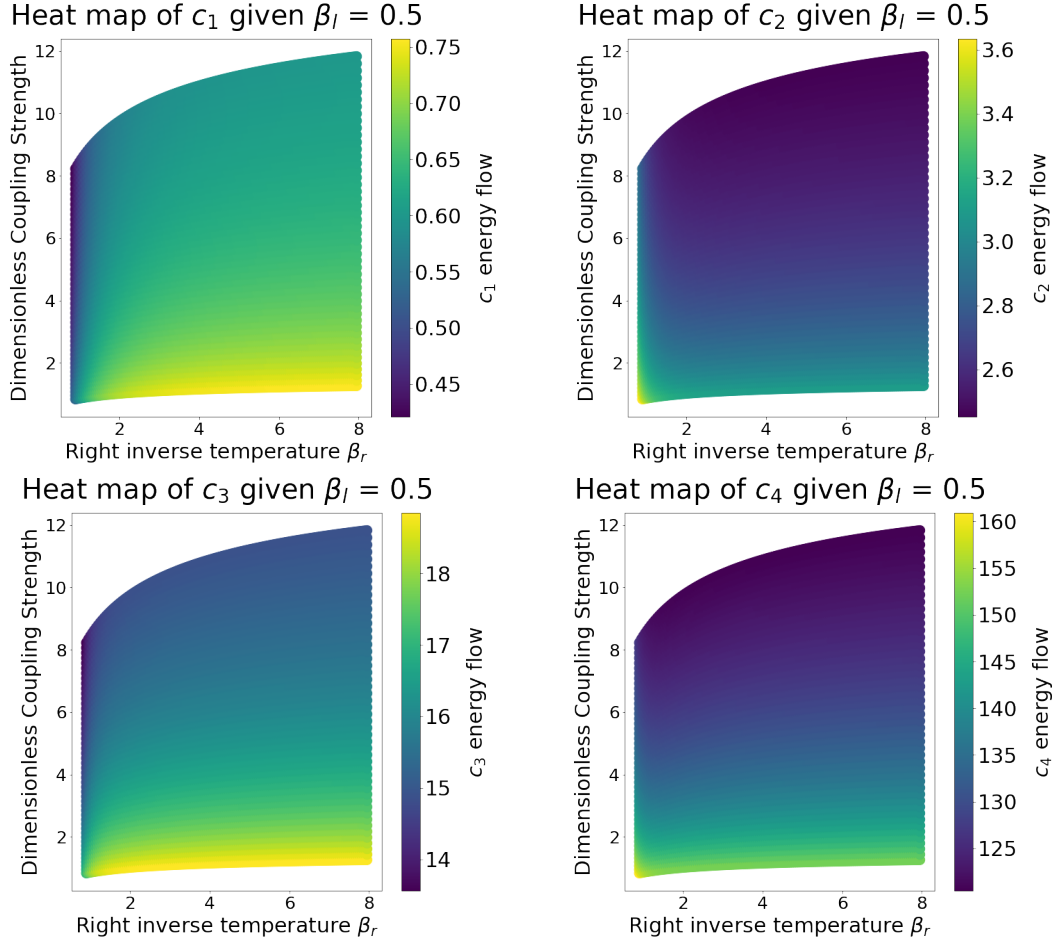


**Figure 6.2:** This plot shows heat maps for energy transport cumulants in the LL gas where the x-axis represents the variation of  $\beta_r$  of the partitioning protocol with fixed  $\beta_l = 0.5$  whilst the y-axis represents the variation of the dimensionless interaction constant. This shows a smooth change in values with no expected complex behaviour. Increasing temperature differences lead to increasing values for the odd cumulants and decreasing values for the even ones. Increasing interaction strength leads to lower values in all four cumulants.

ected by the slowest particle in the neighbourhood. This has the effect of decreasing the total energy transported and thus a decrease across all cumulants.

### 6.5.3 SCGF and probability distribution in the Lieb-Liniger

In order to obtain the SCGF for the LL,  $n(\theta)$  is calculated in the same way as above. Then using the fermion relationship required for the LL,  $\varepsilon(\theta) = \log(n(\theta)^{-1} - 1)$  which provides  $\varepsilon(\theta; \lambda = 0)$ . In order to obtain  $F(\lambda)$  one must solve the flow equation, (6.19), numerically for  $\varepsilon(\lambda)$ . Equation (6.19) is solved numerically using an iterative approach known as Picard's method [126] which works as follows: assume  $y(x) = y(0) + \int_{x_0}^x dx' f(x', y(x'))$  solves the ODE  $dy/dt = f(x, y)$  where  $y_0 = y(x_0)$ .



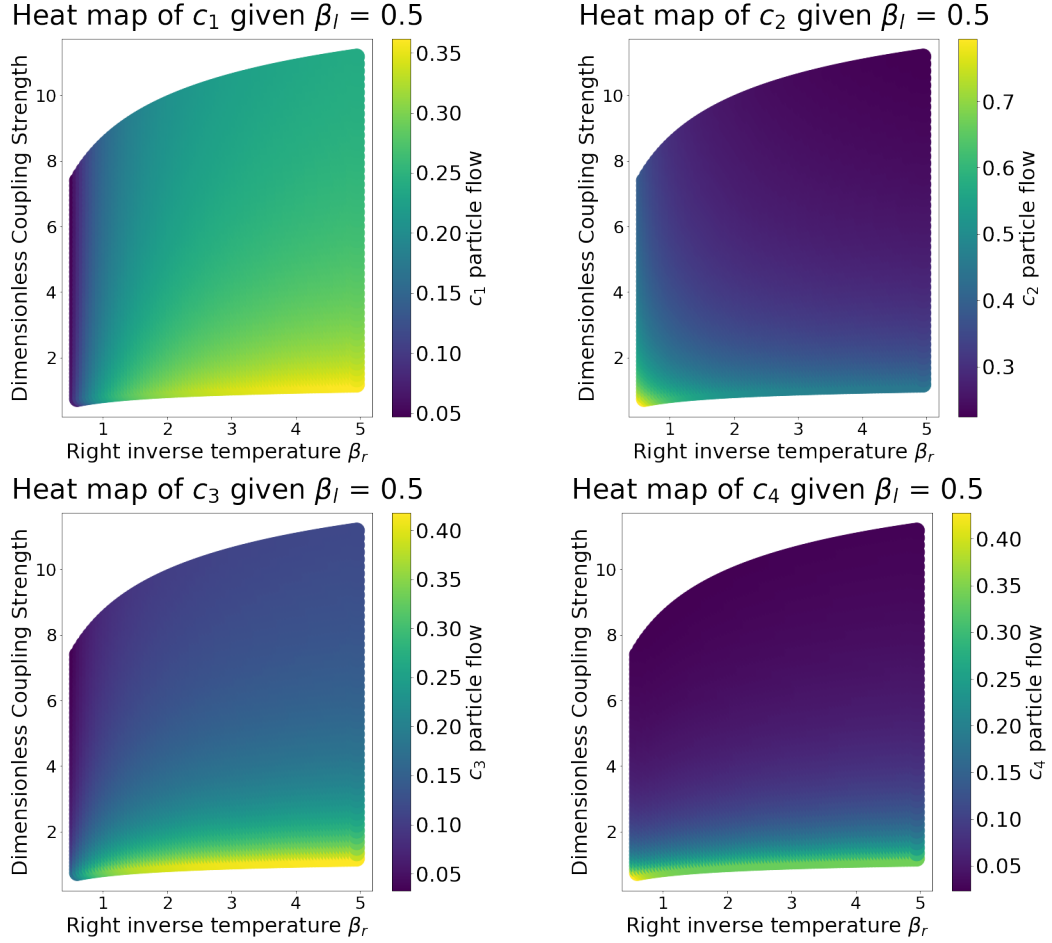


**Figure 6.3:** This plot shows heat maps for particle transport cumulants in the LL gas where the x-axis represents the variation of  $\beta_r$  of the partitioning protocol with fixed  $\beta_l = 0.5$  whilst the y-axis represents the variation of the dimensionless interaction constant. The observed behaviour is identical to that of the energy transport cumulants in fig. 6.2.

Then take an initial guess for the solution  $g_0(x)$ . From here one iterates as follows:  $g_{i+1}(x) = y_0 + \int_{x_0}^x dx' f(x', g_i(x'))$  until convergence is reached. Convergence was found to be fairly rapid, taking 20 or less iterations.

In this manner the SCGFs in fig. 6.4 were obtained. These plots show the resulting SCGF for two sets of values of  $\beta_r$  and  $\beta_l$  with coupling taken as  $c = 1.5$ . Both plots are convex as is required of the SCGF [34], and both grow sharply near the values  $-\beta_r$  and  $\beta_l$ . These are the values at which divergences in the SCGF occur in free Bosonic models (and also in conformal field theory [44]), thus suggesting that at these values, the free Bosonic physics of the LL dominates. Both plots are also seen to display a symmetry which is shown to be the Gallavotti-Cohen relation in the next section. The plot on the left of fig. 6.4 is an equilibrium scenario whilst the plot on the right is a non-equilibrium

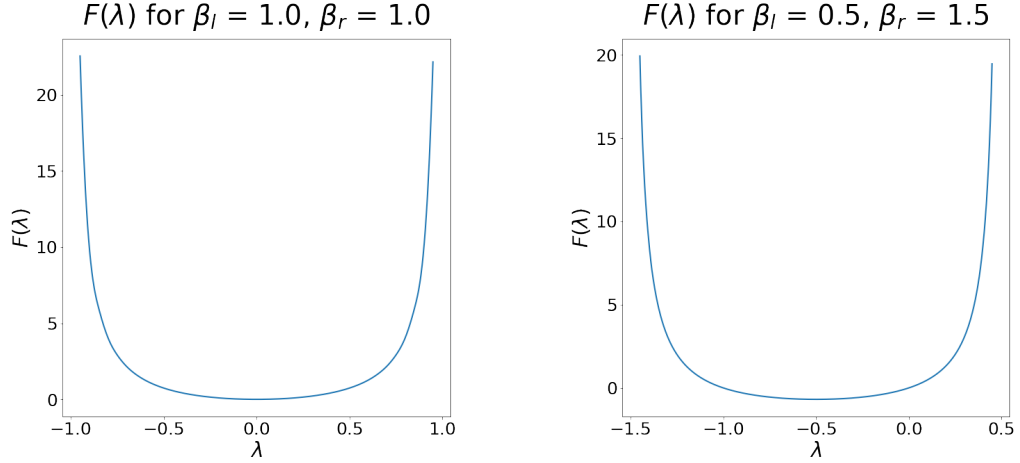


**Figure 6.4:** Figures showing the SCGF for the LL with coupling  $c = 1.5$ . Shapes shown are convex, as required for an SCGF. Sharply growing values at  $-\beta_r$  and  $\beta_l$  match divergences in free Bosonic models suggesting free Bosonic physics of the LL dominates here. There is also symmetry in these plots reminiscent of Gallavotti-Cohen relations. The plot on the left is an equilibrium scenario whilst the plot on the right is a non-equilibrium one - more information on this is gained from fig. 6.5

one. In order to explore the difference in behaviour it is best to obtain the probability distributions in both cases.

In order to obtain a probability distribution from the SCGF recall the rate function is related to the SCGF via a Legendre-Fenchel transform as outlined in section 1.2.2. In turn the rate function defines the probability distribution through the definition of the LDP, (1.1). Thus the probability distribution is found for increasing  $t$  via a numerical Legendre-Fenchel transform of  $F(\lambda)$  above. The probability distributions that correspond to the SCGF plots in fig. 6.4 are found in fig. 6.5. As expected, as time increases there is an increasing peak with suppressed tails, the definition of the large deviation principle. Satisfyingly in the equilibrium case  $\beta_l = \beta_r$  one sees a symmetrical distribution where the average transport is 0. The non-equilibrium case produces a slightly asymmetric curve where there is a steeper slope for lower energy particles and a shallower slope for higher energy particle. This is related to the imbalance in the system partitions resulting in more higher energy particles in the system. The asymmetry is made clearer in fig. 6.6 in which I plot the mirror image of the left side of the probability distributions over the obtained distribution. The asymmetry is seen clearly by the right-hand figure as the curves do not overlap.

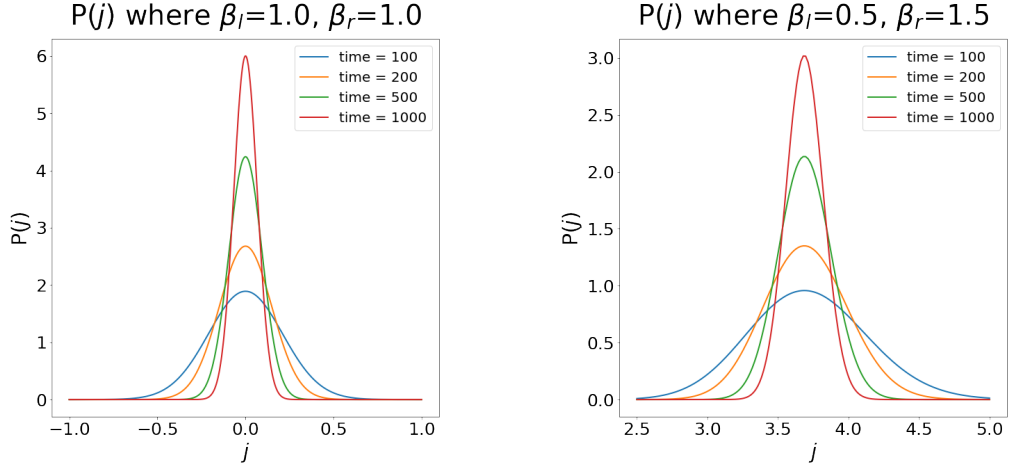


**Figure 6.5:** The figure on the left show the probability distribution obtained by using a numerical inverse Legendre-Fenchel transform on the SCGF of the left figure in fig. 6.4 for increasing system time, an equilibrium scenario. The behaviour is as expected, a growing peak in time at  $j = 0$ , the expected current of an equilibrium system. The figure on the right is the equivalent plot for the non-equilibrium SCGF of the right figure of fig. 6.4.

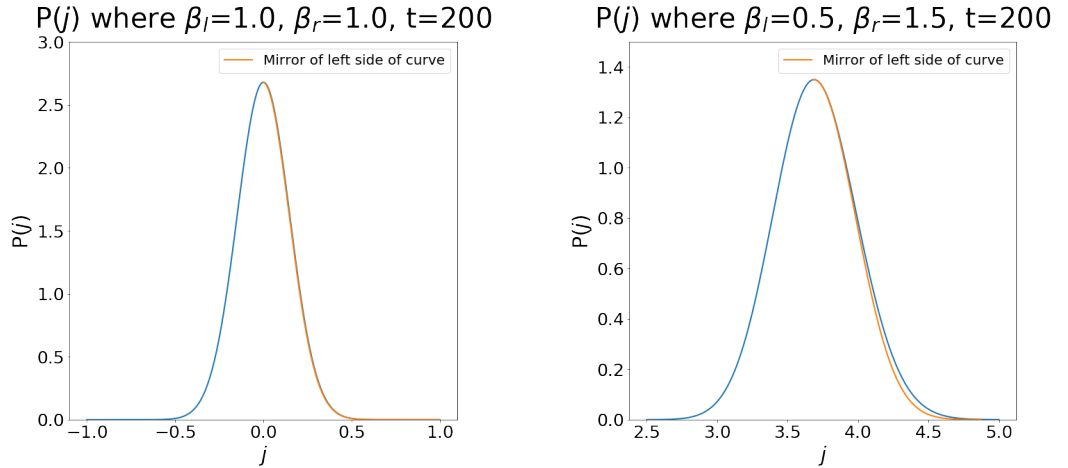


**Figure 6.6:** The figure on the left show the probability distribution for energy transport at a specific time in the equilibrium scenario, notice the curve is proven to be symmetrical. The figure on the right is the equivalent probability distribution for a non-equilibrium state. In this case there exists a slightly asymmetrical curve which is explained by the imbalance defined by the initial conditions of the partitioning protocol.

## 6.6 Fluctuation relation in integrable models

A different check on (6.20) is to confirm the expected non-equilibrium fluctuation relation (1.26) as was done in the case of  $d$ -dimensional CFT in section 5.3. Recall from section 1.3.3 that the FR in a NESS emerging from the partitioning protocol expected to

satisfy,

$$F(\lambda) = F(-\lambda - (\beta_l - \beta_r)). \quad (6.26)$$

Proving that (1.26) is satisfied based on (6.20) through analytical means has proven highly nontrivial. The reason is (6.20) is expressed in terms of the solution to a flow equation which leaves the explicit  $\lambda$ -dependence difficult to obtain. As fluctuation relations involve shifts in  $\lambda$ , undertaking these shifts for a function without an explicit analytical form is difficult. Nevertheless, one may verify the symmetry (1.26) by numerically solving the flow equation (6.19) and evaluating (6.20). This section is largely based on the results found in [54].

Since (1.26) is expected to hold, the FR is exposed by a symmetry in the plot of the SCGF about the point  $(\beta_l - \beta_r)/2$ . I would like to stress that figures in this section are not produced via Monte Carlo simulations but are the numerical solutions for (6.20) under various parameters. Figure 6.7 shows the same curves from fig. 6.4 except here I have inserted the expected symmetry line at  $(\beta_l - \beta_r)/2$  and plotted the mirror image of the left part of the curve over the right side of the curve. The fact that the mirror image is effectively indistinguishable from the actual curve provides numerical evidence that the SCGF is satisfying the FR for this choice of parameters. Note that in the equilibrium case one expects the SCGF to be symmetrical around zero, which is borne out by the left hand plot of fig. 6.4. In order to ensure this symmetry isn't a result of a lucky choice of parameters I computed results for a variety of different parameter choices. Figure 6.8 shows the SCGF for the LL with different temperatures but the same interaction strength  $c$ . Figure 6.9 displays the results of varying the interaction strength while maintaining the same temperatures. Lastly, fig. 6.10 shows HR-specific results using similar parameters as for the previous plots. In all cases the symmetry is prominent which provides strong numerical evidence that the integrable SCGF formula satisfies the FR.

The validity of the fluctuation relation in the LL and HR provide further support both for (6.20), and for the general consistency of the theory of non-equilibrium transport. Clearly an interesting future project would be analytical validation of this fact.

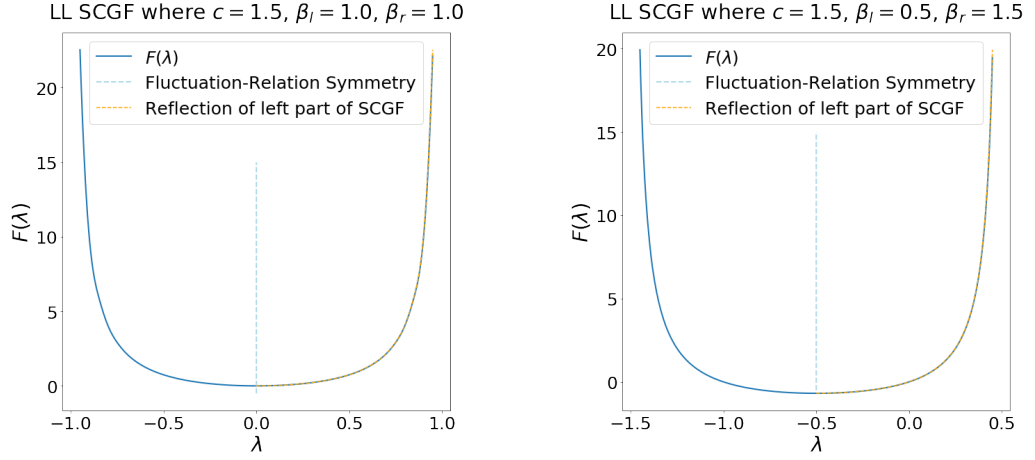


**Figure 6.7:** Numerical evidence for the fluctuation-relation symmetry in the LL. Plot of the energy flow SCGF for the LL using (6.20). These are the same figures as in fig. 6.4 with the expected symmetry line at  $(\beta_l - \beta_r)/2$  and the mirror image of the left part of the curve plotted over the right side of the curve. The fact that the mirror image is effectively indistinguishable from the actual curve provides numerical evidence that the SCGF is satisfying the FR for this choice of parameters. Furthermore, the symmetry point at  $\lambda = 0$  for equilibrium (left figure) is expected.

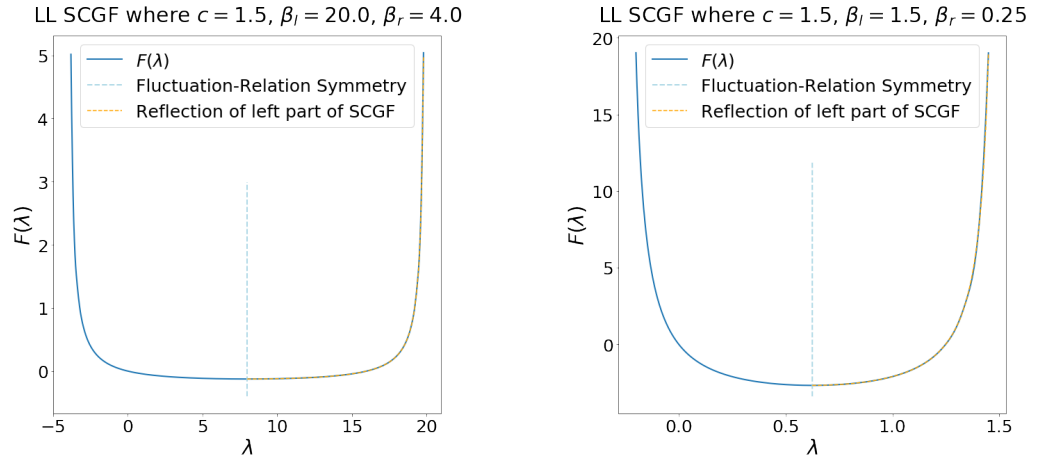


**Figure 6.8:** Energy flow SCGF for the LL using equation (6.20). Both plots use an interaction strength of  $c = 1$ . In (a) the parameters used are  $\beta_l = 20$ ,  $\beta_r = 4$  and in (b)  $\beta_l = 0.25$ ,  $\beta_r = 1.5$ . In both cases a dotted line is plotted for the expected symmetry point at  $(\beta_l - \beta_r)/2$ . Both plots also indicate the symmetry by reflecting the left-hand side of the plot onto the right-hand side of the plot.

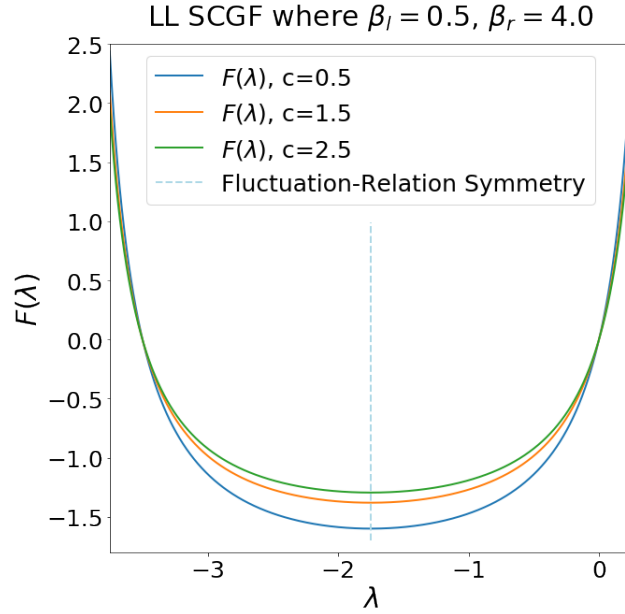


**Figure 6.9:** Same as fig. 6.8 but with  $\beta_l = 1, \beta_r = 5$  and various values of  $c$ . The FR symmetry point,  $(\beta_l - \beta_r)/2$ , is again shown by the dotted line.

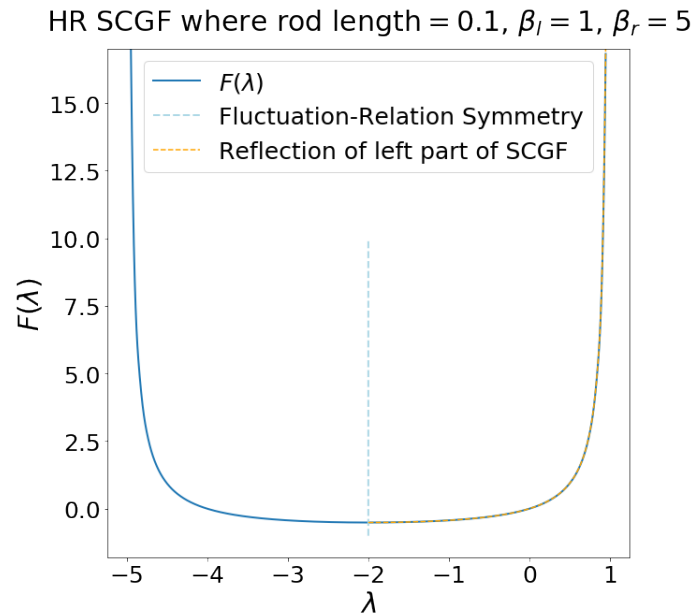


**Figure 6.10:** Plot of the energy flow SCGF for the HR using equation (6.20). For this plot the parameters used are  $\beta_l = 1, \beta_r = 5$  and rod length = 0.1. Once again, the dotted line is the expected FR symmetry point and the curve is reflected to indicate how symmetrical it is.

# Conclusion

The overall aim of this thesis was to investigate transport fluctuations in non-equilibrium states of both classical and quantum systems. The scaled cumulant generating functional from large deviation theory was used to understand and quantify fluctuations in such states. Thus, the goal of this thesis was the calculation of the SCGF for transported quantities. Due to the complexity of general non-equilibrium states, I considered only the ‘simplest’ class of non-equilibrium states, non-equilibrium steady states, which are time invariant. The primary outcome of this work was the development of the Ballistic Fluctuation Formalism, a general approach to obtaining the SCGF for a broad range of systems.

The first original results (unpublished) of this thesis were obtained in chapter 2. In this chapter it was shown that the SCGF can be obtained based on three specific properties: the steady state current, the assumption that the Gallavotti-Cohen relation holds, and the presence of chiral separation. With this I was able to construct a scaled cumulant generating functional for each KdV charge of a CFT, a charge defined by multiples of the energy momentum-tensor and used to exploit the technology of integrable systems within a CFT. In the case that the NESS is obtained via the partitioning protocol, it was found that fluctuations in the transport of a KdV charge can be obtained via the difference of the fluctuations in two independent equilibrium systems. This approach was successful at producing new results and insights for 1D CFTs, however, it was difficult to extend this to systems in which chiral separation was broken. Since the scaled cumulant generating functional requires large time limits, it was natural to turn to a hydrodynamic treatment of transport in non-equilibrium steady states.

Making use of hydrodynamics proved fruitful as it led to the general framework, the BFF, introduced in chapter 3. The BFF was applied to varying systems across the

remaining chapters with much success indicating the effectiveness of the BFF as a unifying principle. This approach, which was published in [51], applies to systems supporting ballistic transport within maximal entropy states attained by the long-time evolution of dynamics governed by Euler hydrodynamics. The BFF is based on two equations: the flow equation, and the fundamental BFF equation. The flow equation is a differential equation that governs how a state should be modified by the conjugate parameter of the SCGF and plays a role similar to linear response theory. The fundamental equation provides a link between states satisfying a flow equation and the SCGF through the equations of state. The fundamental equation can be understood as a re-summation of the cumulant expansion that defines the SCGF into a  $\lambda$ -dependent current. With these equations, the fluctuations in the transport of some ballistic quantity can be obtained using only the equations of state and knowledge of system fluctuations. These fluctuations can be quantified by either the static correlation function or the structure of the maximal entropy states directly. The BFF was shown to fully explain the presence of the extended fluctuation relation while also predicting dynamical phase transitions through the SCGF. The remainder of the thesis focussed on using this framework to unify a range of existing results and further generate new results.

In chapter 4 I applied the BFF to a classical lattice system with stochastic dynamics - the  $\ell$ -TASEP. This chapter involves original but unpublished work. The value of this chapter is two-fold; firstly, it showed how to use the BFF in the case of a classical lattice gas with stochastic dynamics and secondly, the simplicity of the  $\ell$ -TASEP helped confirm and generate insights into the BFF itself and phase transitions. New results for the SCGF of particle transport in the  $\ell$ -TASEP were obtained. Chapter 5 showed how the BFF applied to a conformal field theory in  $d$  dimensions, a quantum theory. This was partly based on work we published in [51] while also introducing some further new but unpublished work. Through the BFF I calculated the SCGF for energy flow and found the existence of the Gallavotti-Cohen fluctuation relation. This chapter further added to the cannon of the BFF by showing how to apply it to a  $d$ -dimensional system and adding this quantum system to its range of applicability.

Chapter 6 is arguably the most valuable application of the BFF in this thesis. The results of this chapter are from our publication [54] with some further unpublished work



added. The application of the BFF to integrable models requires the use of generalised hydrodynamics which represents integrable models in terms of quasi-particles through the thermodynamic Bethe ansatz. Through the BFF I obtained a general expression for the SCGF of transported conserved quantities that is applicable to any model with a TBA description - this represents an important advance in the field of integrability. From the SCGF I obtained analytical expressions for the first four cumulants. These predicted cumulants were applied to the energy transport in a classical Hard Rod gas and compared to cumulants obtained via a Monte-Carlo simulation. This provided sound numerical evidence that the SCGF obtained is correct. The results were then applied to the Lieb-Liniger gas where I obtained new predictions for values of cumulants and the probability distribution of energy transport. Finally, I presented numerical evidence that the integrable SCGF satisfies the Gallavotti-Cohen fluctuation relation.

In summary the BFF has correctly reproduced known results in the TASEP, 1D CFTs, and non-interacting (1D) field theories. It has produced new results in the  $\ell$ -TASEP,  $d$ -dimensional CFT with  $d > 1$  and interacting integrable models of both classical and quantum variety. Thus, the BFF has proven to be an important unifying framework across non-equilibrium states of many different systems.

This thesis has opened up many pathways to further research. In the short term the results of chapter 4 are nearly publishable where a further check is needed on the SCGF in the case  $\ell > 1$  and more calculation in the zero range process is needed. There are also results from sections 6.5.2 and 6.5.3 which may be expanded on and published in the near term. In the medium term there are at least two further important applications for the BFF. Reference [127] obtained an Euler-scale hydrodynamic description for the ballistic transport in the one-dimensional fermionic Hubbard model. In this work they calculate many of the expressions needed in order to apply the BFF, thus opening up the possibility of obtaining the full transport statistics in this model. Another important application would be obtaining the full statistics of the spin transport in spin chains where the required hydrodynamics description already exists in [128]. In the long term one may search the literature for cases where the macroscopic fluctuation theory is applied to systems similar to those in which the BFF applies. For instance, the macroscopic fluctuation theory is applied to the weakly-asymmetric exclusion process which is the

same set-up as the TASEP except that particles hop to the left at approximately the same rate as they hop to the right. From these examples one may be able to obtain some cases or limits in which these two approaches are in agreement. If such a case are possible this may indicate how to incorporate diffusive terms into the BFF, potentially unifying this approach with the MFT. This would result in a framework fully capable of calculating the fluctuations for a general hydrodynamic classical or quantum system in a non-equilibrium state.

## Appendix A

# Appendices to chapter 2

### A.1 Bootstrapping in $d$ -dimensional free massive theories

The results of section 2.2.2 can be generalised further to include free massive theories in  $d$ -dimensions. This is based on results found in [41]. The bootstrapping method of section 2.2.2 is applicable to these systems since they display a chiral splitting in the same way seen for 1D CFTs [41]. In order to make use of bootstrapping I will assume the Gallavotti-Cohen fluctuation relation holds and I assume the system attains a NESS through the partitioning protocol.

In the case of the partitioning protocol, the steady state energy current of a massive case  $d$ -dimensional free field theory was found in [41]. It is given by:

$$j^{ss} = C \left( a_{d+1} [m\beta_l] \frac{1}{\beta_l^{d+1}} - a_{d+1} [m\beta_r] \frac{1}{\beta_r^{d+1}} \right), \quad (\text{A.1})$$

where  $C$  is a constant,  $d$  is the dimension of the theory,  $\beta_{l/r}$  are the Lagrange multipliers in the partitioning protocol,  $m$  is the mass of the particles and  $a$  is some function that depends on the dimensionless constant  $\beta m$  and  $d$ . In the case of free Bosons in  $d$ -dimensions,

$$a_{d+1} [m\beta] \equiv (1/\Gamma(d+1)) \int_0^\infty dp p^d / (\exp(\sqrt{p^2 + m^2\beta^2}) - 1), \quad (\text{A.2})$$

where  $\Gamma$  is the gamma-function. In order to make a connection to the notation of section 2.2.2 instead of considering  $d$ , I consider  $p$  such that  $\beta^{(p)} = \beta^d$ . Thus, for a general

system of massive particles the three inputs required for the Bootstrapping approach are,

$$F(\lambda) = f(\lambda, \beta_r^{(p)}, m) + f(-\lambda, \beta_l^{(p)}, m) \quad (\text{A.3})$$

$$F(\lambda) = F(\beta_r^{(p)} - \beta_l^{(p)} - \lambda) \quad (\text{A.4})$$

$$j_{ss} = C \left( a \left[ m \beta_l^{(p)1/p} \right] \beta_l^{(p)-1-1/p} - a \left[ m \beta_r^{(p)1/p} \right] \beta_r^{(p)-1-1/p} \right), \quad (\text{A.5})$$

These expressions can be used to find an SCGF for the energy flow in a system of massive Bosons/Fermions in  $d$ -dimensions through the method of bootstrapping. Also notice that in this form these expressions are very similar to those obtained in section 2.2.2, except in this case there is an extra function. If one sets  $a_0[x] = 1$ , I get exactly the results from section 2.2.2. Thus, results obtained here are, in principle, more general.

Exactly the same line of argument as in section 2.2.2 is followed. As before I introduce the simplified notation  $\beta^{(p)} \equiv \tilde{\beta}$  and start with the generalised form of (2.13),

$$f(\lambda, \tilde{\beta}, m) = \frac{1}{\lambda^{1/p}} g \left[ \frac{\lambda}{\tilde{\beta}}, m \tilde{\beta}^{1/p} \right] \quad (\text{A.6})$$

$$\text{where, } g[x, w] = a_0[x] w^{1+1/p} + a_1[x] w^{2+1/p} + \mathcal{O}(w^{3+1/p}). \quad (\text{A.7})$$

Again inserting the above results into (A.4) and using (A.3) I can write in terms of dimensionless variables to obtain,

$$\begin{aligned} & \left( g \left[ \frac{\frac{\tilde{\beta}_r}{\lambda} - \frac{\tilde{\beta}_l}{\lambda} - 1}{\frac{\tilde{\beta}_r}{\lambda}}, m \tilde{\beta}_r^{1/p} \right] + (-1)^{1/p} g \left[ \frac{-1 \left( \frac{\tilde{\beta}_r}{\lambda} - \frac{\tilde{\beta}_l}{\lambda} - 1 \right)}{\frac{\tilde{\beta}_r}{\lambda}}, m \tilde{\beta}_l^{1/p} \right] \right) \\ &= \frac{\lambda^{1/p} \left( \frac{\tilde{\beta}_r}{\lambda} - \frac{\tilde{\beta}_l}{\lambda} - 1 \right)^{1/p}}{\lambda^{1/p}} \left( g \left[ \frac{\lambda}{\tilde{\beta}_r}, m \tilde{\beta}_r^{1/p} \right] + (-1)^{1/p} g \left[ -\frac{\lambda}{\tilde{\beta}_l}, m \tilde{\beta}_l^{1/p} \right] \right). \quad (\text{A.8}) \end{aligned}$$

The same change of variables can be used:  $\frac{\tilde{\beta}_r}{\lambda} = \frac{1}{w} + h$ ,  $\frac{\tilde{\beta}_l}{\lambda} = \frac{1}{w} - 1$ . The left hand side is expanded to order  $h^{1+1/p}$  using (A.7), and the right hand side is Taylor expanded to  $\mathcal{O}(h^{1+1/p})$ . Matching the left and right at  $\mathcal{O}(h^{1+1/p})$ , changing the integration variable

$w = \frac{\lambda}{\tilde{\beta}}$  one finds:

$$f[\lambda, \tilde{\beta}, m] = \int d\tilde{\beta} \left( -\frac{a_0 [m\tilde{\beta}^{1/p}]}{\tilde{\beta}^{1+1/p}} + \frac{a_0 [m(\tilde{\beta} - \lambda)^{1/p}]}{(\tilde{\beta} - \lambda)^{1+1/p}} \right). \quad (\text{A.9})$$

Putting this expression back into (A.3) I obtain the general expression for the SCGF. The above results match other known results. In particular by considering  $p = 1$  and  $a_0[m\tilde{\beta}] = c/12$  the results of section 2.2.2 are found, the results for a 1D CFT. Using  $p = 1$  and  $a_0[m\tilde{\beta}] = \int_0^\infty d\varepsilon \left( \varepsilon / e^{\sqrt{\varepsilon^2 - m^2 \tilde{\beta}^2}} - 1 \right)$  one obtains the results found in [41].

## A.2 1D CFT energy transport from classical particles on a ring

The claim was made in section 2.3 that the SCGF for a CFT can be expressed in a Poisson formulation which is strongly associated with systems of classical particles. In this appendix I show that the SCGF for fluctuations of energy transport in a 1D CFT, (2.26) with  $p = 1$ , can be derived from an explicit classical stochastic dynamical system.

It is well known that the SCGF of particle flow of a random walker is given by [8],

$$F_n(\lambda) = p_n(e^{n\lambda} - 1) + q_n(e^{-n\lambda} - 1), \quad (\text{A.10})$$

which is equivalent to the cumulant generating functional of a Poisson process. The Gallavotti-Cohen fluctuation relation are known to hold in such a system and can be written as,

$$F_n(E_n - \lambda) = F_n(\lambda) \text{ where } E_n = \frac{1}{n} \ln \frac{q_n}{p_n}. \quad (\text{A.11})$$

Now consider there are two random walkers in a ring, walkers 1 and 2, they hop to the right with rates  $p_1$  and  $p_2$  and to the left with rates  $q_1$  and  $q_2$  respectively. This situation is illustrated in fig. A.1. Further assume that particle 1 carries one unit of energy and particle 2 carries two units of energy. Since these are two independent processes, the

total SCGF for particle transport is simply a sum and given by,

$$F(\lambda) = p_1(e^\lambda - 1) + q_1(e^{-\lambda} - 1) + p_2(e^{2\lambda} - 1) + q_2(e^{-2\lambda} - 1), \quad (\text{A.12})$$

where the vale in front of  $\lambda$  defines the amount of energy carried by the particle. The assumption is made that fluctuation relations must hold over the combined system, this is equivalent to the requirement that  $E_1 = E_2$ . This results in the following constraint,

$$\ln \frac{q_2}{p_2} = 2 \ln \frac{q_1}{p_1}. \quad (\text{A.13})$$

Finally, I enforce the condition of (A.13) on (A.12) by assuming  $p_2 = p_1^2$  and  $q_2 = q_1^2$ . This leads to,

$$\begin{aligned} F^{(2)}(\lambda) &= p(e^\lambda - 1) + q(e^{-\lambda} - 1) + p^2(e^{2\lambda} - 1) + q^2(e^{-2\lambda} - 1) \\ &= \sum_{\varepsilon=1,2} p^\varepsilon (e^{\varepsilon\lambda} - 1) + \sum_{\varepsilon=1,2} q^\varepsilon (e^{-\varepsilon\lambda} - 1) \\ &= \sum_{\varepsilon=1,2} e^{\varepsilon \ln p} (e^{\varepsilon\lambda} - 1) + \sum_{\varepsilon=1,2} e^{\varepsilon \ln q} (e^{-\varepsilon\lambda} - 1). \end{aligned} \quad (\text{A.14})$$

In the case of  $\nu$  different particle types one may then write,

$$F^{(\nu)}(\lambda) = \sum_{i=0}^{\nu} \left( e^{\varepsilon_i \ln p} (e^{\varepsilon_i \lambda} - 1) + e^{\varepsilon_i \ln q} (e^{-\varepsilon_i \lambda} - 1) \right), \quad (\text{A.15})$$

where  $\varepsilon_i$  is the amount of energy carried by the  $i^{\text{th}}$  particle.

If one considers a very large number of energy carriers each carrying increasing amounts of energy, then with the appropriate rescaling of  $p = \beta_r/\nu$  and  $q = \beta_l/\nu$ , this expression is equivalent to the CFT expression found in (2.26) with  $p = 1$ ,

$$F_{\text{CFT}}(\lambda) = C \int_0^\infty d\varepsilon \left( e^{-\varepsilon \beta_r} (e^{\lambda \varepsilon} - 1) + e^{-\varepsilon \beta_l} (e^{-\lambda \varepsilon} - 1) \right). \quad (\text{A.16})$$

This exposes a clear relationship between the energy transport in a 1D CFT case and a system comprised of an infinite number of random walkers on a ring each carrying an energy from the continuous range of energies available.

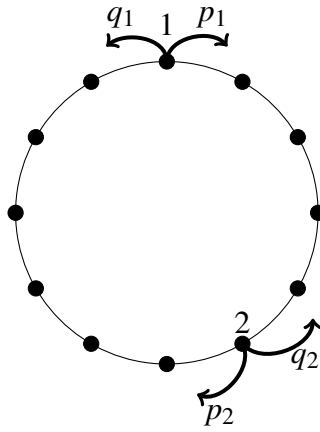


**Figure A.1:** Figure showing two independent random walkers on a ring, where particle 1/2 hopping with rate  $p_1/p_2$  to the right and  $q/q'$  to the left.

## Appendix B

# Macroscopic fluctuation theory

As was stated in the introduction, there already exists a highly successful approach to calculating rate functions which through a Legendre-Fenchel transform gives the SCGF. This successful approach is known as Macroscopic fluctuation theory (MFT) [48]. I provide a very brief introduction to MFT as this thesis presents the results of research that may hopefully be merged with MFT at some future date. This is not intended to be a detailed exposé. These notes follow [48, 129] closely.

In essence the MFT acts as a non-equilibrium generalisation of Einstein equilibrium fluctuation theory [48]. Landau and Lifshitz present Einstein fluctuation theory in [130] based on the following expression for the probability of a fluctuation in an equilibrium system in contact with an environment:

$$\mathbb{P} \approx e^{-\frac{R_{min}}{T_0}}, \text{ where } R_{min} = \Delta E - T_0 \Delta S + P_0 \Delta V. \quad (\text{B.1})$$

$R_{min}$  represents the minimal work needed to produce the fluctuation under a reversible transformation.  $\Delta E$ ,  $\Delta S$  and  $\Delta V$  are the corresponding variations of energy, entropy and volume. The environment is represented through its temperature  $T_0$  and pressure  $P_0$ . MFT extends this type of estimate for application in a NESS.

As in the ballistic fluctuation formalism developed in [51] and presented in chapter 3, the MFT relies on a hydrodynamics description of the system. However, the MFT applies to diffusive systems where the state of interest can be completely described by the density  $\rho(x, t)$  and the corresponding current  $j(x, t)$  which satisfy the continuity equation

$$\partial_t \rho + \nabla \cdot j = 0, \quad (\text{B.2})$$



and the constitutive equation, or equations of state,

$$j = J(t, \rho) = -D(\rho)\nabla\rho + \chi(\rho)E(t), \quad (\text{B.3})$$

where  $D(\rho)$  is the diffusion constant  $\chi(\rho)$  is the mobility constant and  $E(t)$  is some external field being applied to the system. For the MFT one also assumes  $D(\rho)$  and  $\chi(\rho)$  satisfy the local Einstein relation,

$$D(\rho) = \chi(\rho)f_0''(\rho), \quad (\text{B.4})$$

with  $f_0(\rho)$  the equilibrium specific free energy.

The equation underlying the MFT is a large deviation formula (like the LDP introduced in chapter 1) for joint fluctuations of the density and the current,

$$\mathbb{P}((\rho_\varepsilon(t), j_\varepsilon(t))) \asymp e^{-\varepsilon^d \mathcal{R}_t(\rho, j)}, \quad (\text{B.5})$$

where the similarity to the Einstein fluctuation relation is quite clear. Here  $\varepsilon^d$  is the ratio between the microscopic length scale and the macroscopic one and represents the order of the number of particles in a macroscopic volume. The term  $\mathcal{R}_t(\rho, j)$  is comprised of two terms and can thought of as the cost to the system of the joint fluctuation of interest,

$$\mathcal{R}_t(\rho, j) = V(\rho, t=0) + \mathcal{I}_t(\rho, j), \quad (\text{B.6})$$

where  $V(\rho, t=0)$  represents the cost to create the initial condition and  $\mathcal{I}_t(\rho, j)$  is the cost to follow the trajectory from the initial condition until  $(\rho_\varepsilon(t), j_\varepsilon(t))$  is actually achieved. The cost of the trajectory followed is defined by:

$$\mathcal{I}_t(\rho, j) = \frac{1}{4} \int_0^t dt' \int dx [j - J(\rho)] \chi^{-1}(\rho) [j - J(\rho)]. \quad (\text{B.7})$$

which is related to the energy dissipated by the extra current  $[j - J(\rho)]$ . In [48] the form of this expression is explained through an analogy with an electric circuit. If  $\chi^{-1}(\rho)$  is analogous to the role of resistor and  $[j - J(\rho)]$  is the electric current, then the power radiated according to Ohms law is  $P = I^2 R$  which is equivalent to the above expression.

The MFT then uses this fundamental formula to calculate quantities as needed. I outline how the MFT is used to calculate fluctuations of time-integrated currents as these are the quantities of interest in this thesis. Starting with the probability of interest,

$$\mathbb{P}\left(\int_0^t dt j_\varepsilon(t) = tJ\right) \asymp e^{-\varepsilon^d t \Phi_t(J)}, \quad (\text{B.8})$$

where  $t$  is the total time and  $\Phi_t(J)$  is the rate function for the current. In [48] they show,

$$\Phi_t(J) = \frac{1}{t} \inf_{(\rho, j) \in \mathcal{A}_t} \mathcal{I}_t(\rho, j), \quad (\text{B.9})$$

where  $\mathcal{A}_t$  is defined by the set of paths  $(\rho, j)$  that have average current  $J$  with initial density  $\rho_0$  i.e.

$$\mathcal{A}_t = \left\{ (\rho, j) : \frac{1}{t} \int_0^t dt' j_\varepsilon(t') = J, \partial_t \rho = -\nabla \cdot j, \rho(0) = \rho_0 \right\}. \quad (\text{B.10})$$

The reason for the infimum over the paths is the rate function is applicable in the large scaling limit. Only by considering the smallest values of the rate function does one obtain the correct contributions.

With the rate function one can do a Legendre-Fenchel transform in order to find the current SCGF. This marks out the approach taken in the MFT. Clearly diffusion plays an important role in this method while a big advantage of this method is it is not constrained to 1D systems as the BFF is. The downside is in a system with ballistic transport, the MFT will not hold due to the dependence on diffusive terms.

## Appendix C

# Appendices to chapter 4

### C.1 Zero range process flow equation

This section explains the zero-range process, a classical lattice model with stochastic dynamics. This model is of particular importance in deriving the hydrodynamic equation for the  $\ell$ -TASEP of chapter 4. I also provide a very brief overview on obtaining a flow equation for the zero-range process from the BFF.

#### C.1.1 ZRP primer

The Zero Range process (ZRP) is used to find the hydrodynamic equations that govern the  $\ell$ -ASEP. The ZRP is a lattice model where any number of particles can occupy a lattice site. These particles move left and right with rates  $\omega_i q$  and  $\omega_i p$  respectively where  $\omega_i$  is related to the occupation number of site  $i$ , and  $p$  and  $q$  are fixed model parameters. As the hopping rate of a particle is only affected by the site it occupies, this is a zero-range interaction.

The ZRP is an interesting model as different choices of  $\omega_i$  can alter the system quite dramatically. For instance, choosing  $\omega_i = 1$  provides the starting point for the mapping between the ZRP and holes of the  $\ell$ -TASEP. Alternatively choosing  $\omega_i = \frac{i}{i+1}$ , encodes a long range interaction which in the hydrodynamic limit can be used to represent the Hard Rods gas of section 6.4 with a constant velocity [105].

In this appendix I briefly show how one would apply the results of BFF in order to obtain a flow equation for the ZRP.

### C.1.2 ZRP flow equation

As in the  $\ell$ -TASEP in order to obtain a flow equation I require knowledge of the static correlation function and the equations of state which dictate how the current depends on the particle density. For ease recall the flow equation in this case, (3.31), is given by,

$$\partial_\lambda q_i(\lambda) = \sum_j \text{sgn}(A(\lambda))_{i*}^j C_{ji}(\lambda). \quad (\text{C.1})$$

In the ZRP, as in the  $\ell$ -TASEP, there is only one conserved quantity, the particle density  $\rho_Z(x, y)$ . Thus I use  $q_i = \rho_Z$  and  $A_i^j$  and  $C_{ij}$  are simply numbers and not matrices.

In the ZRP the static correlation,  $C$ , is the same form as in the  $\ell$ -TASEP, (4.2) [105],

$$C = z_Z \frac{\partial \rho_Z}{\partial z_Z}, \quad (\text{C.2})$$

where  $z_Z$  is the fugacity defined as was done in (4.3),

$$Z_Z = \sum_{n=0}^{N_{\max}} z_Z^n Z_n, \quad (\text{C.3})$$

with  $Z_Z$  the non-equilibrium partition function and  $Z_n$  the  $n$ -particle partition function.

The equations of state are found from the ZRP Euler scaling limit. Reference [106] shows this to be  $j_Z = z_Z$  i.e. the current is equivalent to the fugacity in the system. This leads to a flux Jacobian,

$$A = \frac{\partial j_Z}{\partial \rho_Z} = \frac{\partial z_Z}{\partial \rho_Z}. \quad (\text{C.4})$$

Then using the flow equation (C.1),

$$\begin{aligned} \frac{\partial \rho_Z}{\partial \lambda} &= \text{sgn}(A(\lambda)) C(\lambda) \\ &= \text{sgn}\left(\frac{\partial z_Z(\lambda)}{\partial \rho_Z(\lambda)}\right) z_Z(\lambda) \frac{\partial \rho_Z(\lambda)}{\partial z_Z(\lambda)}. \end{aligned} \quad (\text{C.5})$$

Recall from here one will use the fundamental equation of BFF, (3.38), in order to obtain the SCGF. Thus, at this juncture it makes sense to consider a flow equation on  $z_Z$  since

$j_Z = z_Z$ . Using chain rule on the left-hand side above one obtains,

$$\frac{\partial z_Z(\lambda)}{\partial \lambda} = \text{sgn} \left( \frac{\partial z_Z(\lambda)}{\partial \rho_Z}(\lambda) \right) z_Z(\lambda). \quad (\text{C.6})$$

In order to solve this equation, one needs the fugacity-density relationship where In the ZRP the fugacity-density relationship is defined by:

$$\rho_Z = z_Z \frac{d}{dz_Z} \log Z_Z, \quad Z_Z = \sum_{n=0}^{\infty} Z_n z_Z^n, \quad Z_n = \prod_{m=1}^n \frac{1}{\omega_m}, \quad Z_0 = 1. \quad (\text{C.7})$$

Thus, with specific choices of  $\omega_m$  one obtains results for the ZRP current SCGF.

It is worth mentioning that given the flux Jacobian is equivalent to the collective velocity used in [93, 131], the phase transitions predicted by the flow equation will be in exact agreement with [109, 131].

## C.2 $\ell$ -TASEP hydrodynamic quantities

This section follows the arguments of [104–106]. The hydrodynamic equations for the  $\ell$ -TASEP are found through a mapping to the Zero-range process (ZRP). The ZRP is introduced in detail in appendix C.1 above. Specifically, there exists a map from the  $\ell$ -TASEP on a periodic lattice of length  $L$  with  $N$  particles to the closed ZRP of length  $N$  and  $L - \ell N$  particles with ZRP rates given by  $\omega_i = 1$ . This is equivalent to saying that the motion of holes in the  $\ell$ -TASEP map to a ZRP process [106].

### C.2.1 Hydrodynamic current

The following argument follows [106] closely.

One can show that mapping the  $\ell$ -TASEP to the ZRP with  $\omega_i = 1$  as described above is equivalent to two relationships: firstly, the particle density of the ZRP,  $\rho_Z(y, t)$  is related to the  $\ell$ -TASEP density via,

$$\rho_Z(y, t) = 1/\rho(x, t) - \ell, \quad (\text{C.8})$$

Secondly the position of the  $i^{\text{th}}$  TASEP particle at time  $t$ ,  $k(i, t)$ , is related to the number

of ZRP particles at site  $j$ ,  $\xi_{j,t}$  via,

$$k(i,t) = \sum_j \xi_{j,t} + \ell(i+1). \quad (\text{C.9})$$

In order to obtain a relationship between the continuum position in the  $\ell$ -TASEP,  $x$ , and that of the ZRP,  $y$ , consider the Euler scaling limit of (C.9) controlled via some parameter  $\nu$  that goes to  $\infty$ . Then in the Euler scaling,  $t \rightarrow \nu t$ ,  $k = x\nu$ ,  $i = x\nu$ . Expanding in  $1/\nu$ , one finds a continuum relation for the position of the TASEP particle,

$$x(y,t) = \int_0^y du (\rho_Z(u,t)) - \frac{(1/\nu)}{2} [\rho_Z(y,t) - \rho_Z(0,t)] + \ell(y - (1/\nu)) + \mathcal{O}((1/\nu)^2). \quad (\text{C.10})$$

The hydrodynamic equations for the ZRP are found through the large  $x, t$  limit of its master equation,

$$\partial_t \xi_{i,t} = p z_{i+1,t} + q z_{i-1,t} - (p+q) z_{i,t}, \quad (\text{C.11})$$

with site independent hopping rates  $p$  and  $q$  (i.e.  $\omega_i = 1$ ) as per the  $\ell$ -TASEP mapping and  $z_{i,t}$  is the probability that a site  $i$  is non-empty at time  $t$ . This can be taken to the continuum limit such that  $z_{i,t}$  becomes the fugacity which allows one to use the fact that for the ZRP, if  $\omega_i = 1$  then  $z = \rho_Z(1 + \rho_Z)^{-1}$ . The resulting expression combined with the mappings defined by (C.8) and (C.10) produces the hydrodynamics equation for the  $\ell$ -TASEP,

$$\partial_t \rho = -\partial_x \left( \rho \frac{1 - \ell \rho}{1 - (\ell - 1) \rho} \right), \quad (\text{C.12})$$

which immediately identifies the  $\ell$ -TASEP current as (4.5) at Euler scaling.

### C.2.2 $\ell$ -TASEP fugacity

Since the ZRP has a stationary process, and a mapping exists between these two systems, the stationary weights of the  $\ell$ -TASEP must be distributed equally among all configurations on the ring. To understand the stationary states recall (4.2),  $Z = \sum_N^{N_{\max}} z^n Z_n$ .

Since all states contribute equally  $Z_N$  is simply the number of possible different

$N$ -particle configurations on length  $L$  i.e. :

$$Z_n = \binom{L - (\ell - 1)N}{N}. \quad (\text{C.13})$$

This object allows one to calculate the fluctuations in the density. In particular in the hydrodynamic limit, the partition sum is approximated by its maximum term and the steady state fugacity is given by [106]:

$$z = \frac{\rho(1 - (\ell - 1)\rho)^{\ell-1}}{(1 - \ell\rho)^\ell}. \quad (\text{C.14})$$

This completes the key results needed for the  $\ell$ -TASEP.

## Appendix D

# Appendices to chapter 6

### D.1 Derivation of TBA for Lieb-Liniger

In this section I will give a brief overview of the thermodynamic Bethe ansatz (TBA) as applied to the Lieb-Liniger model. Recall that the TBA is a thermodynamic limit of the Bethe ansatz which is used to find the spectrum of the ground state in integrable models (section 6.1.1). I introduced the Lieb-Liniger model in section 6.5 as a gas of interacting bosons in 1D where the interaction occurs when two bosons meet. The Hamiltonian was given as,

$$H = \int dx \left( \frac{1}{2m} \partial_x \psi^\dagger \partial_x \psi + c \psi^\dagger \psi^\dagger \psi \psi \right). \quad (\text{D.1})$$

in the following I assume  $m = 1$ . This derivation of the TBA closely follows [117] which is based on [132].

The starting point is the Bethe equations for the Lieb-Liniger model given by:

$$e^{ip_j L} = \prod_{k \neq j}^N \frac{p_j - p_k + ic}{p_j - p_k - ic}, \quad (\text{D.2})$$

where  $L$  is system size and the  $p_i$  are the Bethe particle momenta and  $c$  is the interaction strength from the Lieb-Liniger Hamiltonian. From this the S-matrix can be read off as,

$$S(p_l, p_m) = S(p_l - p_m) = \frac{p_l - p_m + ic}{p_l - p_m - ic}. \quad (\text{D.3})$$

Since these are non-relativistic Bosons the dispersion relation is given by the usual



$$E(p) = p^2.$$

The goal is to get the density of states in the momentum space. In other words, I obtain a relationship for the number of states and the momentum. To begin I rewrite the S-matrix as,

$$S(p) = -e^{i \arctan p/c} \equiv -e^{i\psi(p)}. \quad (\text{D.4})$$

With this definition the Bethe equations can be re-written as

$$2\pi I_j = p_j L - i \sum_k \log S(p_j - p_k) = p_j L + \sum_k (\psi(p_j - p_k) + \pi), \quad (\text{D.5})$$

which is defined up to the integer  $I_j$  defining the branch of the logarithm taken. The integers are in one-to-one correspondence with solutions to the Bethe equations. To prove this Yang and Yang created the Yang-Yang functional [132]. It is an unnecessary detour to introduce this functional explicitly but what this relationship shows is these  $I_j$  can be viewed as quantum numbers for the system. These quantum numbers can be used to obtain a density of states in the thermodynamic limit.

Having obtained quantum numbers, I move to the thermodynamics. In order to do this a deeper understanding between the quantum numbers and the momenta is required.

Start by defining a counting function  $c(p)$  where:

$$Lc(p) = \frac{L}{2\pi} p + \frac{1}{2\pi i} \sum_k \log S(p - p_k). \quad (\text{D.6})$$

By comparing this with (D.5) it is clear that for a state with quantum numbers given by  $\{I\}$  the particle momenta correspond to the  $p$ 's for which  $Lc(p_j) = I_j$ . Similarly, any allowed quantum number  $J$  that is  $\notin \{I\}$  is a hole with momentum  $Lc(p) = J$ . This picture can be argued for physically as follows: start by noticing the counting function is monotonically increasing, then since each particle carries an energy  $p^2$ , in the  $N$ -particle system has quantum numbers running between  $-(N-1)/2$  to  $(N-1)/2$  in intervals of 1. An excited state is then understood as particles on the same quantum number. Once one of these particles leaves the ground state it is understood as leaving a hole behind in the ground state. This is a counting function as it counts the number of states in some

interval  $\Delta p$  as each momenta corresponds to one quantum number via this function.

Using this picture, it is now possible to move to a thermodynamic limit of the system. However, before doing I introduce densities that will be useful in this limit. Defining a particle density  $\rho_p(p)$  such that  $L\rho_p(p)\Delta p$  is the number of particles with momentum between  $p$  and  $\Delta p$  and similarly a density of holes  $\rho_h(p)$ . The total number of states between  $p$  and  $\Delta p$  is defined by the counting function. Thus,

$$\rho_s(p) = \rho_p(p) + \rho_h(p) = \frac{dc(p)}{dp}, \quad (\text{D.7})$$

where the discrete derivatives have been replaced by a continuous derivative consistent with the thermodynamic limit and  $\rho_s$  is used to define the total density of states in the system. Further going into the thermodynamic limit the second term of the counting function, (D.6), can be expressed as follows,

$$\begin{aligned} \lim_{N \rightarrow \infty} \frac{1}{L} \sum_{k \neq j}^N \log S(p - p_k) &= \lim_{N \rightarrow \infty} \sum_{k \neq j}^N \log S(p - p_k) \frac{1}{L} \frac{p_k - p_{k-1}}{p_k - p_{k-1}} \\ &= \int_{-\infty}^{\infty} dp' \log S(p - p') \rho(p'). \end{aligned} \quad (\text{D.8})$$

Then in the continuum limit, (D.7) becomes,

$$\rho_s = \rho_p(p) + \rho_h(p) = \frac{1}{2\pi} + T\rho(p), \quad (\text{D.9})$$

where I am using the notation that  $T$  is an operator where its action on a test function,  $X(p)$  is

$$TX(p) \equiv \int_{-\infty}^{\infty} dp' \varphi(p - p') X(p'), \quad \text{where, } \varphi(q) = \frac{1}{2\pi i} \frac{d \log S}{dq}. \quad (\text{D.10})$$

Equation (D.9) is the first, important, equation needed in the TBA. Specifically, it gives the density of states as a function of momentum. This relation is the thermodynamic equivalent of the Bethe equations. From this expression one obtains the other important equation of the TBA, the statement of pseudo energy.

To obtain the pseudo energy one requires the TBA free energy. The free energy density is defined as usual via  $f = e - \beta^{-1}s$  with  $e$  the energy density and  $s$  the entropy

density. From the densities above it is natural to write the energy density as the energy of a particle multiplied by the density of particles summed over all possible momenta i.e.  $e = \int_{-\infty}^{\infty} dp E(p) \rho_p(p)$ . The entropy density is found by starting with the definition of the entropy for a given discrete momentum interval as the logarithm of the available states,

$$\Delta S(p_j) = \log \frac{(L \Delta p_j \rho_s(p_j))!}{(L \Delta p_j \rho_p(p_j))! (L \Delta p_j \rho_h(p_j))!}, \quad (\text{D.11})$$

Then in the thermodynamic limit one can use Stirling's approximation and in the continuum limit,

$$s = \int_{-\infty}^{\infty} dp \rho_s \log \rho_s - \rho_p \log \rho_p - \rho_h \log \rho_h. \quad (\text{D.12})$$

Putting these expressions together, the free energy in terms of TBA quantities is,

$$f = \int_{-\infty}^{\infty} dp (E(p) \rho_p - \beta^{-1} (\rho_s \log \rho_s - \rho_p \log \rho_p - \rho_h \log \rho_h)). \quad (\text{D.13})$$

The thermodynamic equilibrium is defined by the stationary point of the free energy. Thus, consider the variation in  $f$  by  $\rho_p$  and  $\rho_h$ . In order to do this vary (D.9) to find,

$$\delta \rho_h = -\delta \rho_p + T \delta \rho. \quad (\text{D.14})$$

With this,

$$\begin{aligned} \delta f &= \int_{-\infty}^{\infty} dp \left( E(p) \delta \rho_p - \beta^{-1} \left( \log \frac{\rho_s}{\rho_p} \delta \rho_p + \log \frac{\rho_s}{\rho_h} \delta \rho_h \right) \right) \\ &= \int_{-\infty}^{\infty} dp \delta \rho_p \left( E(p) - \beta^{-1} \left( \log \frac{\rho_h}{\rho_p} + T \log \left( \frac{\rho_p}{\rho_h} + 1 \right) \right) \right). \end{aligned} \quad (\text{D.15})$$

Finally introducing a term called the pseudo energy defined by,

$$\frac{\rho_h}{\rho_p}(p) = e^{\beta \varepsilon(p)}, \quad (\text{D.16})$$

then since in equilibrium  $\delta f = 0$  this sets up the following self-consistent expression for

the pseudo energy,

$$\varepsilon(p) = E(p) - \beta^{-1} \log(1 + e^{-\beta \varepsilon}). \quad (\text{D.17})$$

This is equivalent to the result quoted in section 6.1.1.

## D.2 Integrable SCGF specialisation to the Lesovik-Levitov formula

This appendix closely follows the results of [54, appendix A].

In free-fermion models, there is a well-known formula for the SCGF for particle transport through an impurity between two “leads”, the celebrated Lesovik-Levitov formula [39]. In this appendix I show the general result for the SCGF in integrable models I presented in (6.20), can be used to correctly reproduce the results of Lesovik-Levitov considered in the case where there is no impurity, i.e. the pure transmission case. Since free fermions are an integrable model, I specialise (6.20) to the case of free Fermionic particles with differential scattering amplitude  $\varphi(\theta - \alpha) = 0$  in a state defined by the partitioning protocol and considering particle transport as opposed to energy transport often considered in this thesis. In this section I use the simplest case of free, massless and chargeless fermions which must have a linear dispersion relation. In the pure transmission case, the Lesovik-Levitov formula takes the form [133]

$$F(\lambda) = \int_{-\infty}^{\infty} \frac{d\omega}{2\pi} \log \left[ 1 - n_l(\omega)(1 - n_r(\omega))(1 - e^\lambda) - n_r(\omega)(1 - n_l(\omega))(1 - e^{-\lambda}) \right], \quad (\text{D.18})$$

where  $n_{r(l)}(\omega)$  is the Fermi occupation function for the initial left (right) reservoirs, with inverse temperatures  $\beta_{r(l)}$  and chemical potentials  $\mu_{r(l)}$ ,

$$n_{r(l)}(\omega) = \frac{1}{e^{\beta_{r(l)}(\omega - \mu_{r(l)})} + 1}. \quad (\text{D.19})$$

Here  $\omega$  plays the role of an energy; it is not bounded from below because of the linear dispersion relation.

Since this is a system of massless non-interacting fermions, there should be two types of particles in the system, right-movers and left-movers defined by  $\sigma = \pm 1$ . This

is due to the fact that massless fermions can be described by a CFT which was shown to display chiral separation in section 2.1. These massless particles then have momentum  $p(\theta, \sigma) = \theta$ ; while the energy function takes the form  $E(\theta, \sigma) = \sigma\theta$  leaving the velocity  $v(\theta, \sigma) = \sigma$  via  $v = dE/dp$ . Since this is a free theory, the effective velocity of the modes,  $v^{\text{eff}}$ , is this velocity and the dressing operation is trivial (due to  $\varphi(\theta - \alpha) = 0$ ). The non-equilibrium steady state in free-fermion models is known [134], and, in the notation of this thesis, has TBA pseudoenergy given by

$$\varepsilon(\theta, \sigma) = \beta_l(\theta - \mu_l)\Theta(\sigma) + \beta_r(-\theta - \mu_r)\Theta(-\sigma). \quad (\text{D.20})$$

This explicitly shows the expected chiral separation as left-movers and right-movers are independently thermalised with respect to the initial left and right states of the partitioning protocol. Now I need to obtain a solution to the flow equation for integrable models, (6.19), in this situation. Due to the simplicity of the system this is easily obtained and shown to be,

$$\varepsilon(\theta, \sigma; \lambda) = [\beta_l(\theta - \mu_l) - \lambda]\Theta(\sigma) + [\beta_r(-\theta - \mu_r) + \lambda]\Theta(-\sigma), \quad (\text{D.21})$$

where  $-\text{sgn}(v^{\text{eff}}) = -\Theta(\sigma) + \Theta(-\sigma)$  and  $\varepsilon(\theta, \sigma; \lambda = 0)$  is given by (D.20). Then using the integrability SCGF presented in (6.20) combined with the above it is easy to show that,

$$F(\lambda) = \int_{-\infty}^{\infty} \frac{d\theta}{2\pi} \sum_{\sigma} \left( \log(1 + e^{-\varepsilon(\theta, \sigma; \lambda)}) - \log(1 + e^{-\varepsilon(\theta, \sigma; 0)}) \right). \quad (\text{D.22})$$

Changing variable to  $\omega = \sigma\theta$ , followed by some simple algebraic manipulations, it can be seen this agrees with (D.18).

### D.3 Calculating $c_3$ and $c_4$ from integrable SCGF

This section closely follows our publication, [54, appendix B]. In this section I obtain the general expressions for the first four scaled cumulants predicted by the integrability

SCGF (6.20) through  $c_n = \partial_\lambda^n F(\lambda) \Big|_{\lambda=0}$ . For ease of reference (6.20) is reproduced here,

$$F(\lambda) = - \int \frac{d\theta}{2\pi} E'(\theta) \left( \text{sgn}(v^{\text{eff}}(\theta; \lambda)) (F(\varepsilon(\theta; \lambda)) - F(\varepsilon(\theta; 0))) \right. \\ \left. - \int_0^\lambda d\lambda' \delta(v^{\text{eff}}(\theta; \lambda')) (\partial_{\lambda'} v^{\text{eff}}(\theta; \lambda')) (F(\varepsilon(\theta; \lambda')) - F(\varepsilon(\theta; 0))) \right), \quad (\text{D.23})$$

This appendix makes use of a flow equation on the state  $n(\theta; \lambda)$ . To obtain this I make use of the fact that  $f = -d \log n / d\varepsilon$  with the flow equation on the pseudo energy, (6.19), to get

$$\partial_\lambda n(\theta; \lambda) = \text{sgn}(v^{\text{eff}}(\theta; \lambda)) h_{i*}^{\text{dr}}(\theta; \lambda) n(\theta; \lambda) f(\theta; \lambda). \quad (\text{D.24})$$

Calculating  $\lambda$ -derivatives of (D.23) requires the following identities, gleaned from understanding the integral-operator structure of the dressing operator, (6.6):

$$\partial_\lambda X^{\text{dr}}(\theta; \lambda) = (s f h^{\text{dr}} X^{\text{dr}})^{\text{dr}}(\theta; \lambda) - f(\theta; \lambda) s(\theta; \lambda) h^{\text{dr}}(\theta; \lambda) X^{\text{dr}}(\theta; \lambda), \quad (\text{D.25})$$

$$\int d\theta n(\theta) X(\theta) Y^{\text{dr}}(\theta) = \int d\theta n(\theta) X^{\text{dr}}(\theta) Y(\theta), \quad (\text{D.26})$$

where  $s(\theta; \lambda) = \text{sgn}(v^{\text{eff}}(\theta; \lambda))$ , and  $X(\theta)$  and  $Y(\theta)$  stand for any two quantities within the GHD description.

The first expression, (D.25), is found by using an integral-operator structure of the dressing i.e.  $X^{\text{dr}} = (1 - \varphi n(\lambda))^{-1} X$  with  $\mathcal{N} \equiv n(\alpha) \delta(\theta - \alpha)$  and  $\varphi \equiv \varphi(\theta - \alpha)$ . Then the derivative on the operator is found,  $\partial_\lambda (1 - \varphi n(\lambda))^{-1} X = (1 - \varphi n(\lambda))^{-1} \varphi \partial_\lambda n(\lambda) (1 - \varphi n(\lambda))^{-1} X$ . Using (D.24) with the definition of the dressing as the action of the operator to the right gives (D.25).

The second expression, (D.26) is easier to understand by using the definition of the dressing

$$X^{\text{dr}}(\theta) = X(\theta) + \int d\alpha \varphi(\theta, \alpha) n(\alpha) X(\alpha) \\ + \int d\alpha \varphi(\theta, \alpha) n(\alpha) \int d\alpha' \varphi(\alpha, \alpha') n(\alpha') X(\alpha') + \dots \quad (\text{D.27})$$

Using this definition,

$$\begin{aligned}
\int d\theta n(\theta)X(\theta)Y^{dr}(\theta) &= \int d\theta n(\theta)X(\theta)Y(\theta) \\
&\quad + \int d\alpha n(\alpha)Y(\alpha) \int d\theta \varphi(\theta, \alpha)n(\theta)X(\theta) \\
&\quad + \int d\alpha' n(\alpha')Y(\alpha') \int d\alpha \varphi(\alpha, \alpha')n(\alpha) \\
&\quad \times \int d\theta \varphi(\theta, \alpha)n(\theta)X(\theta) + \dots
\end{aligned} \tag{D.28}$$

where I have rearranged the functions being integrated over. Integration variables are relabelled in a leading way, in the second term,  $\theta \rightarrow \alpha$  and  $\alpha \rightarrow \theta$ , while in the third term  $\theta \rightarrow \alpha'$  and  $\alpha' \rightarrow \theta$ . This leads to,

$$\begin{aligned}
\int d\theta n(\theta)X(\theta)Y^{dr}(\theta) &= \int d\theta n(\theta)Y(\theta) \left( X(\theta) + \int d\alpha \varphi(\alpha, \theta)n(\alpha)X(\alpha) \right. \\
&\quad \left. + \int d\alpha \varphi(\alpha, \theta)n(\alpha) \int d\alpha' \varphi(\alpha', \alpha)n(\alpha')X(\alpha') + \dots \right).
\end{aligned} \tag{D.29}$$

With the assumption that,  $\varphi(x, y) = \varphi(y, x)$ , the identity of (D.26) is obtained. With this I can produce expressions for the cumulants.

Going forward I use the  $\lambda$ -dependent state  $n(\theta; \lambda)$  which is defined by (D.24). The  $\lambda$ -dependent current is given by the expression

$$j(\lambda) = \int \frac{d\theta}{2\pi} E'(\theta) n(\theta; \lambda) h_{i^*}^{dr}(\theta; \lambda). \tag{D.30}$$

At  $\lambda = 0$  this correctly produces the steady-state current as given by the first expression in (6.8). This expression for the current is obtained by starting with the GHD expectation values of the current, (6.8), then using  $v^{\text{eff}} = (E')^{dr}/(p')^{dr}$  and (6.6) with (D.24) I obtain the expression for  $j(\lambda)$ .

To assist with readability, the  $\theta$ -dependence in the notation below is dropped with the understanding that all terms inside the  $\theta$  integrals are  $\theta$  dependent. Furthermore, the following simplified notation is introduced:  $s(\lambda) \equiv \text{sgn}(v^{\text{eff}}(\theta; \lambda))$  and  $H(\lambda) \equiv h_{i^*}^{dr}(\theta; \lambda)$ .

The second cumulant  $c_2$  is found by taking a  $\lambda$ -derivative of the  $\lambda$ -dependent cur-

rent and setting  $\lambda = 0$ ,

$$\begin{aligned}\partial_\lambda \langle j(\lambda) \rangle &= \int \frac{d\theta}{2\pi} E' [\partial_\lambda n(\lambda) H(\lambda) + n(\lambda) \partial_\lambda H(\lambda)] \\ &= \int \frac{d\theta}{2\pi} E' [s(\lambda) H^2(\lambda) n(\lambda) f(\lambda) + n(\lambda) (sfH^2)^{\text{dr}}(\lambda) - n(\lambda) f(\lambda) s(\lambda) H^2(\lambda)] \\ &= \int \frac{d\theta}{2\pi} (E')^{\text{dr}}(\lambda) n(\lambda) s(\lambda) f(\lambda) H^2(\lambda),\end{aligned}\tag{D.31}$$

where in the second line I used (D.24) and (D.25) while the third line required (D.26). At  $\lambda = 0$  this correctly reproduces  $c_2$  from the literature [90].

The cumulants obtained via higher-order derivatives require special care as these expressions require calculating terms  $\partial_\lambda s(\lambda)$ . Recall  $s(\lambda)$  is a sign function and the derivatives of this produce a  $\delta$ -function. The  $\delta$ -function leads to terms evaluated at  $\theta^*(\lambda)$  where  $v^{\text{eff}}(\theta^*(\lambda); \lambda) = 0$ . This can be problematic, as in the partitioning protocol considered,  $n(\theta^*(\lambda))$  is ill-defined. This is the problem that in principle should lead back to the discussion on co-propagating modes discussed in section 3.5. However, for  $c_3$  the ambiguity resolves fairly straightforwardly. On taking the derivative of  $\partial_\lambda j(\lambda)$  there is a term that contains  $\partial_\lambda \text{sgn}(v^{\text{eff}}(\theta; \lambda)) = \delta(v^{\text{eff}}(\theta; \lambda)) \partial_\lambda v^{\text{eff}}(\theta; \lambda)$ . Then recalling that from the definition of  $v^{\text{eff}}$  in section 6.1.2,  $(E')^{\text{dr}}(\theta; \lambda) = v^{\text{eff}}(\theta; \lambda) (p')^{\text{dr}}(\theta; \lambda)$ . Thus there is a term  $\int \frac{d\theta}{2\pi} (p')^{\text{dr}}(\theta; \lambda) v^{\text{eff}}(\theta; \lambda) \delta(v^{\text{eff}}(\theta; \lambda)) \partial_\lambda v^{\text{eff}}(\theta; \lambda) n(\lambda) f(\lambda) H^2(\lambda)$ . The  $\delta$ -function sets  $v^{\text{eff}} = 0$  which ensures I do not need to evaluate  $n(\theta^*(\lambda))$ . The remaining terms all follow from use of (D.24), (D.25) and (D.26) which leads to

$$\begin{aligned}\partial_\lambda^2 \langle j(\lambda) \rangle &= \int \frac{d\theta}{2\pi} [(sf(E')^{\text{dr}}H)^{\text{dr}}(\lambda) n(\lambda) s(\lambda) f(\lambda) H^2(\lambda) \\ &\quad + 2(E')^{\text{dr}}(\lambda) n(\lambda) s(\lambda) f(\lambda) H(\lambda) (sfH^2)^{\text{dr}}(\lambda) \\ &\quad + (E')^{\text{dr}}(\lambda) n(\lambda) f(\lambda) H^3(\lambda) \tilde{f}(\lambda)] \\ &= \int \frac{d\theta}{2\pi} (E')^{\text{dr}}(\lambda) n(\lambda) s(\lambda) f(\lambda) H(\lambda) [s(\lambda) H^2(\lambda) \tilde{f} + 3(sfH^2)^{\text{dr}}(\lambda)],\end{aligned}\tag{D.32}$$

where  $\tilde{f} = -(\text{dlog } f/\text{d}\varepsilon + 2f)$  and  $s^2(\lambda) = 1$  was used throughout. The final expression (6.22) for  $c_3$  is obtained by recalling again the identities  $(E')^{\text{dr}} = v^{\text{eff}}(p')^{\text{dr}}$ ,  $|v^{\text{eff}}| = v^{\text{eff}} \text{sgn}(v^{\text{eff}})$ , and  $\rho_p = n(p')^{\text{dr}}/(2\pi)$  before finally setting  $\lambda = 0$ .

This expression for  $c_3$  was not obtained before our work in [54]. In principle the



same process can be seen to generate all orders of cumulants, however one pays with increasing complexity of the required calculations. I will show how to obtain  $c_4$  as this introduces one more illustrative difficulty to overcome. This calculation involves the same steps as above, first using (D.24) and (D.25) followed by acting on the term gained from  $\partial_\lambda(E')^{\text{dr}}$  with (D.26). However, a further complication arises when considering the term  $\partial_\lambda(sfH^2)^{\text{dr}}(\lambda)$ . I explain the specific issue and how to overcome it but will not repeat manipulations already covered in the calculations of  $c_2$  and  $c_3$ .

In order to calculate  $\partial_\lambda(sfH^2)^{\text{dr}}(\lambda)$ , consider the integral representation of a dressed object. From (6.6), the dressing operator is  $h^{\text{dr}}(\theta) = h(\theta) + \int \frac{d\alpha}{2\pi} \varphi(\alpha, \theta) n(\alpha) h^{\text{dr}}(\alpha)$ . With this definition

$$\begin{aligned} \partial_\lambda(sfH^2)^{\text{dr}}(\lambda) &= \partial_\lambda(s(\theta; \lambda)f(\theta; \lambda)H^2(\theta; \lambda)) \\ &\quad + \partial_\lambda \int \frac{d\alpha}{2\pi} \varphi(\alpha, \theta) n(\alpha; \lambda) s(\alpha; \lambda) f(\alpha; \lambda) H(\alpha; \lambda)^2 \\ &\quad + \partial_\lambda \int \frac{d\alpha}{2\pi} \varphi(\alpha, \theta) n(\alpha; \lambda) \\ &\quad \times \int \frac{d\alpha'}{2\pi} \varphi(\alpha', \alpha) n(\alpha'; \lambda) s(\alpha'; \lambda) f(\alpha'; \lambda) H(\alpha'; \lambda)^2 + \dots, \end{aligned} \quad (\text{D.33})$$

where I have displayed only the first three terms of the infinite sequence arising from the iterative equation defined by the dressing operator. Everything is as before except the issue involving evaluation at the co-propagation mode,  $n(\theta^*(\lambda))$ , cannot be resolved as in  $c_3$ . To get around this issue, consider splitting the integrals above such that  $\int d\theta s(\theta^*(\lambda)) = -\int_{-\infty}^{\theta^*(\lambda)} d\theta + \int_{\theta^*(\lambda)}^{\infty} d\theta$ . Then using the Leibniz integral rule, the boundary terms which come from  $\partial_\lambda \int d\theta s(\theta^*(\lambda))$  cancel each other out which removes the ambiguity from (D.33). This is not unexpected since the sign function entered the initial calculations as a shorthand. In fact, it is possible to do all calculations without the explicit use of this function, instead computing under split integrals from the start so that there is never a question of ambiguity. With this issue resolved I write

$$\begin{aligned} \partial_\lambda(sfH^2)^{\text{dr}}(\lambda) &= 3 \left( fsH(fsH^2)^{\text{dr}} \right)^{\text{dr}}(\lambda) - f(\lambda)s(\lambda)H(\lambda)(fsH^2)^{\text{dr}}(\lambda) \\ &\quad + (f\tilde{f}H^3)^{\text{dr}}(\lambda). \end{aligned} \quad (\text{D.34})$$

The rest of the calculation, although tedious, follows the same principles as before. For

comparative purposes I write  $c_4$  in the same more formal notation as used in (6.23):

$$c_4 = \int d\theta \rho_p f v^{\text{eff}} \left\{ (h_{j_*}^{\text{dr}})^4 s \hat{f} \tilde{f} + 3s((sf(h_{j_*}^{\text{dr}})^2)^{\text{dr}})^2 + 4h_{j_*}^{\text{dr}} s(f\tilde{f}(h_{j_*}^{\text{dr}})^3)^{\text{dr}} \right. \\ \left. + 6\tilde{f}(h_{j_*}^{\text{dr}})^2 (sf(h_{j_*}^{\text{dr}})^2)^{\text{dr}} + 12h_{j_*}^{\text{dr}} s(sf h_{j_*}^{\text{dr}} (sf(h_{j_*}^{\text{dr}})^2)^{\text{dr}})^{\text{dr}} \right\}, \quad (\text{D.35})$$

where  $\hat{f} = -(\text{dlog}(f\tilde{f})/\text{d}\epsilon + 3f)$ .

This last statement has important ramifications for the caveat stated in section 3.5. In this section I discussed the role of co-propagating modes in phase transitions and stated there was a difference between “isolated” and non-isolated modes. The fact that it is even possible to split integrals from the start so that there is never a question of ambiguity is the signature of a non-isolated co-propagating mode.

integrable

## D.4 Occupation function in integrable models

In this section I outline how to obtain (6.24), an exact expression for the occupation function of the Euler equations under the partitioning protocol. I will show that,

$$n(\theta) = n_l(\theta)\Theta(\theta - \theta^*) + n_r(\theta)\Theta(\theta^* - \theta), \quad (\text{D.36})$$

where the indices  $l$  and  $r$  are reference to the initial occupation functions for the left and right partitions in the partitioning protocol. This section follows very closely the work in [122].

Starting with the Euler equation,

$$\partial_t n(x, t; \theta) + v^{\text{eff}}(x, t; \theta) \partial_x n(x, t; \theta) = 0. \quad (\text{D.37})$$

and partitioning protocol defining initial conditions.

In the Euler scaling limit  $n(x, t; \theta) = n(x/t; \theta)$ . Setting  $\xi = x/t$  and changing variables in the Euler equation results in the following equation,

$$\left( \xi - v^{\text{eff}}(\xi; \theta) \right) \partial_\xi n(\xi; \theta) = 0. \quad (\text{D.38})$$

where the initial condition becomes the boundary conditions,

$$n_l(\theta) = \lim_{\xi \rightarrow -\infty} n(\xi; \theta), \quad n_r(\theta) = \lim_{\xi \rightarrow +\infty} n(\xi; \theta). \quad (\text{D.39})$$

Then clearly

$$n(\theta; \xi) = n_l(\theta) \Theta(\theta - \theta^*(\xi)) + n_r(\theta) \Theta(\theta^*(\xi) - \theta), \quad (\text{D.40})$$

solves the differential equation if  $v^{\text{eff}}(\xi; \theta^*) = \xi$ .

Finally since I focus on the interface of the partitioning protocol which by definition is considered as,  $x = 0 \implies \xi = 0$ .

## D.5 Thermal distribution of hard rod gas

The hard rod (HR) gas provides a simple model in which to test results for integrable models. In this appendix I explain what inputs are used for the theoretical predictions of  $c_1, c_2, c_3$  and  $c_4$  plotted in fig. 6.1. This section follows [54, appendix D] closely.

To obtain the theoretical values for the cumulants, the following are required: the conserved quantity  $h(\theta)$ ; the occupation function  $n(\theta)$  together with the related pseudoenergy  $\varepsilon(\theta)$  and particle density  $\rho_p(\theta)$ , the dressing operation, the effective velocity  $v^{\text{eff}}(\theta)$ , and the statistical factor  $f(\theta)$ . Here  $\theta$  is the velocity and I take unit mass.

As stated in section 6.4, in the HR gas the differential scattering amplitude is given by  $\varphi(\theta, \alpha) = -a$  where  $a$  is the rod length. The constant interaction term simplifies the dressing operation, giving

$$h^{\text{dr}}(\theta) = h(\theta) - \frac{a}{1+ab} \int \frac{d\alpha}{2\pi} n(\alpha) h(\alpha) \quad (\text{D.41})$$

with

$$b = \int \frac{d\alpha}{2\pi} n(\alpha). \quad (\text{D.42})$$

This produces further simplifications of  $v^{\text{eff}}(\theta)$  since  $v^{\text{eff}}(\theta) = (E')^{\text{dr}}(\theta)/(p')^{\text{dr}}(\theta)$ . Further, in the HR gas  $f(\theta; \lambda) = 1$  and

$$n(\theta) = e^{-\varepsilon(\theta)}, \quad (\text{D.43})$$

as this is a gas of classical particles with free energy function  $F(\varepsilon) = e^{-\varepsilon}$ . The particle density is given by  $\rho_p(\theta) = n(\theta)(p')^{\text{dr}}((\theta))/(2\pi)$  which, using  $p'(\theta) = 1$  and (D.41), is easily shown to give

$$\rho_p(\theta) = \frac{1 - a\rho}{2\pi} n(\theta), \quad \text{where } \rho = \int d\alpha \rho_p(\alpha) = \frac{b}{1 + ab}. \quad (\text{D.44})$$

Since the differential scattering phase is constant in the HR gas, the pseudoenergy can be expressed as  $\varepsilon(\theta) = w(\theta) + z$ , where the constant  $z$  satisfies

$$z = ade^{-z}, \quad d = \int \frac{d\alpha}{2\pi} e^{-w(\alpha)}. \quad (\text{D.45})$$

The equation for  $z$  is solved using the Lambert-W function as  $z = W(ad)$ .

In section 6.4 I was concerned with energy currents. This situation is defined by  $h(\theta) = \theta^2/2$  where I assume mass,  $m = 1$ . For the HR gas in the steady state arising from the partitioning protocol, the exact expression for  $n(\theta)$  in terms of the occupation functions  $n_l(\theta)$  and  $n_r(\theta)$  in the initial left and right baths of the protocol is provided in appendix D.4 above. In this instance I use a more general version of the initial states where they are fixed using two boosted thermal distributions. In order to apply the result of the appendix above I only need to describe what form  $n(\theta)$  takes for thermal distributions in the HR gas; Galilean boosting is simply a shift of  $\theta$ . To obtain a thermal distribution in the HR gas, one may naively assume that fixing the source term  $w(\theta)$  of the pseudoenergy (6.2) to be Gaussian is sufficient. However, we show that for truly thermal distributions, the starting rod density per unit length must also be fixed in a particular way.

To fix a thermal state, I choose a thermal term defined by  $w^{(\text{th})}(\theta) = \beta\theta^2/2$ . It is now clear that using the thermal,  $w^{(\text{th})}(\theta)$ , will affect the particle density. The thermal  $d^{(\text{th})}$  is a Gaussian integral giving  $d^{(\text{th})} = 1/\sqrt{2\pi\beta}$ . This is used to find  $\varepsilon^{(\text{th})} = \beta\theta^2/2 + W(ad^{(\text{th})})$ . Then, using  $n(\theta) = e^{-\varepsilon(\theta)}$  with (D.44),

$$\rho_p^{(\text{th})} = \frac{e^{-\varepsilon^{(\text{th})}(\theta)}}{2\pi(1 + ab^{(\text{th})})} = \frac{e^{-\beta\theta^2/2} e^{-W(ad^{(\text{th})})}}{2\pi(1 + W(ad^{(\text{th})}))}. \quad (\text{D.46})$$

This is how the initial thermal densities are constructed for the Monte Carlo simulation of

the hard rod gas. Since I investigate boosted thermal distributions, we use such Gaussian distributions with non-zero means; the above details remain unaffected other than in the final equality  $\theta \rightarrow \theta - \mu$ .

## D.6 Details of Monte Carlo simulation of hard rod gas

I describe the Monte Carlo procedure used to obtain  $c_2$ ,  $c_3$  and  $c_4$  for the HR gas in the partitioning protocol presented in fig. 2. Since it is the same simulation, this appendix closely follows [54, appendix D]. In the partitioning protocol the system is split into two halves defined by different boosted thermal distributions for the left and right side of the partition (see appendix D.5 above). This defines both the rod velocities, through sampling from a Gaussian distribution, and the rod densities, through (D.46). On the left side of the partition I used a Gaussian with a mean of 8 and standard deviation of 15, on the right a mean of  $-3$  and standard deviation of 10. The initial length scale in the system is defined by the distance between the leftmost rod of the left partition and the rightmost rod of the right partition. To ensure that the system is dense enough to display interesting behaviour but not so dense as to obstruct the dynamics, I enforce the initial length scale to be half-populated by rods, where I have taken into account the rod lengths. The choices of the initial distributions, the initial density and the rod number uniquely determine the initial length scale and the rod length. Specifically, as the initial rod density is given by thermal distributions,  $\rho_{p,\beta_r}^{(\text{th})}$ ,  $\rho_{p,\beta_l}^{(\text{th})}$  defined by the initial partition temperatures, then choosing the number of rods,  $N$ , in the simulation results in the fixing of the initial length scale,  $L$ , via  $L(\rho_{p,\beta_r}^{(\text{th})} + \rho_{p,\beta_l}^{(\text{th})}) = N$ . Then as I require the system to be half filled at the start of the simulation, this imposes  $Na/L = 1/2$  where  $a$  is rod density and is thus also fixed. For the simulation in this thesis I used  $10^5$  rods. Since the system dynamics are deterministic, the stochasticity is contained within the initial conditions where the initial rod velocities are randomly drawn from Gaussian distributions. Then for a given realisation of initial velocities, I count the total amount of energy that passes through the midpoint of the system during a long time interval  $t$ . To gain statistics on the energy flow, I allow multiple realisations of initial rod velocities and record the total energy flow for each. From the data collected the scaled cumulants can be determined.

# Bibliography

- [1] G. E. Crooks. On thermodynamic and microscopic reversibility. *J. Stat. Mech.: Theory Exp*, 2011(07):P07008, 2011.
- [2] D. D. Briske, A. W. Illius, and J. M. Anderies. *Nonequilibrium Ecology and Resilience Theory*, pages 197–227. Springer International Publishing, Cham, 2017.
- [3] W. H. Renwick. Equilibrium, disequilibrium, and nonequilibrium landforms in the landscape. *Geomorphology*, 5(3):265 – 276, 1992. Proceedings 23rd Binghamton Symposium in Geomorphology.
- [4] V.P. Crawford, M.A. Costa-Gomes, and N. Iriberry. Structural models of nonequilibrium strategic thinking: Theory, evidence, and applications. *Journal of Economic Literature*, 51(1):5–62, 2013.
- [5] S. Ornes. Core concept: How nonequilibrium thermodynamics speaks to the mystery of life. *PNAS*, 114(3):423–424, 2017.
- [6] L. F. Santos and E. J. Torres-Herrera. *Nonequilibrium Quantum Dynamics of Many-Body Systems*, pages 231–260. Springer, Cham, 2017.
- [7] D.V. Schroeder. *An introduction to thermal physics*. San Francisco, CA : Addison Wesley, 2000.
- [8] H. Touchette and R. J. Harris. *Large Deviation Approach to Nonequilibrium Systems*, chapter 11, pages 335–360. John Wiley & Sons, Ltd, 2013.
- [9] R. Kubo, M. Toda, and N. Hashitsume. *Statistical Physics II Nonequilibrium Statistical Mechanics*. Springer, Berlin, Heidelberg, 1991.
- [10] L. E. Reichl. *A modern course in statistical physics*. Arnold, London, 1980.

- [11] J. Topping. Investigations on the theory of the Brownian movement. *Physics Bulletin*, 7(10):281–281, 1956.
- [12] R. Kubo. The fluctuation-dissipation theorem. *Rep. Prog. Phys*, 29(1):255–284, 1966.
- [13] M. Campisi, P. Hänggi, and P. Talkner. Colloquium: Quantum fluctuation relations: Foundations and applications. *Rev. Mod. Phys.*, 83:771–791, 2011.
- [14] W. Sutherland. Xviii. ionization, ionic velocities, and atomic sizes. *The London, Edinburgh, and Dublin Philosophical Magazine and Journal of Science*, 3(14):161–177, 1902.
- [15] J. B. Johnson. Thermal agitation of electricity in conductors. *Phys. Rev.*, 32:97–109, 1928.
- [16] H. Nyquist. Thermal agitation of electric charge in conductors. *Phys. Rev.*, 32:110–113, 1928.
- [17] H.B. Callen and T.A. Welton. Irreversibility and generalized noise. *Phys. Rev.*, 83:34–40, 1951.
- [18] M. S. Green. Markoff random processes and the statistical mechanics of timedependent phenomena. *J. Chem. Phys*, 20(8):1281–1295, 1952.
- [19] M. S. Green. Markoff random processes and the statistical mechanics of timedependent phenomena. ii. irreversible processes in fluids. *J. Chem. Phys*, 22(3):398–413, 1954.
- [20] R. Kubo. Statistical-mechanical theory of irreversible processes. i. general theory and simple applications to magnetic and conduction problems. *J. Phys. Soc. Jpn.*, 12(6):570–586, 1957.
- [21] D. J. Evans, E. G. D. Cohen, and G. P. Morriss. Probability of second law violations in shearing steady states. *Phys. Rev. Lett.*, 71:2401–2404, 1993.
- [22] G. Gallavotti and E. G. D. Cohen. Dynamical ensembles in nonequilibrium statistical mechanics. *Phys. Rev. Lett.*, 74:2694–2697, 1995.

- [23] U. Seifert. Stochastic thermodynamics, fluctuation theorems and molecular machines. *Rep. Prog. Phys.*, 75(12):126001, 2012.
- [24] D. J. Searles and D. J. Evans. The fluctuation theorem and Green-Kubo relations. *J.Chem. Phys.*, 112(22):9727–9735, 2000.
- [25] C. Jarzynski. Nonequilibrium equality for free energy differences. *Phys. Rev. Lett.*, 78:2690–2693, 1997.
- [26] G. E. Crooks. Entropy production fluctuation theorem and the nonequilibrium work relation for free energy differences. *Phys. Rev. E*, 60:2721–2726, 1999.
- [27] P. Talkner, E. Lutz, and P. Hänggi. Fluctuation theorems: Work is not an observable. *Phys. Rev. E*, 75:050102, 2007.
- [28] N. Garnier and S. Ciliberto. Nonequilibrium fluctuations in a resistor. *Phys. Rev. E*, 71:060101, 2005.
- [29] Y. Utsumi, D. S. Golubev, M. Marthaler, K. Saito, T. Fujisawa, and G. Schön. Bidirectional single-electron counting and the fluctuation theorem. *Phys. Rev. B*, 81:125331, 2010.
- [30] K. Feitosa and N. Menon. Fluidized granular medium as an instance of the fluctuation theorem. *Phys. Rev. Lett.*, 92:164301, 2004.
- [31] S. An, J. Zhang, M. Um, D. Lv, Y. Lu, J. Zhang, Z. Yin, H. T. Quan, and K. Kim. Experimental test of the quantum Jarzynski equality with a trapped-ion system. *Nat. Phys*, 11:193, 2014.
- [32] O.E. Lanford. *Entropy and equilibrium states in classical statistical mechanics*, pages 1–113. Springer, Berlin, Heidelberg, 1973.
- [33] R.S. Ellis. *Entropy, Large Deviations, and Statistical Mechanics*. Springer-Verlag New York, 1985.
- [34] H. Touchette. The large deviation approach to statistical mechanics. *Phys. Rep.*, 478(1):1 – 69, 2009.



- [35] H. Spohn. *Large Scale Dynamics of Interacting Particles*. Springer-Verlag Berlin Heidelberg, 1991.
- [36] H. Touchette. A basic introduction to large deviations: Theory, applications, simulations. *arXiv e-prints*, arXiv:1106.4146, 2011.
- [37] B. Buca and T. Prosen. Exactly solvable counting statistics in open weakly coupled interacting spin systems. *Phys. Rev. Lett.*, 112:067201, 2014.
- [38] J. P. Carollo, F. and Garrahan, I. Lesanovsky, and C. Pérez-Espigares. Fluctuating hydrodynamics, current fluctuations, and hyperuniformity in boundary-driven open quantum chains. *Phys. Rev. E*, 96:052118, 2017.
- [39] L.S. Levitov and G.B. Lesovik. Charge distribution in quantum shot noise. *Jetp Let.*, 58:230, 1993.
- [40] K. Saito and A. Dhar. Fluctuation theorem in quantum heat conduction. *Phys. Rev. Lett.*, 99:180601, 2007.
- [41] B. Doyon, A. Lucas, K. Schalm, and M. J. Bhaseen. Non-equilibrium steady states in the Klein–Gordon theory. *J. Phys. A*, 48(9):095002, 2015.
- [42] T. Yoshimura. Full counting statistics in the free Dirac theory. *J. Phys. A: Math. and Th.*, 51(47):475002, 2018.
- [43] A. Komnik and H. Saleur. Quantum fluctuation theorem in an interacting setup: Point contacts in fractional quantum hall edge state devices. *Phys. Rev. Lett.*, 107:100601, 2011.
- [44] D. Bernard and B. Doyon. Energy flow in non-equilibrium conformal field theory. *J. Phys. A*, 45(36):362001, 2012.
- [45] D. Bernard and B. Doyon. Non-equilibrium steady states in conformal field theory. *Ann. Henri Poincaré*, 16(1):113–161, 2015.
- [46] L. Bertini, A. De Sole, D. Gabrielli, G. Jona-Lasinio, and C. Landim. Macroscopic fluctuation theory for stationary non-equilibrium states. *J. Stat. Phys.*, 107(3):635–675, 2002.

- [47] B. Derrida. Non-equilibrium steady states: fluctuations and large deviations of the density and of the current. *J. Stat. Mech.: Th. and Exper.*, 2007(07):P07023–P07023, 2007.
- [48] L. Bertini, A. De Sole, D. Gabrielli, G. Jona-Lasinio, and C. Landim. Macroscopic fluctuation theory. *Rev. Mod. Phys.*, 87:593–636, 2015.
- [49] C. B. Mendl and H. Spohn. Current fluctuations for anharmonic chains in thermal equilibrium. *J. Stat. Mech.: Theory Exp*, 2015(3):P03007, 2015.
- [50] H. Spohn. Nonlinear fluctuating hydrodynamics for anharmonic chains. *J. Stat. Phys.*, 154(5):1191–1227, 2014.
- [51] B. Doyon and J. Myers. Fluctuations in ballistic transport from Euler hydrodynamics. *arXiv e-prints*, arXiv: 1812.02082, 2019.
- [52] B. Schmittmann and R.K.P. Zia. Statistical mechanics of driven diffusive systems. In B. Schmittmann and R.K.P. Zia, editors, *Statistical Mechanics of Driven Diffusive System*, volume 17 of *Phase Transitions and Critical Phenomena*, pages 3 – 214. Academic Press, 1995.
- [53] C. T. MacDonald, J. H. Gibbs, and A. C. Pipkin. Kinetics of biopolymerization on nucleic acid templates. *Biopolymers*, 6(1):1–25, 1968.
- [54] J. Myers, M.J. Bhaseen, R. Harris, and B. Doyon. Transport fluctuations in integrable models out of equilibrium. *arXiv e-prints*, arXiv: 1812.02082, 2018.
- [55] B. Altaner. Nonequilibrium thermodynamics and information theory: Basic concepts and relaxing dynamics. *J. Phys. A.*, 50(45):454001, 2017.
- [56] X. Zhang, H. Qian, and M. Qian. Stochastic theory of nonequilibrium steady states and its applications. part i. *Phys. Rep.*, 510(1):1 – 86, 2012. Stochastic Theory of Nonequilibrium Steady States and Its Applications: Part I.
- [57] H. Spohn and J.L. Lebowitz. Stationary non-equilibrium states of infinite harmonic systems. *Commun. Math. Phys*, 54(2):97–120, 1977.

- [58] M. Spillane and C.P. Herzog. Relativistic hydrodynamics and non-equilibrium steady states. *J. Stat. Mech.: Theory Expt*, 2016(10):103208, 2016.
- [59] H. Hinrichsen. Non-equilibrium phase transitions. *Physica A*, 369(1):1 – 28, 2006. Fundamental Problems in Statistical Physics.
- [60] M. Heyl. Dynamical quantum phase transitions: a review. *Rep. Prog. Phys*, 81(5):054001, 2018.
- [61] C. Flindt and J.P. Garrahan. Trajectory phase transitions, Lee-Yang zeros, and high-order Cumulants in full counting statistics. *Phys. Rev. Lett.*, 110:050601, 2013.
- [62] D Collin, F Ritort, C Jarzynski, S B Smith, I Tinoco, and C Bustamante. Verification of the Crooks fluctuation theorem and recovery of RNA folding free energies. *Nature*, 437(7056):231–234, 2005.
- [63] S. An, J. Zhang, M. Um, D. Lv, Y. Lu, J. Zhang, Z. Yin, H.T. Quan, and K. Kim. Experimental test of the quantum Jarzynski equality with a trapped-ion system. *Nat. Phys*, 11:193, 2014.
- [64] M. Esposito, U. Harbola, and S. Mukamel. Nonequilibrium fluctuations, fluctuation theorems, and counting statistics in quantum systems. *Rev. Mod. Phys.*, 81:1665–1702, 2009.
- [65] C. Jarzynski and D. K. Wójcik. Classical and quantum fluctuation theorems for heat exchange. *Phys. Rev. Lett.*, 92:230602, 2004.
- [66] D. Bernard and B. Doyon. Time-reversal symmetry and fluctuation relations in non-equilibrium quantum steady states. *J. Phys. A*, 46(37):372001, 2013.
- [67] A. Torrielli. Lectures on Classical Integrability. *J. Phys.*, A49(32):323001, 2016.
- [68] J.S. Caux and J. Mossel. Remarks on the notion of quantum integrability. *J. Stat. Mech.: Theory Exp.*, 2011(02):P02023, 2011.
- [69] S. Parke. Absence of particle production and factorization of the S-matrix in 1 + 1 dimensional models. *Nuc. Phys. B*, 174(1):166 – 182, 1980.

- [70] D. Bombardelli. S-matrices and integrability. *J. Phys. A*, 49(32):323003, 2016.
- [71] E. T. Jaynes. Information theory and statistical mechanics. *Phys. Rev.*, 106:620–630, 1957.
- [72] E. T. Jaynes. Information theory and statistical mechanics. ii. *Phys. Rev.*, 108:171–190, 1957.
- [73] L. Vidmar and M. Rigol. Generalized Gibbs ensemble in integrable lattice models. *J. Stat. Mech.: Theory Exp.*, 2016(6):064007, 2016.
- [74] B. Wouters, J. De Nardis, M. Brockmann, D. Fioretto, M. Rigol, and J.-S. Caux. Quenching the anisotropic Heisenberg chain: exact solution and generalized Gibbs ensemble predictions. *Phys. Rev. Lett.*, 113:117202, 2014.
- [75] B. Pozsgay, M. Mestyán, M. A. Werner, M. Kormos, G. Zaránd, and G. Takács. Correlations after quantum quenches in the XXZ spin chain: failure of the generalized Gibbs ensemble. *Phys. Rev. Lett.*, 113:117203, 2014.
- [76] E. Ilievski, J. De Nardis, B. Wouters, J.-S. Caux, F. H. L. Essler, and T. Prosen. Complete generalized Gibbs ensembles in an interacting theory. *Phys. Rev. Lett.*, 115:157201, 2015.
- [77] C. Gogolin and J. Eisert. Equilibration, thermalisation, and the emergence of statistical mechanics in closed quantum systems. *Rep. Prog. Phys.*, 79(5):056001, 2016.
- [78] J. De Nardis, D. Bernard, and B. Doyon. Diffusion in generalized hydrodynamics and quasiparticle scattering. *SciPost Phys.*, 6:49, 2019.
- [79] B. Doyon. Exact large-scale correlations in integrable systems out of equilibrium. *SciPost Phys.*, 5:54, 2018.
- [80] J. Cardy. Conformal field theory and statistical mechanics. In *Les Houches Summer School: Session 89: Exact Methods in Low-Dimensional Statistical Physics and Quantum Computing Les Houches, France, June 30-August 1, 2008*, 2008.
- [81] D. Tong. Lectures on string theory. *arXiv e-prints*, arXiv:0908.0333, 2009.

- [82] E. M. Brehm and D. Das. On KdV characters in large  $c$  CFTs. *arXiv e-prints*, arXiv: 1901.10354, 2019.
- [83] V. V. Bazhanov, S.L. Lukyanov, and A. B. Zamolodchikov. Integrable structure of conformal field theory, quantum KdV theory and Thermodynamic Bethe Ansatz. *Commun. Math. Phys.*, 177(2):381–398, 1996.
- [84] D. Bernard and B. Doyon. Conformal field theory out of equilibrium: a review. *J. Stat. Mech: Theory Exp.*, 2016(6):064005, 2016.
- [85] I. Affleck. Universal term in the free energy at a critical point and the conformal anomaly. In J. L. CARDY, editor, *Finite-Size Scaling*, volume 2 of *Current Physics Sources and Comments*, pages 347 – 349. Elsevier, 1988.
- [86] H. W. J. Blöte, J. L. Cardy, and M. P. Nightingale. Conformal invariance, the central charge, and universal finite-size amplitudes at criticality. *Phys. Rev. Lett.*, 56:742–745, 1986.
- [87] Wolfram Research, Inc. Mathematica, Version 12.0.
- [88] H. Gould and J. Tobochnik. Statistical and thermal physics (STP) package, 2008.
- [89] O. A. Castro-Alvaredo, B. Doyon, and T. Yoshimura. Emergent hydrodynamics in integrable quantum systems out of equilibrium. *Phys. Rev. X*, 6:041065, 2016.
- [90] B. Doyon and H. Spohn. Drude weight for the Lieb-Liniger Bose gas. *SciPost Phys.*, 3:039, 2017.
- [91] R. Chetrite and H. Touchette. Nonequilibrium Markov processes conditioned on large deviations. *Ann. Henri Poincaré*, 16(9):2005–2057, 2015.
- [92] F. Carollo, J. P. Garrahan, I. Lesanovsky, and C. Pérez-Espigares. Making rare events typical in Markovian open quantum systems. *Phys. Rev. A*, 98:010103, 2018.
- [93] A. B. Kolomeisky, G. M. Schtz, E. B. Kolomeisky, and J. P. Straley. Phase diagram of one-dimensional driven lattice gases with open boundaries. *J. Phys. A: Math. Gen.*, 31(33):6911–6919, 1998.

- [94] T. Bodineau and B. Derrida. Distribution of current in nonequilibrium diffusive systems and phase transitions. *Phys. Rev. E*, 72:066110, 2005.
- [95] J.P. Garrahan, R. L. Jack, V. Lecomte, E. Pitard, K. van Duijvendijk, and F. van Wijland. First-order dynamical phase transition in models of glasses: an approach based on ensembles of histories. *J. Phys. A*, 42(7):075007, 2009.
- [96] C. P. Espigares, P. L. Garrido, and P. I. Hurtado. Dynamical phase transition for current statistics in a simple driven diffusive system. *Phys. Rev. E*, 87:032115, 2013.
- [97] P. I. Hurtado, C. P. Espigares, J. J. del Pozo, and P. L. Garrido. Thermodynamics of currents in nonequilibrium diffusive systems: Theory and simulation. *J. Stat.Phys.*, 154(1):214–264, 2014.
- [98] P.T. Nyawo and H. Touchette. A minimal model of dynamical phase transition. *EPL*, 116(5):50009, 2016.
- [99] A. Lazarescu. Generic dynamical phase transition in one-dimensional bulk-driven lattice gases with exclusion. *J. Phys. A*, 50(25):254004, 2017.
- [100] A. Bressan. *Hyperbolic Conservation Laws: An Illustrated Tutorial*, pages 157–245. Springer Berlin Heidelberg, Berlin, Heidelberg, 2013.
- [101] L. Piroli, J. De Nardis, M. Collura, B. Bertini, and M. Fagotti. Transport in out-of-equilibrium XXZ chains: Nonballistic behavior and correlation functions. *Phys. Rev. B*, 96:115124, 2017.
- [102] Z. Chen, J. de Gier, I. Hiki, and T. Sasamoto. Exact confirmation of 1d nonlinear fluctuating hydrodynamics for a two-species exclusion process. *Phys. Rev. Lett.*, 120:240601, 2018.
- [103] A. Lazarescu. Exact Large Deviations of the Current in the Asymmetric Simple Exclusion Process with Open Boundaries. *arXiv e-prints*, arXiv:1311.7370, 2013.
- [104] G. Schnherr and G. M. Schtz. Exclusion process for particles of arbitrary extension: hydrodynamic limit and algebraic properties. *J. Phys. A: Math. Gen.*, 37(34):8215–8231, 2004.

- [105] G. Schönherr. Hard rod gas with long-range interactions: Exact predictions for hydrodynamic properties of continuum systems from discrete models. *Phys. Rev. E*, 71:026122, 2005.
- [106] D. D. Erdmann-Pham, K. Dao Duc, and Y. S. Song. Hydrodynamic Limit of the Inhomogeneous  $\ell$ -TASEP with Open Boundaries: Derivation and Solution. *arXiv e-prints*, arXiv:1803.05609, 2018.
- [107] F. Spitzer. Interaction of markov processes. *Advances in Mathematics*, 5(2):246 – 290, 1970.
- [108] E. Levine, D. Mukamel, and G. M. Schütz. Zero-range process with open boundaries. *J. Stat. Phys.*, 120(5):759–778, 2005.
- [109] G. M. Schütz and R. J. Harris. Hydrodynamics of the zero-range process in the condensation regime. *J. Stat. Phys.*, 127(2):419–430, 2007.
- [110] J. de Gier and F. H. L. Essler. Large deviation function for the current in the open asymmetric simple exclusion process. *Phys. Rev. Lett.*, 107:010602, 2011.
- [111] A. Lazarescu and K. Mallick. An exact formula for the statistics of the current in the TASEP with open boundaries. *J. Phys. A: Math. Theor.*, 44(31):315001, 2011.
- [112] H.T. Yau.  $(\log t)^{2/3}$  law of the two dimensional asymmetric simple exclusion process. *Ann. Math*, 159:377–405, 2004.
- [113] M. Uchiyama, T. Sasamoto, and M. Wadati. Asymmetric simple exclusion process with open boundaries and Askey–Wilson polynomials. *J. Phys. A: Math. Gen.*, 37(18):4985–5002, 2004.
- [114] M. J. Bhaseen, B. Doyon, A. Lucas, and K. Schalm. Energy flow in quantum critical systems far from equilibrium. *Nat. Phys.*, 11:509, 2015.
- [115] A. Lucas, K. Schalm, B. Doyon, and M. J. Bhaseen. Shock waves, rarefaction waves, and nonequilibrium steady states in quantum critical systems. *Phys. Rev. D*, 94:025004, 2016.

- [116] B. Doyon, T. Yoshimura, and J.S. Caux. Soliton gases and generalized hydrodynamics. *Phys. Rev. Lett.*, 120:045301, 2018.
- [117] S. J. van Tongeren. Introduction to the thermodynamic Bethe ansatz. *J. Stat. Mech.: Theory Exp.*, 49(32):323005, 2016.
- [118] A.B. Zamolodchikov. Thermodynamic Bethe ansatz in relativistic models: Scaling 3-state potts and Lee-Yang models. *Nucl. Phys. B*, 342(3):695 – 720, 1990.
- [119] J. Mossel and J.S. Caux. Generalized TBA and generalized Gibbs. *J. Phys. A*, 45(25):255001, 2012.
- [120] B. Bertini, M. Collura, J. De Nardis, and M. Fagotti. Transport in out-of-equilibrium  $xxz$  chains: Exact profiles of charges and currents. *Phys. Rev. Lett.*, 117:207201, 2016.
- [121] C. Boldrighini, R. L. Dobrushin, and Yu. M. Sukhov. One-dimensional hard rod caricature of hydrodynamics. *J.Stat. Phys.*, 31(3):577–616, 1983.
- [122] B. Doyon and H. Spohn. Dynamics of hard rods with initial domain wall state. *J. Stat. Mech.: Theory Exp*, 2017(7):073210, 2017.
- [123] B. Efron and R. J. Tibshirani. *An Introduction to the Bootstrap*. Number 57 in Monographs on Statistics and Applied Probability. Chapman & Hall/CRC, Boca Raton, Florida, USA, 1993.
- [124] Y. Jiang, Y. Chen, and X. Guan. Understanding many-body physics in one dimension from the Lieb–Liniger model. *Chin. Phys. B*, 24(5):050311, 2015.
- [125] G.Lang, F. Hekking, and A. Minguzzi. Ground-state energy and excitation spectrum of the Lieb-Liniger model : accurate analytical results and conjectures about the exact solution. *SciPost Phys.*, 3:003, 2017.
- [126] W. E. Boyce, R. C. DiPrima, and D. B. Meade. *Boyce’s elementary differential equations and boundary value problems*. [Hoboken, NJ] : Wiley, global edition edition, 2017. ”Based on Boyce, Diprima and Meade’s Elementary differential equations and boundary value problems. 11th edition [2017]. John Wiley and Sons Singapore Pte. Ltd.”–Title page verso.



- [127] E. Ilievski and J. De Nardis. Ballistic transport in the one-dimensional Hubbard model: The hydrodynamic approach. *Phys. Rev. B*, 96:081118, 2017.
- [128] A. Urichuk, Y. Oez, A. Klümper, and J. Sirker. The spin Drude weight of the XXZ chain and generalized hydrodynamics. *arXiv e-prints*, arXiv:1808.09033, 2018.
- [129] G. Jona-Lasinio. Lecture notes - macroscopic fluctuation theory 1: foundations and some applications, 2015.
- [130] L. D. Landau and E. M. Lifshitz. *Course of theoretical physics. Vol. 5: Statistical physics*. Pergamon Press, Oxford, 1968.
- [131] S. Großkinsky, G. M. Schütz, and H. Spohn. Condensation in the zero range process: Stationary and dynamical properties. *J. Stat. Phys.*, 113(3):389–410, 2003.
- [132] C. N. Yang and C. P. Yang. Thermodynamics of a onedimensional system of bosons with repulsive deltafunction interaction. *J. Math. Phys.*, 10(7):1115–1122, 1969.
- [133] D. Bernard and B. Doyon. Full counting statistics in the resonant-level model. *J. Math. Phys.*, 53(12):122302, 2012.
- [134] S. Tasaki. Nonequilibrium stationary states of noninteracting electrons in a one-dimensional lattice. *Chaos, Solitons Fractals*, 12(14):2657 – 2674, 2001. Irreversibility, Probability and Complexity.